1982

An investigation of sand transport phenomena in the Rappahannock River estuary, Virginia

Charles Joseph Natale
College of William and Mary - Virginia Institute of Marine Science

AN INVESTIGATION OF SAND TRANSPORT PHENOMENA IN THE RAPPAHANNOCK RIVER-ESTUARY, VIRGINIA

A Thesis

Presented to

The Faculty of the School of Marine Science

The College of William and Mary in Virginia

In Partial Fulfillment

Of the Requirements for the Degree of

Master of Arts

---

by

Charles Joseph Natale, Jr.

1982

APPROVAL SHEET

This thesis is submitted in partial fulfillment of the requirements for the degree of

Master of Arts

Charles Joseph Natale Jr.
Author

Approved,

John M. Zeigler, Ph.D.
Chairman

Robert J. Byrne, Ph.D.

John D. Boon, III, Ph.D.

Maynard M. Nichols, Ph.D.

Dexter S. Haven, M.S.

TABLE OF CONTENTS

TABLE OF CONTENTS (Continued)

TABLE OF CONTENTS (Continued)

DEDICATION

I would like to dedicate this work to my wife Donna, for without her support and constant encouragement, this work would not have been possible.

ACKNOWLEDGEMENTS

I am eternally indebted to Drs. John M. Zeigler, John D. Boon, III and Robert J. Byrne for their constant guidance and encouragement throughout my graduate career.

I would also like to thank Dr. Maynard M. Nichols and Mr. Dexter S. Haven for their careful review and constructive criticisms throughout this research investigation. I am grateful to Dr. Wayne L. Newell of the United States Geological Survey for graciously supplying his information on the geology surrounding the Rappahannock River.

I am especially grateful to Brett A. Burdick for his unselfish attention and input of ideas towards the development of this research investigation, Adam A. Frisch and Harold F. Hennigar for their help with Fourier grain shape analysis, Cindy T. Fischler and Ellen J. Travelstead for their help in the sediment textural analysis and D. Scott Fenstermacher, George R. Thomas and Bruce H. Comyns for their assistance in the fieldwork.

Finally, a special thanks to Cynthia D. Gaskins for her excellent job in typing this manuscript.

LIST OF TABLES

LIST OF FIGURES

LIST OF FIGURES (Continued)

LIST OF FIGURES (Continued)

ABSTRACT

Quantitative evidence supplied by bottom sediment textural analysis, Fourier grain-shape analysis and Q-mode factor analysis indicate that river-borne sand-sized sediment originating in the upper reaches of the Rappahannock is actively transported downstream and ultimately delivered to the estuarine sediment regime. Current velocity observations in the upper estuary as well as suspended sediment concentrations measured at stream gaging stations, indicate that short-term extreme hydrological events such as periodic river flooding provide a plausible transport mechanism to move river-borne sands into the estuarine sediment regime. Events of this nature can disrupt average partly-mixed estuarine circulation patterns by displacing the salt-wedge to a more seaward position, increase stratification and create a net-seaward river-type flow within the affected portions of the estuary; thus, allowing high concentrations of river-borne sediments associated with the high freshwater inflow to move into the estuary and become incorporated into the estuarine sediment regime.

Bottom sediment textural analysis indicates that the two major landward sources of sand-sized sediment to the Rappahannock Estuary are the Piedmont-derived river sands and sand-sized sediment derived from the constant denudation of fastland bluff sediments which directly outcrop along certain reaches of the Rappahannock River. Sand-sized sediment is consistently present within all the bottom sediment samples taken from the estuary channel as well as along its flanking shoals.

Fourier grain-shape analysis serves to differentiate the Piedmont-derived river sands from the fastland bluff sands in that the sand-sized sediment derived from each of these provenances possess highly contrastable shape attributes. Based upon the distribution of Fourier harmonic amplitudes of ninety-four sand-shape samples over a defined range Fourier harmonic amplitude class intervals, it is found that the river sands and fastland bluff sands represent two statistically non-similar sand-shape populations. The distribution of Fourier harmonic amplitudes also suggests that these two non-similar sand-shape populations mix together within the river's active transport system landward of the Rappahannock Estuary. The proportional mixing of these two sand-shape populations and subsequent downriver transport results in the delivery of both shape populations into the estuarine sediment regime where they may become deposited and/or redistributed within the estuarine sediments.

Q-mode factor analysis is employed in order to determine the relative extent of the proportional mixing of the two non-similar sand-shape populations within the active transport system of the Rappahannock River-Estuary via the grain-shape information supplied by Fourier analysis. Q-mode analysis determined that three compositionally distinct end-members, or factor components, are sufficient enough to encompass 98.5% of the total grain-shape variance contained within the distribution of Fourier harmonic amplitudes for the ninety-four sand-shape samples. Based upon the distribution these samples within the defined factor (variable) space, it is quantitatively determined that various percentages of the Piedmont-derived river sands are present within the bottom sediments of the Rappahannock Estuary both in the estuary channel as well as along its flanking shoal areas. Thus, Fourier grain-shape analysis proves as a useful geological tool in that it quantitatively determines that river-borne sand-sized sediment is present within the Rappahannock estuarine sediment regime.

AN INVESTIGATION OF SAND TRANSPORT PHENOMENA IN THE RAPPAHANNOCK RIVER-ESTUARY, VIRGINIA

INTRODUCTION

There has been much speculation as to whether the drowned river-valley systems of the Atlantic Coastal Plain are sources or sinks for sediments; moreover, whether sand-sized sediments originating within the fluvial reaches of these rivers are actively transported downstream into the estuarine sediment regime (Simmons, 1955; Meade, 1969, 1972; Nichols, 1972, 1977; Krone, 1972). This speculation arises as a result of the dynamic nature of estuarine circulation patterns and how these patterns affect sediment transport processes. Pritchard (1967) developed a simplistic estuarine circulation model which proposes that a two-layered flow system develops with a net-landward bottom transport and a net-seaward surface transport. This model is based on the fact that freshwater entering upstream must eventually be transported seaward, and the more dense saline water must force its way upstream to maintain a continuity of flow. Pritchard (1954) has also shown that the maximum velocities of the freshwater occur at or near the surface while maximum near bottom velocities occur at or near the bed. Surface velocities generally decrease with depth and near bottom velocities decrease with distance from the bottom. Consequently, a point or layer of no-net motion occurs, or zero velocity, close to the fresh-saltwater interface.

It should be pointed out that this classical estuarine circulation model is overly simplified and represents a generalized estuarine

circulation scheme. This has been demonstrated by Elliot (1978) who observed meterologically induced circulation patterns in the Potomac Estuary, a Chesapeake Bay Tributary. Observations were made over a period of one year (1974-1975) based upon current measurements at three levels within the estuary. Six distinct circulation patterns were recognized: classical "Pritchard Flow" associated with a partially mixed estuary (surface outflow-bottom inflow) occurred 43% of the total time, reverse estuary, three layered, reverse three layered, discharge and storage accounted for 57% of the total time. In short, it must be recognized that estuarine circulation patterns tend to be highly variable and that average or "classical flow patterns" do not always persist.

In terms of sediment transport processes in estuaries, most observations have been made during relatively stable conditions of average or low river inflow and have centered around questions concerning the transport processes of fine grained silts and clays. This is chiefly due to the observed fact that unlike river channels which tend to be paved with coarser sediments, estuarine sediments are mainly composed of muds rather than sand. Many studies have examined fine particle flocculation processes and its effects upon estuarine sedimentation patterns. Krone (1972) proposes that during average flow conditions, moderately stratified estuaries are essentially a closed system in terms of suspended sediment transport processes. Suspended sediments (chiefly silts and clays) in estuaries are being continually deposited, resuspended and recycled due to the hydraulic nature of the characteristic bi-directional flow regime (Figure 1). In addition, the deposition of river-borne suspended sediments has been observed near the

Figure 1. A diagram of estuarine shoaling processes and sediment transport patterns (from Krone, 1972).

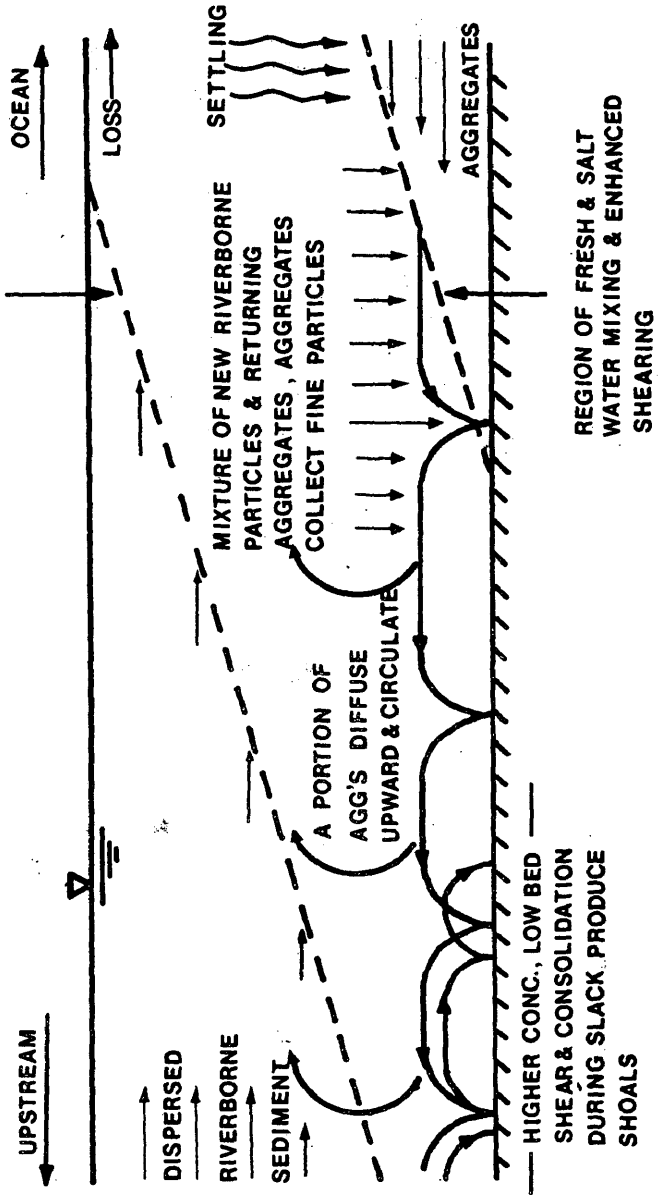
OCEAN
LOSS
SETTLING
UPSTREAM
DISPERSED
RIVERBORNE
SEDIMENT
MIXTURE OF NEW RIVERBORNE PARTICLES & RETURNING AGGREGATES, AGGREGATES COLLECT FINE PARTICLES
A PORTION OF AGG'S DIFFUSE UPWARD & CIRCULATE
AGGREGATES
HIGHER CONC., LOW BED SHEAR & CONSOLIDATION DURING SLACK PRODUCE SHOALS
REGION OF FRESH & SALT WATER MIXING & ENHANCED SHEARING

landward limit of saltwater intrusion where river waters converge and mix with the more dense saline bottom waters. Due to the turbulent nature of this convergence zone, suspended sediment concentrations increase significantly and this phenomenon has been referred to as the Turbidity Maximum Zone (Nichols, 1972).

In the past, few observations document the effects of high inflow or flooding events which tend to disrupt average estuarine circulation patterns. The response of an estuary to the high influx of flood waters is that the salt intrusion is displaced seaward and large influxes of river-borne sediments are introduced to the head of the estuary. This has been recorded by Inglis and Allen (1957); Meade (1972); Nichols (1977); Nichols, et al. (1981). Nichols, et al. (1981) obtained field observations of a flooding event (Operation HIFLO) in the Rappahannock River Estuary during March and April, 1978. Freshwater discharges of up to 358 m^3 per second were recorded, an inflow that occurs once every year on the average. During four days of peak flooding (March 26-March 29, 1978), the salt intrusion was displaced 13 km seaward and 21,000 tons of sediment, about 30% of the annual average river input, was supplied to the estuary head. This information does suggest that periodic flooding events can produce dramatic effects upon the hydraulic regime as well as sediment transport processes of an estuary, and although flooding events are short term, they may very well have long term implications upon the sedimentalogical scheme of a particular estuary.

Since most estuarine sediment transport studies have concentrated on the transport processes associated with fine grained silts and clays, very little is known about the distribution of sand-size

sediments in an estuary. Also, very little information exists about the number of potential sources of sand, the relative importance of one source versus another in contributing sand to the estuarine sediment regime. Moreover, what are the potential transport mechanisms within the river-estuary system capable of transporting sand and introducing it to the estuarine sediment regime, since the classical transport mechanisms for suspended silts and clays may not apply to the coarser materials.

Therefore, the research objective of this investigation is to attempt to gain quantitative insight into the question as to whether river-borne sand-sized sediment originating in the upper reaches of the Rappahannock River is ultimately transported into the estuarine sediment regime. In addition, evaluate plausible transport mechanisms which may provide the opportunity for river-borne sands to move into the Rappahannock Estuary.

I. PHYSICAL CHARACTERISTICS OF THE RAPPAHANNOCK RIVER-ESTUARY SYSTEM IN VIRGINIA

Rappahannock River-Estuary Geography

The Rappahannock River-Estuary system is located within the Middle Atlantic Coastal Plain of Southeastern Virginia and is one of four major tributaries which are characterized as drowned river-valley systems that drain into the Chesapeake Bay (Figure 2). The fluvial reaches of the Rappahannock drain both the Piedmont and Coastal Plain physiographic provinces while the estuarine reaches drain only the Coastal Plain. The river trends in a northwest to southeast direction. River length is approximately 295 km (184 miles) and the drainage basin covers an area of 7032 km^2 (2,715 mi^2) which accounts for approximately 6.8% of Virginia's total area (United States Geological Survey, 1978). The Rappahannock is bordered by the Potomac River to the north and the Piankatank, York and James Rivers to the south.

The Rappahannock River-Estuary is chosen for this study since it is a relatively long, straight, funnel-shaped estuary that is in an essentially pristine state. The river has not been extensively modified by major dams and only minor channel dredging has been done, primarily in the upper river, in order to maintain navigability. The Corrotoman River (18.5 km from the mouth at Windmill Point) is the only major sub-tributary draining into the Rappahannock; otherwise, only smaller tidal creeks are operative along its reaches. In addition,

Figure 2a. Map of the Chesapeake Bay Region.

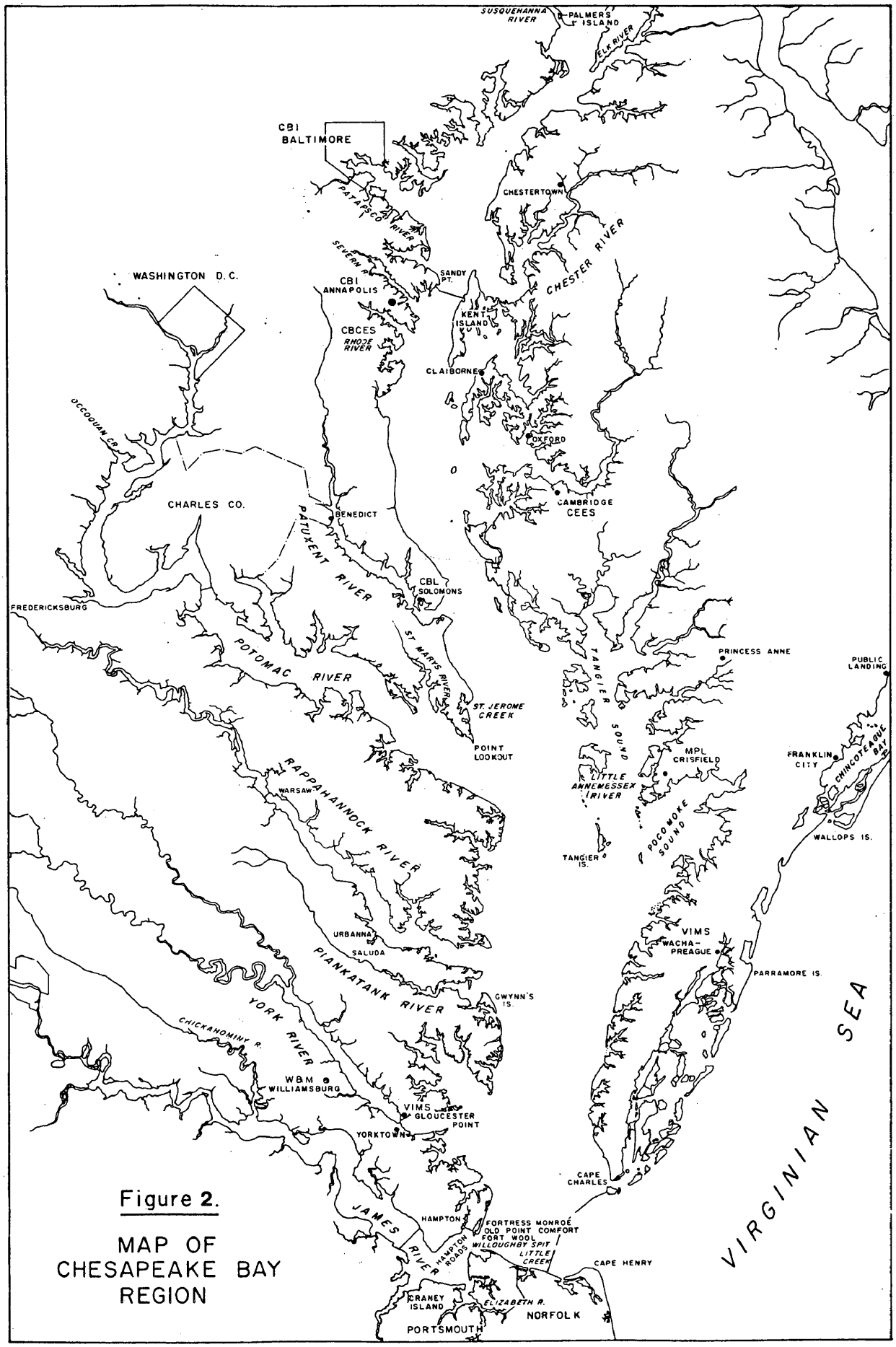

Figure 2.

MAP OF CHESAPEAKE BAY REGION

Figure 2b. Location map of the Rappahannock River basin in Virginia.

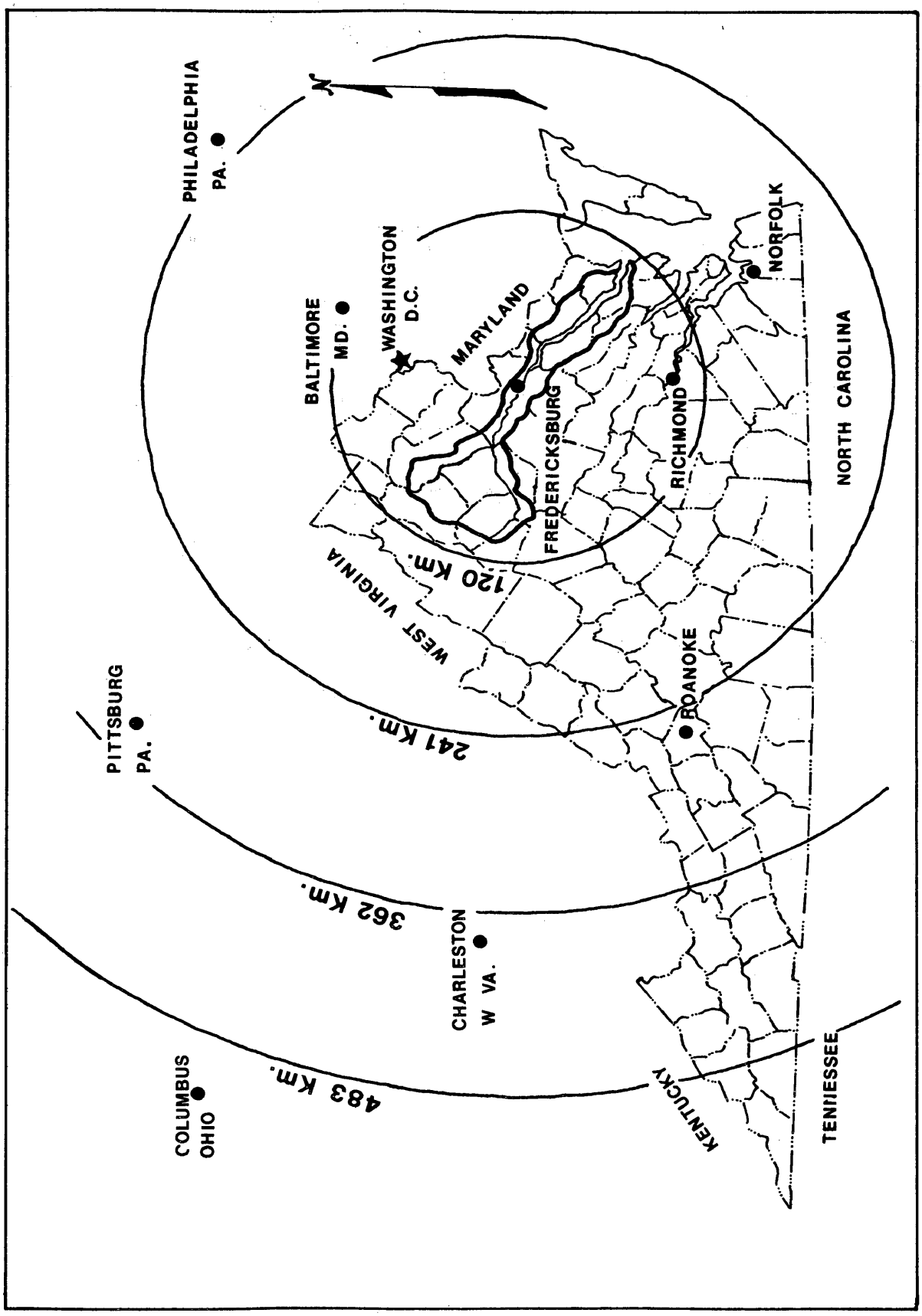

FIG. 2b. LOCATION MAP RAPPAHANNOCK RIVER BASIN IN VIRGINIA.

its river flow and sediment discharge are monitored at a number of points, particularly at Remington and Fredericksburg, by the United States Geological Survey.

Rappahannock River - Geology

The geology of the Rappahannock River has been recently investigated by W.L. Newell and E. Rader (1982, in press). Dr. Newell was kind enough to discuss his findings (via Personal Communications), and his information will be presented in a generalized scheme for the purpose of relating the effects of the local geology on the distribution of sand within the river-estuary system.

The geology surrounding the Rappahannock River-Estuary is generally described in terms of three depositional environments:

1.) Quaternary fluvial terraces.
2.) Quaternary restricted estuary deposits (reworked terraces and marine silts and clays).
3.) Tertiary marine deposits underlying uplands composed of nearshore marine and fluvial sediments.

Figure 3 shows a generalized depiction of the basic geological framework surrounding the Rappahannock River-Estuary. The sedimentary deposits flanking the upper river within the Piedmont province, above the fall line at Fredericksburg, Virginia, are described as Quaternary fluvial terraces underlain by lower Cretaceous deposits. The present day river channel sediments in the upper reaches of the river from the Piedmont down into the coastal plain to the proximity of Skinkers Neck are analogous to the earlier terrace deposits in this area and are representative of the sedimentary material actively transported out of the Piedmont reaches and into the coastal plain reaches.

Figure 3. Surrounding geology of the Rappahannock River-Estuary System, Virginia.

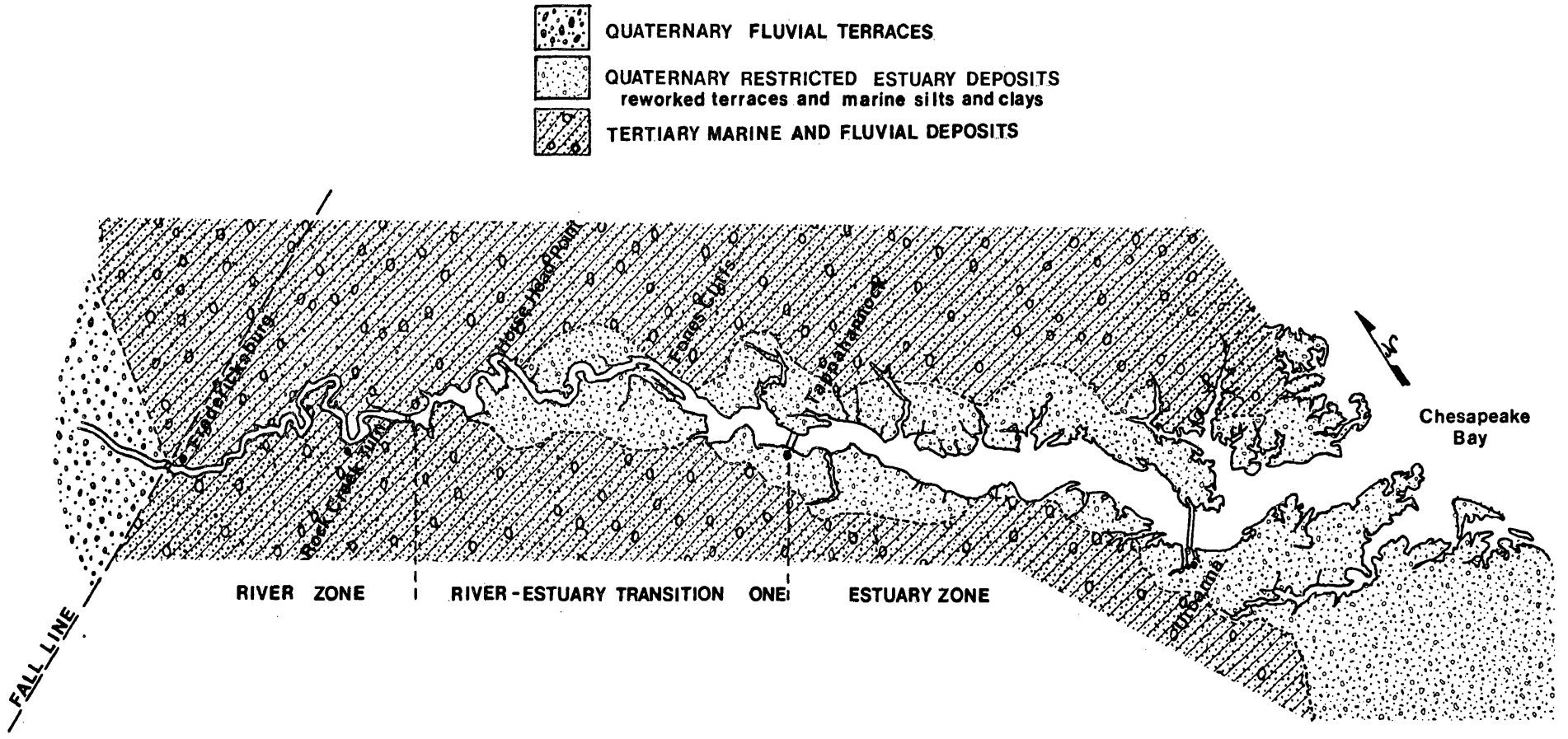
QUATERNARY FLUVIAL TERRACES
QUATERNARY RESTRICTED ESTUARY DEPOSITS
reworked terraces and marine silts and clays
TERTIARY MARINE AND FLUVIAL DEPOSITS
Fredericksburg
Rock Creek Mills
Hoses Head Point
Foxes Cliffs
Tappahannock
Chesapeake Bay
FALL LINE
RIVER ZONE
RIVER-ESTUARY TRANSITION ZONE
ESTUARY ZONE

From Skinkers Neck down into the lower estuarine reaches, subaerially exposed sedimentary material directly flanking the river is derived from a complex array of sources depending upon the relative elevations of the material above mean sea level. Upland sedimentary materials (> 35 ft (10 m) contour) directly outcropping along the flanks of the river at Rock Creek Turn, Horse Head Point and Fones Cliffs are composed of Tertiary fluvial deposits underlain by Tertiary nearshore marine and marine deposits. These deposits are associated with the Nanjemoy, Aquia, Calvert and Choptank formations.

Sedimentary material flanking the Rappahannock River at lower elevations (20-35 ft (6-10 m) contours) is described as restricted estuary late Quaternary terrace deposits composed of reworked marine silts and clays. The term restricted estuary is used in the sense that these proto-estuarine deposits were confined to the salt-wedge zone.

Unconsolidated Tertiary fastland sediments that are in direct contact with the river along reaches such as Rock Creek Turn, Horse Head Point and Fones Cliffs are in a constant state of denudation. Consequently, this sedimentary material is continually being introduced into the river's active transport system along with the native sediments occupying these reaches. Therefore, the sedimentary material comprising these bluffs must be considered as a viable source of sand-sized sediment to the river-estuary's active transport system.

Classification and Hydrological Characteristics

The Rappahannock Estuary is classified as a moderately stratified, partially-mixed, type B, estuary under Pritchard's (1967) classification scheme. During periodic high freshwater inflows, the estuary responds

by an increase in stratification and may transform into a highly stratified, salt-wedge, type A, flow regime. Once the estuary recovers from such an event, it then reverts back to its average moderately stratified flow regime (Nichols, 1977; 1981).

Tidal Characteristics

The mean tidal range at the mouth of the Rappahannock River (Windmill Point) is 36 cm. In the proximity of the average position of the head of the estuary at Tappahannock (69 km from the mouth), the tidal range is 51 cm. Freshwater reaches above Tappahannock are tidally influenced up to Fredericksburg (172 km from the mouth) which has a tidal range of 85 cm. Spring tidal ranges are 45 cm at the mouth, 58 cm at Tappahannock and 97 cm at Fredericksburg (National Ocean Survey, 1982).

The Rappahannock River is tidally classified as mainly semidiurnal. Hicks (1964) has shown that there is a slight indication of tidal inequalities within the lower portions of the Rappahannock River. Based on the ratio of the sum of the amplitudes of the major diurnal constituents (K_1 and O_1) to the sum of the amplitudes of the major semidiurnal constituents (M_2 and S_2), a value of 0.266 is obtained at the river mouth (Windmill Point). This value falls into the mixed, mainly semidiurnal type classification of Hicks (a ratio of 0.25 to 1.5 is characterized as mixed, mainly semidiurnal). Thus, although the tidal classification of the Rappahannock is mainly semidiurnal, there is evidence that a slight tidal inequality does exist.

Tidal Current Velocities

Tidal current velocities within the Rappahannock Estuary typically range from 10 cm/sec to 40 cm/sec for both the flood and ebb phases.

Tidal current velocities may vary along the length of the estuary, depending on the rates of river discharge and the phase of the tide in order to maintain a continuity of flow. During average flow conditions, there is a net non-tidal circulation in the Rappahannock Estuary. This circulation follows a two-layered bi-directional flow pattern with a net-seaward surface flow and a net-landward bottom flow. The near-surface mean non-tidal velocity is typically on the order of magnitude of around 1.5 cm/sec seaward, while the return near-bottom mean non-tidal velocity is on the order of magnitude of around 4.5 cm/sec landward.

During periodic high freshwater inflows to the estuary, bi-directional circulation patterns are disrupted with certain portions of the estuary, depending upon the magnitude of the flooding event. During Operation HIFLO (1978), near bottom net-velocities quickly changed direction from landward to seaward at the head of the estuary and ebb flow accelerated. Consequently, high freshwater inflow changed the circulation pattern at the head of the estuary from a two-layered estuarine circulation to a seaward river-type circulation at all depths. Tidal current velocities were recorded as high as 76 cm/sec at the surface and 54 cm/sec near the bottom over the longer duration ebb phase. Average current velocities during Operation HIFLO ranged from 58 cm/sec over the ebb phase and 31 cm/sec over the shorter duration flood phase.

River Discharge

Stream gaging stations located on the Rappahannock River, which measure flow discharge rates as well as suspended sediment concentrations

on a daily basis are maintained by the United States Geological Survey. These stream gaging stations are located at Remington (215 km from the mouth) and Fredericksburg, Virginia (172 km from the mouth).

At Remington, Virginia, average river discharge over the past 36 years is 18.80 m^3/sec (369 mm/yr); the maximum discharge recorded is 2,500 m^3/sec on October 16, 1942; and a minimum discharge of .079 m^3/sec on September 13, 1966. Peak flood discharge rates measured during Operation HIFLO from March 26-29, 1978 averaged 87.23 m^3/sec with a maximum flood discharge rate of 128.8 m^3/sec occurring on March 27, 1978 at Fredericksburg, Virginia; average river discharge over the past 71 years is 46.61 m^3/sec (356 mm/yr); the maximum discharge recorded is 3,960 m^3/sec on October 16, 1942; and a minimum discharge of 0.14 m^3/sec on October 11, 1930. Peak flood discharge rates measured during Operation HIFLO from March 26-29, 1978 averaged 200 m^3/sec with a maximum flood discharge rate of 325.68 m^3/sec occurring on March 27, 1978 (United States Geological Survey, 1977-1980).

Suspended Sediment Discharge

Suspended sediment measurements are recorded on a daily basis at stream gaging stations along the Rappahannock River at Remington and Fredericksburg, Virginia. At Remington, Virginia, the maximum recorded daily suspended sediment load (the quantity of suspended sediment passing a section in a specific period) was 55,600 tons on September 26, 1975 and a minimum daily load of .21 tons on September 12, 1978. The total suspended sediment load for the year 1977-1978 was 186,026.98 tons, 1978-1979 was 253,327.20 tons and 1979-1980 was 101,926.40 tons. During Operation HIFLO, one of five high runoff events during 1977-1978

sediment influx reached 4,800 tons/day at Remington or about 10 times the daily average.

At Fredericksburg, Virginia, maximum rates of suspended sediment discharge (the rate at which dry weight of sediment passes a section of stream) for 1977-1978 occurred during Operation HIFLO from March 26-29, 1978 where peak suspended sediment influx to the estuary head had reached 12,300 tons/day over the 4 days of peak freshwater inflow. For 1978-1979, peak suspended sediment influx occurred around March 27, 1979 with values ranging around 2,690 tons/day. For 1979-1980, highest values of suspended sediment discharge occurred during early October, 1979 with values ranging around 648 tons/day (United States Geological Survey, 1978; 1979; 1980).

Salinity Characteristics

Salinity data in the Rappahannock River from 1977-1980, collected by the Virginia Institute of Marine Science slack water sampling surveys, show that during the spring and early fall, salinity values at the mouth of the Rappahannock River (at Windmill Point) range from 12-14^{o}/oo at the surface and 15-17^{o}/oo at the bottom with a depth averaged salinity of 14.5^{o}/oo. Maximum recorded depth averaged salinity within this period was 19.57^{o}/oo on September 15, 1980 which corresponds to an extremely dry summer of that year.

Both surface and bottom salinity values gradually decrease with distance upstream from the mouth, and during average flow conditions, the 1^{o}/oo isohaline is usually located in the proximity of Tappahannock, Virginia, which is 69 km from the mouth. During extremely dry seasons such as the summer of 1980, when river discharge rates were very low, the 1^{o}/oo isohaline can be located as far as 115 km upstream from the

mouth near Port Royal, Virginia (126 km from the mouth). During periodic high freshwater inflows, which can occur up to 5 times a year, the salt wedge can be displaced in a seaward direction. Field observations during such an event (Operation HIFLO) indicate that during maximum stratification on March 30, 1978, the $1^{o}/oo$ surface salinity was displaced 13 km seaward, from its 21-year average position of 72 km from the mouth to 59 km from the mouth (Nichols, et al., 1981).

Hydrographic Zonation

For the purpose of this study, the Rappahannock River-Estuary is divided into three hydrographic zones. The extent of these zones are based upon the distribution of depth averaged salinity distribution as determined from both long-term data, 21-year average of the location of the $1^{o}/oo$ isohaline, and short-term data; salinity measurements from 1978-1980 (collected by the Virginia Institute of Marine Science). The zonal boundaries, for purposes of simplification, are associated with identifiable landmarks which are in close proximity to the actual salinity boundaries. Thus, the three hydrographic zones are:

1.) Estuary Zone: from the mouth at Windmill Point to Tappahannock, Virginia (69 km from the mouth).

2.) River-Estuary Transition Zone: from Tappahannock, Virginia to Port Royal, Virginia (126 km from the mouth).

3.) River Zone: from Port Royal, Virginia to the Rappahannock head waters within the Piedmont (240 km from the mouth).

Fastland Erosion Rates Within the Rappahannock River

In the estuaries of Virginia, shoreline erosion is a continuing geological process which has been operating for thousands of years. Accelerated erosion of the fastlands surrounding these estuaries has been attributed to the gradual rise in sea level caused by the waning of glacial ice sheets. Erosion rates experienced in the Rappahannock River are on the same order of magnitude as the surrounding estuaries (i.e. James, York and Potomac) and are slightly greater than the shoreline erosion rates of the Chesapeake Bay proper (Hardaway and Anderson, 1981).

Shoreline erosion rates within the Rappahannock River range from -0.3 to -0.6 m/yr (-1.0 to -2.0 ft/yr). The average rate of erosion along the north side of the river is -0.18 m/yr. The average rate of erosion along the south side of the river is slightly greater at -0.3 m/yr (Hardaway and Anderson, 1981). Erosion rates along bluffed reaches of the river as well as certain portions of the shoreline along the middle and lower reaches of the estuary may exceed -0.6 m/yr (Hardaway and Anderson, 1981; Byrne and Anderson, 1977).

II. STATEMENT OF PROBLEMS REQUIRING INVESTIGATION

In order to properly evaluate the research objectives of this investigation, inherent central problems must be addressed.

1.) Is river-borne sand-sized sediment derived from landward provenances of the upper reaches of the Rappahannock River actively transported downstream and ultimately delivered and dispersed within the estuarine sediment regime?

2.) If it is generally true that river-borne sands are inhibited from further downstream transport pass the salt intrusion during average, partially-mixed estuarine circulation patterns, do periodic high freshwater inflows to the estuary provide a plausible transport mechanism to move river-borne sands into the estuarine sediment regime?

3.) What are the potential pathways that exist within the river-estuary's active transport system which are capable of transporting and dispersing river-borne sand-sized sediment into and within the estuarine sediment regime?

III. FIELD INVESTIGATIONS

Sediment Sampling

One hundred and sixty-one bottom sediment samples were acquired from the Rappahannock River-Estuary from the fall line at Fredericksburg to just outside the river mouth at Windmill Point (Figure 4). Sampling periods occurred during the summer and fall of 1980 and the spring and summer of 1981. The bottom sediment surface sampling was implemented via portable hand-grabs, Smith-McIntyre surface grabs and 12 box core stations (65 cm depth of penetration). Water depths at each sampling location were recorded by calibrated lead line and electronic fathometer readings. Sample station locations were recorded by dead reckoning, Loran C and latitude-longitude.

The bottom sediment sampling scheme was developed in order to determine the textural composition of bottom sediments and to evaluate the relative distribution of sand within the Rappahannock River-Estuary system. Bottom surface sediments were collected in two fashions:

1.) Lateral (cross-sectional) sampling.

2.) Spot sampling.

Thirty-eight cross-sectional sampling stations (115 samples) were established from Fredericksburg (172 km from the mouth) downriver to Morattico (46 km from the mouth). The average distance between cross-sections was 2.5 km within the riverine zone, 5 km within the river-estuary transition zone and 8.0 km within the estuary. At each cross-section

Figure 4. Sediment sampling locations in the Rappahannock River-Estuary System.

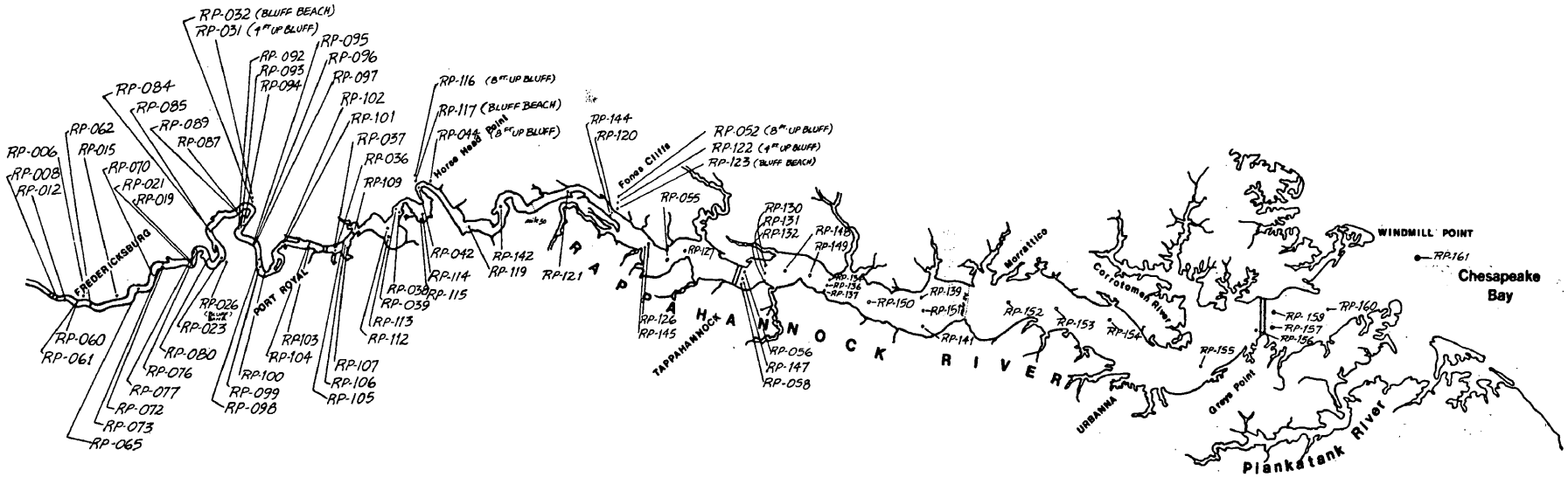

SEDIMENT SAMPLING LOCATIONS

station, sediment sampling began on the south side of the river, moved into the channel and then onto the northern side. The sample frequency was usually dictated by the width of the river at a particular station. The sample frequency generally increased with an increase in river width. Usually three to four bottom sediment samples were taken across each cross-section within the river and river-estuary transition zone. Five to seven samples were taken across each cross-section within the estuary zone. Additional cross-sectional sampling stations were established where current meter arrays were deployed during Operation HIFLO (just downriver of the Tappahannock Bridge). This enabled the textural composition of the bottom sediments at the current mooring locations to be determined.

Spot samples of bottom sediments were taken in the channel as well as along the shoals in between cross-section station locations. This was done mainly to determine the spatial distribution and continuity of sand-sized sediment between cross-section stations. In addition, sixteen spot samples were taken from fastland bluffs (subaerially exposed sedimentary formations) which directly outcropped along certain reaches of the river such as Rock Creek Turn, Horse Head Point and Fones Cliffs. At these locations, vertical spot samples were taken at 8 ft and 4 ft up the bluff face as well as the bluff beach material at the foot of the bluff. These samples were taken so that the textural composition of the fastland bluff sediments could be determined.

Granulometric Analysis

Each sediment sample is first homogenized. A 50-gram aliquot is then removed from the homogenized sample for analysis. Each sample

is wet sieved at 62μm (4ϕ) to separate the sand-size fraction. Pipette analysis is performed on the residual wash material in order to separate the silt (4ϕ - 8ϕ) and clay (> 8ϕ) size fractions. Each of the three size fractions are then oven-dried and weighed. The percent composition of sand, silt and clay is determined from the fractioned weight of the constituents.

Rappahannock River-Estuary Bottom Sediment Textural Characteristics

Channel Bottom Sediments

Figure 5 shows that the channel bottom sediments consists of three textural types: (1) sand, (2) an admixture of clayey sand or clayey silt, and (3) silty clay. Figure 5a shows the textural distribution of all channel bottom sediment samples within the river-estuary system. Figure 5b indicates that sand is the dominant sediment type within the river channels. Gravel, very coarse and coarse sand occupied the river channels near Fredericksburg and progressively fine downstream to a medium sand near Port Royal. Figure 5c shows that in the river-estuary transition zone, channel bottom sediments are characterized as admixtures of clayey sand or clayey silt. The coarser, clayey sands are the dominant sediment type from Port Royal down to Fones Cliffs. Medium to fine sand is contained within the samples from these reaches. Clayey silts characterize the channel bottom sediments approaching the head of the estuary from Fones Cliffs to Tappahannock. Fine sand is the dominant sand-size fraction contained within the samples along this reach. Figure 5d shows that in the estuary, channel bottom sediments are characterized as silty clay with low percentages of sand. Fine sand to very fine sand are contained within the estuary

Figure 5. Sediment textural composition and distribution of Rappahannock Channel bottom sediments.

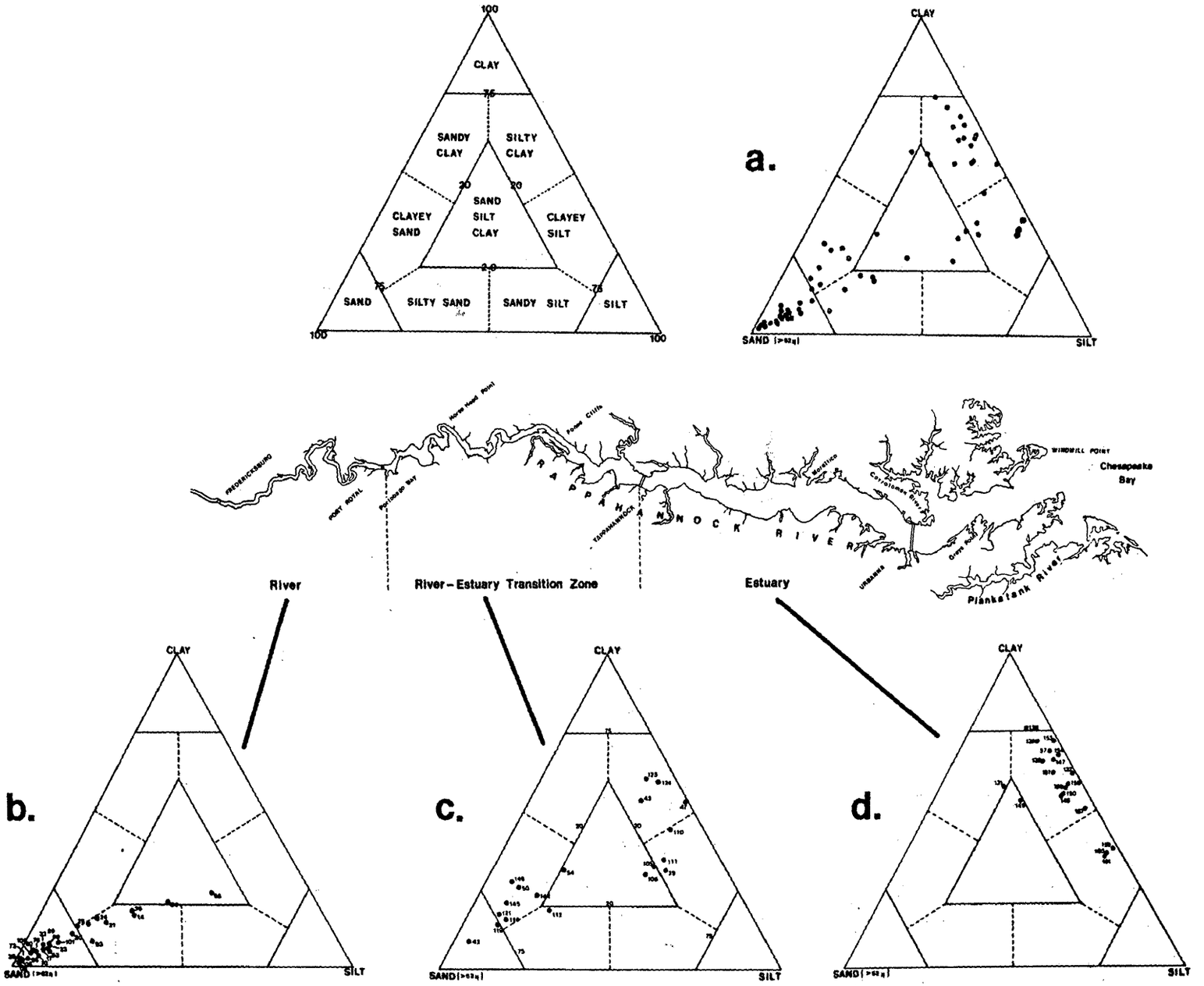

CHANNEL BOTTOM SEDIMENTS

channel samples. It is interesting to note that the three channel samples taken at the mouth (RP158 and RP160) and just outside the mouth (RP161) show a coarsening into a clayey silt sediment type.

Fluvial Channel-bars and Flanking Shoals

Figures 6a-f show the distribution of bottom sediment textural characteristics of the fluvial channel-bars and the northern and southern shoaling areas which flank the river and estuary's central channel. It is particularly noticeable that the textural distribution of bottom sediments occupying the northern flank are very similar to the textural distribution of bottom sediments occupying the southern flank for all three hydrographic zones.

Figures 6a-b show the distribution of bottom sediment textural characteristics within the river zone for the northern and southern channel-bars. An interesting dichotomy appears to exist within the textural distribution of these samples. The bottom sediments are characterized either as sand or silty clay with a few samples falling into the sand-silt-clay admixtures. This trend may be attributed to the local morphology of the fluvial meanders present within this zone and changes in the momentum of river flow associated with meander morphology. An increase in flow momentum on the concave or outside of a meander bend would tend to winnow fine sediments, hence conducive to coarser-sized sediment deposition. A decrease in the flow momentum on the convex or inside of a meander bend would be conducive to the deposition of finer sediments such as silts and clays. This type of situation would lead to the deposition of coarser material (sand)

on a channel-bar located close to the outside edge of a meander bend while deposition of finer material (silty clays) may be associated with a channel bar located close to the inside edge of a meander bend.

Figures 6b-c show the distribution of bottom sediment textural characteristics of samples from the north and south shoals flanking the river channel within the river-estuary transition zone. Near Port Royal, sand (> 75%) occupies both the north and south flanks of the river channel. Downriver from Port Royal, the bottom sediments occupying the wide shoaling areas flanking the river channel at Nanzatico Bay (northern flank) and Portobago Bay (southern flank) are characterized as silty clays. Approaching Horse Head Point where fastland bluffs flank the river channel on the northern side, the textural composition of bottom sediments markedly coarsens to sandy clay at Devils Elbow (southern flank) and Horse Head Point (northern flank). Downriver from Horse Head Point near Blind Point and Leedstown, the textural composition of the bottom sediments along both the northern and southern flanks of the river channel show a marked fining of sediment texture into silty clays. Approaching the Fones Cliffs area, where again fastland bluffs flank the river channel on the northern side, the textural composition of the northern shoal coarsens markedly into sand (Blandfield Point and Mulberry Point) while the textural composition of the southern shoal is characterized as silty clay down to Tappahannock (Paynes Island, Mulberry Point and Mallorys Point).

The trends in textural composition of the shoaling areas flanking the river channel within the river-estuary transition present important evidence; a marked coarsening of sediment texture within the close proximity of Horse Head Point and Fones Cliffs indicates that the

fastland sedimentary outcrops in these areas are a potential source of coarse sediments (sands and gravels) to the river's active transport system.

The textural composition of the samples removed from the sedimentary material composing the bluffs at Horse Head Point and Fones Cliffs are characterized as sandy clay. The bluff beach sedimentary material at the base of the bluffs is characterized as sand. It must also be mentioned that bluff and bluff beach samples contained from 1.0 to 14% gravel.

Figures 6e-f show the distribution of bottom sediment textural characteristics of samples from the north and south shoals flanking the central channel within the estuary zone from Tappahannock to Morattico (46 km from the mouth). Shoaling areas within the estuary are much more extensive both laterally and longitudinally due to a gradual increase in the river-estuary's cross-sectional area from 3.0 km near Tappahannock to 5.0 km near Urbanna (mid-estuary) and to 6.5 km at the mouth of the estuary (Windmill Point).

At Tappahannock, the textural composition of bottom sediments on the northern shoal are characterized as an admixture of sand, silt and clay while the southern shoal is characterized as silty clay. Down-estuary from Tappahannock at Jones Point, Wares Wharf, and Sharps (near Morattico), a lateral gradational trend develops on the shoaling areas, particularly along the northern shoal. In these areas, sand grades outward towards the channel into sand, silt, clay of clayey sand and subsequently into silty clay in deeper water.

Figure 6. Sediment textural composition and distribution of the northern and southern shoal sediments.

NORTHERN SHOAL

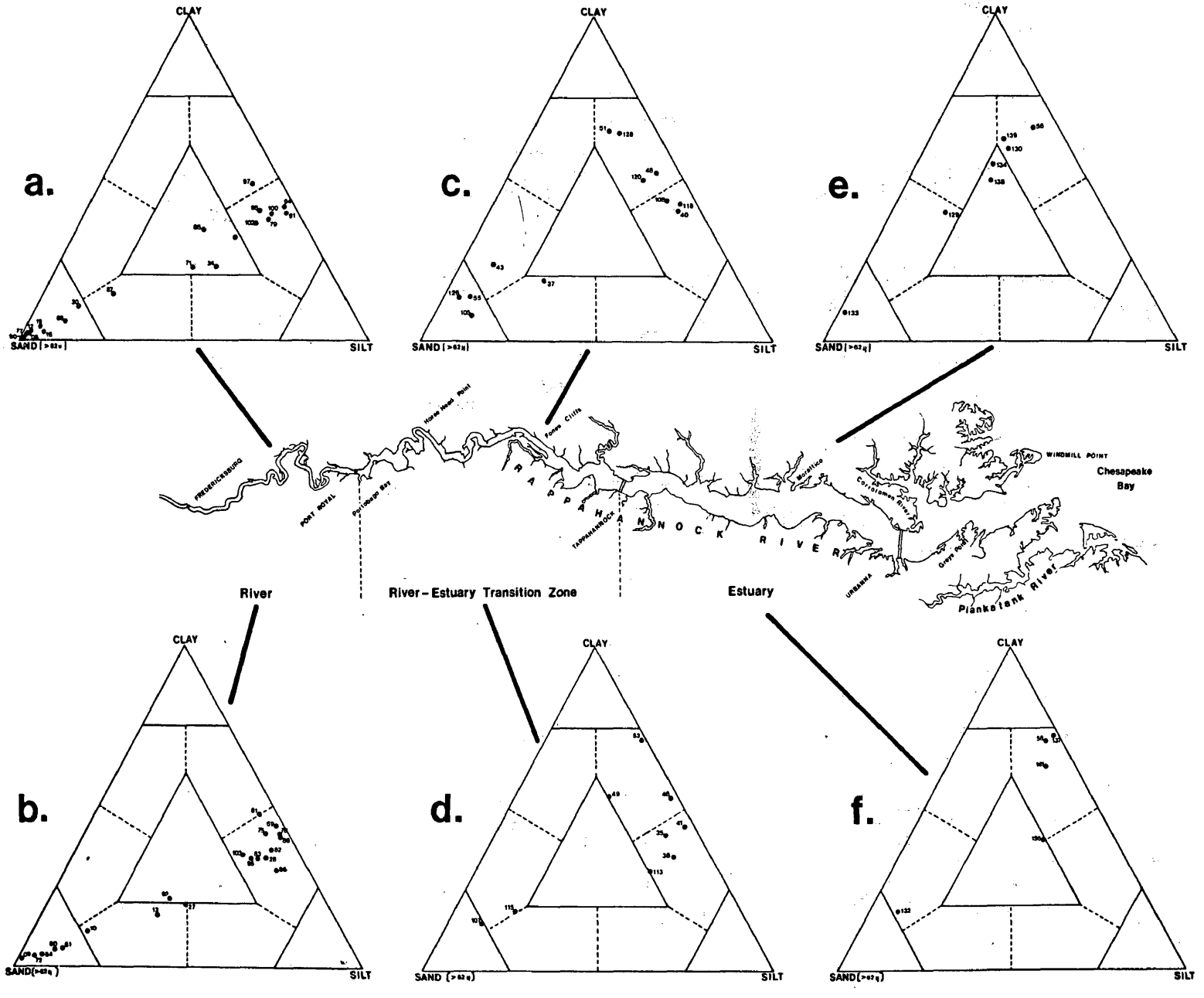

SOUTHERN SHOAL

Percent Sand Composition of Bottom Sediment Samples

Figure 7 shows the percent sand composition (by weight; > 62μ) versus distance from the mouth for the channel bottom sediments, river channel-bars and flanking shoals. A three-point (15 km) running mean is employed in order to smooth out the trends in the data.

Channel Bottom Sediments

Figure 7a shows the percent sand composition of the channel bottom sediments versus distance from the mouth with a corresponding three-point (15 km) running mean superimposed upon the initial percentage plot. High percentages of sand (65-98%; with a mean value of 86.3%) occupy the channel bottom within the river zone of the Rappahannock from the fall line near Fredericksburg down to Port Royal, Virginia. In the river-estuary transition zone from Port Royal to Tappahannock, interesting trends develop. The percentage of sand in the channel bottom sediments shows a marked decrease from 90% at Port Royal down to 20% near Portobago Bay. Just downriver from Portobago Bay, at Devils Elbow, the percentage of sand occupying the channel bottom drastically increases from 20% (near Portobago Bay) to 72%. At Horse Head Point where the fastland bluffs flank the northern side of the river, the percentage of sand in the channel shows a further increase to 85%. Downriver from Horse Head Point, the percentage of sand occupying the river channel gradually decreases from 85% down to 74% at Blind Point and to 37% at Leedstown. Downriver from Leedstown, approaching Fones Cliffs where, again, fastland bluffs outcrop on the northern flank of the river channel, the percentage of sand occupying the river channel along this reach again increases to 70% near

Blandfield Point. Downriver from the Fones Cliffs area, approaching the head of the estuary, the percentage of sand drops to 65% at Mulberry Point and then markedly decreases to 21% at Naylors Point and Tappahannock.

Within the estuary, the percentage of sand occupying the central channel of the estuary is variable (from 2-24% with an average value of 7.1%). Higher percentages of sand occupying the estuary channel occur at the head of the estuary with values of 24% at Jones Point and 21% at Wellford. In the middle estuary, the central channel's cross-sectional area gradually increases in width towards the mouth from 1.1 km at Morattico to 3.0 km at Urbanna and to 3.7 km at the mouth. The percentage of sand varies inversely in that it decreases from 7% at Sharps to 1.0% at Morattico and to 2.8% near Urbanna. The percentage of sand occupying the lower estuary central channel varies from 4.3% at Towles Point to 19% at Greys Point and 5% at Mosquito Point. The channel outside the estuary mouth at Windmill Point contains 6% sand.

River Channel Bars and Flanking Shoals

Figure 7b shows the percentage of sand comprising the bottom sediment samples of the river channel-bars and shoaling areas on the northwestern and southeastern flanks of the river-estuary central channel. Figure 7c shows the three-point (15 km) running mean analogue of Figure 7b.

Within the river zone, the percentage of sand contained within the sediments occupying the river channel-bars show a wide range of variability from as high as 90% composition to as low as 4%. Sediments on the channel-bars located near the outside edge of a meander bend

Figure 7. Percent sand composition of bottom sediments with distance from the mouth for both the channel bottom sediments and the northern and southern shoal sediments.

a.

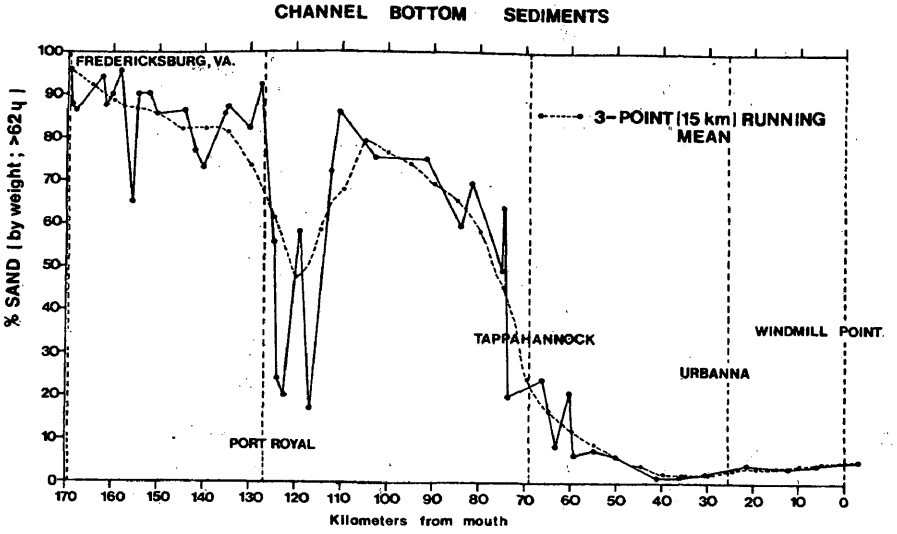
CHANNEL BOTTOM SEDIMENTS
FREDERICKSBURG, VA.
3-POINT (15 km) RUNNING MEAN
% SAND (by weight; >62 μ)
TAPPAHANNOCK
WINDMILL POINT
URBANNA
PORT ROYAL
Kilometers from mouth

b.

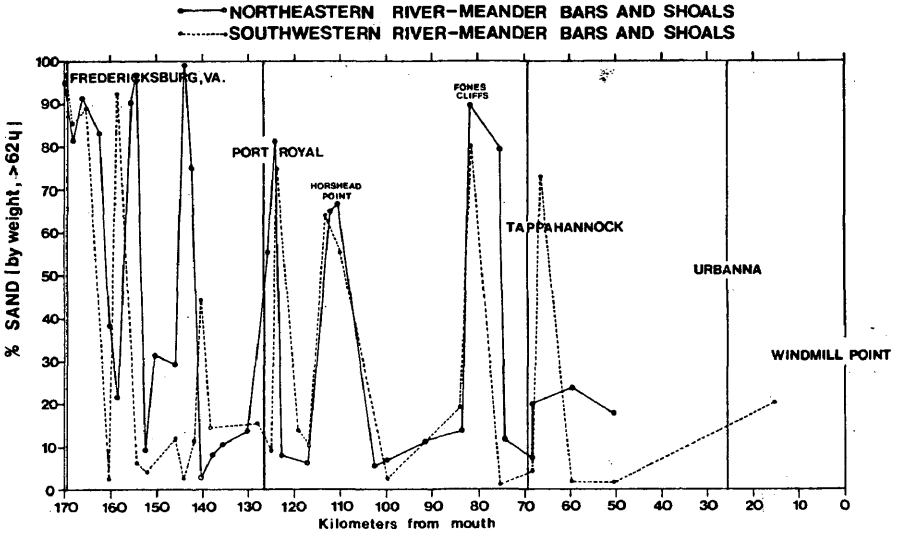
NORTHEASTERN RIVER-MEANDER BARS AND SHOALS
SOUTHWESTERN RIVER-MEANDER BARS AND SHOALS
FREDERICKSBURG, VA.
FONES CLIFFS
PORT ROYAL
HORSHEAD POINT
TAPPAHANNOCK
URBANNA
WINDMILL POINT
% SAND (by weight, >62 μ)
Kilometers from mouth

c.

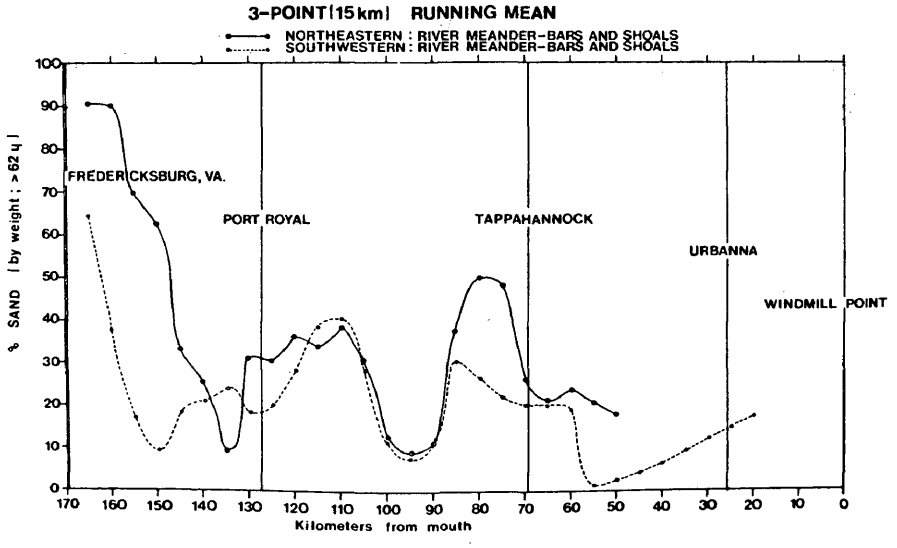
3-POINT (15 km) RUNNING MEAN
NORTHEASTERN : RIVER MEANDER-BARS AND SHOALS
SOUTHWESTERN : RIVER MEANDER-BARS AND SHOALS
FREDERICKSBURG, VA.
PORT ROYAL
TAPPAHANNOCK
URBANNA
WINDMILL POINT
% SAND (by weight; >62 μ)
Kilometers from mouth

consistently show high percentages of sand (Fredericksburg bar: 94% on northern flank; Bernard Bar: 85% on southern flank; Snowden Bar: 89% on southern flank; Hop Yard Bar: 65.2% on northern flank). Sediments contained on the channel bars located near the inside edge of a meander bend show a lower percentage of sand (Fredericksburg Bar: 70.6%, southern flank; Bernard Bar: 13% on northern flank; Snowden Bar: 38% on northern flank; Hop Yard Bar: 2.2% on southern flank).

Within the river-estuary transition zone, the percentage of sand within the samples occupying the northern and southern shoaling areas show interesting trends. Firstly, the distribution of sand percentages of samples along the northern shoals strongly correlate with the distribution of sand percentages of samples along the southern shoals. Secondly, high percentages of sand occur on both the northern and southern shoaling areas in the close proximity to where fastland bluff sediments directly outcrop along the flanks of the river, particularly along areas such as Horse Head Point and Fones Cliffs.

Downriver from Port Royal, the percentage of sand on both the northern and southern shoals is low at around 10%. At Horse Head Point, the percentage of sand markedly increases to 67% on the northern shoal and 65% on the southern shoal. Downriver from Horse Head Point, the percentage of sand then gradually decreases to approximately 10% for both the northern and southern shoals. Further downriver, approaching Fones Cliffs, the percentage of sand, again, dramatically increases to as much as 90% on the northern shoal and 80% on the southern shoal. Approaching the head of the estuary, downriver towards Tappahannock, the percentage of sand again tends to gradually decrease to around 20% along both the northern and southern shoaling areas.

Within the estuary, the percentage of sand comprising the samples along the northern and southern shoals appears to vary, depending on where the sample was taken with respect to distance channelward from the shoreline. Samples close to the shoreline generally contain higher percentages of sand (72% at Jones Point, southern flank; 87% at Wares Wharf, northern flank; 27% at Sharps, northern flank). Lesser percentages of sand occur within the samples moving outward towards the estuary channel (17% at Jones Point, southern flank; 24% at Wares Wharf, northern flank; 17% at Sharps, northern flank; 8% at Sharps, southern flank). Although no cross-sectional sediment sampling stations were taken down-estuary pass Morattico, spot sampling along the shoaling areas of the lower estuary seem to indicate a similar trend, in that, along the shoaling areas of the estuary, the percentage of sand grades outward by gradually decreasing from the shoreline towards the estuary channel.

Mineralogic Composition

Representative sand samples from the river, fastland bluffs and estuary were observed under a lietz compound microscope in order to qualitatively examine the mineralogic composition and physical characteristics of the sand-sized particles. The same samples observed from the river zone show high percentages of quartz particles (approximately 80%) and virtually no feldspar (approximately 2%); micas do not seem to be present in these samples. Heavy minerals such as tourmaline and hornblende are the second most abundant mineralogic constituents (approximately 18%) of the river sand samples.

The fastland bluff sand samples from Horse Head Point and Fones Cliffs also show high percentages of quartz (approximately 70%),

although a greater abundance of feldspar minerals are contained in the bluff samples than in the river samples (approximately 20%). Micas are not present. Heavy minerals such as illeminite, tourmaline, hornblende zircon and possibly garnet (spessartite) are present in lesser amounts (approximately 10%) within the bluff sand-sized sediments than the rivers.

Sand samples from the estuary again indicate that quartz is the most abundant mineralogic constituent of the sand fraction (approximately 60-70%); generally, feldspars comprise of approximately 10% of these samples. Mica is present within the estuary samples in varying amounts (approximately 5-10%). Higher amounts of mica occur in samples taken near areas where creek systems drain into the estuary (Totuskey Creek, Lancaster Creek and Parrots Creek) indicating a possible upland source. High amounts of organic material such as fecal pellets and foraminifera tests are also present in varying amounts (approximately 10-20%) within the estuary sand samples.

Physical Characteristics of Sand Samples

The most striking difference in physical characteristics of the sand samples under microscopic examination is the readily apparent contrast between the shape characteristics of the river quartz sand particles and the fastland bluff quartz sand particles. The fluvial quartz particles are characterized as highly angular, low sphericity. Conversely, the fastland bluff quartz sand particles are characterized as sub-rounded to rounded, low to high sphericity (Powers, 1973). The quartz particle shapes of the sand samples from the estuary appear to be comprised of a mixture of both quartz sand-shape characteristics (river and bluff sands). In the estuary, quartz

particle shapes range from angular to rounded and low, medium and high sphericity. This could suggest that quartz sand-sized sediment located within the estuary may be a result of mixing processes of the two landward sand sources; namely, the river and fastland bluffs. An in depth, quantitative examination of the distribution of quartz particle shape characteristics throughout the river-estuary system in relation to the two identifiable landward sources will be presented in a later section.

Evaluation of Current Velocities, Boundary Shear Stresses and Sediment Transport Response During a Freshwater Inlfow in the Rappahannock Estuary (Operation HIFLO, 1978)

Operation HIFLO was planned to observe and evaluate the response of an estuary to high freshwater inflow and high influx of suspended sediment. Synoptic measurements of flow, salinity and suspended sediment were obtained at slack water along the 172 km river-estuary between March-April 1, 1978. Current velocity observations within the estuary (near Tappahannock; 69 km from the mouth) began on March 23 and ended on April 14, 1978.

For the purposes of this research project, accumulated data on time-series measurements of current velocities within the estuary, particularly velocities within the boundary layer (1 m off the bed), and suspended sediment measurements recorded during Operation HIFLO, are examined in order to evaluate the question as to whether these periodic high freshwater inflows to the estuary could provide a plausible transport mechanism for river-borne sand to enter the estuarine sediment regime. In addition, some of the pertinent questions addressed by Nichols, et al. (1981) have a direct bearing upon the aforementioned statement such as: How far seaward does the sediment

load from an event go before settling to the bed? How do the hydrodynamic conditions for sediment transport change?

Operation HIFLO Storm and Runoff

The storm event associated with Operation HIFLO reached the Chesapeake Bay Region on March 27, 1978. Rainfall on the Rappahannock watershed began on March 25, 1978 and continued for approximately 38 hours to March 27, 1978. Precipitation rates on the Rappahannock totaled 3.0 to 4.5 cm on the Piedmont watershed and 5.0 to 9.5 cm on the Coastal Plain watershed. The high water crest moved downstream from Remington to Fredericksburg (48 km) in 8.2 hours. Runoff water levels reached a peak of 2.1 m at Fredericksburg on March 27, 1978 which was equivalent to a discharge of 358 m/sec (12,800 cfs). A runoff event of this magnitude is seven times the annual average discharge (46.6 m^3/sec; 1,800 cfs). The March 27 discharge was one of five high runoff events during 1977-1978. The HIFLO discharge has an average recurrence interval of once a year (Nichols, et al., 1981).

Sediment Influx

Sediment influx reached 4,800 tons/day at Remington on March 27, 1978, nearly 10 times the daily average for 1978 (509 tons/day). Farther downstream at Fredericksburg, peak suspended sediment influx to the estuary head reached 12,300 tons/day over 4 days (March 26-29, 1978) with 89% of the suspended sediment finer than .062 mm (4ϕ; 62.5μ) and 11% being greater than .062 mm (United States Geological Survey, 1977-1978). Table 1 shows a comparison of HIFLO sediment loads and peak discharges with other high freshwater inflow events recorded by the United States Geological Survey stream gaging station at Remington,

TABLE I

COMPARISON OF HIFLO SEDIMENT LOADS AND PEAK DISCHARGES WITH OTHER EVENTS RECORDED BY THE UNITED STATES GEOLOGICAL SURVEY AT REMINGTON SINCE 1951
(from Nichols, et al., 1981)

Date	Storm Sediment Load, tons	Storm Period, Arbitrary, days	Peak Discharge m/s
Aug. 19, 1955	43,900	7	1263
Mar. 20, 1963	82,100	10	195
June 22, 1972 (Agnes)	41,500	11	1296
Mar. 20, 1975	71,300	9	501
Sept. 26, 1975	107,300	6	397
Jan. 27, 1978	50,710	4	109
Mar. 27, 1981 (HIFLO)	8,146	4	358

Virginia since 1951. Relatively speaking, "HIFLO" was not a major flooding event in the Rappahannock System.

Salinity Response

The Rappahannock Estuary's response to high freshwater inflow was a lowered salinity and an associated increase in stratification. At Tappahannock (69 km from the mouth), surface salinities decreased within twenty-four hours after rainfall began from 1.5°/oo at 0200 on March 26, to nearly zero at 1100 on March 27. By March 28, one day after high inflow at Fredericksburg, the most landward limit of salty water (0.5 ppt in surface water) was displaced 12.8 km (8 miles) downstream of its position prior to high inflow (72 km from the mouth). The indirect effect of the high freshwater inflow was to freshen the estuary by 2-4°/oo and to maintain this lowered level for about 20 days. The estuary retained its salt intrusion as well as its partially mixed flow regime through all stages of high inflow (Nichols, et al., 1981).

Current Velocity Observations and Flow Response

Current velocity observations during "Operation HIFLO" were taken at current mooring station R-1A which was located within the estuary's central channel at the head of the estuary (66.5 km from the mouth; 37°55'10" N, 76°49'17" W), Figure 8. At R-1A, measurements of speed, tilt and direction were made by two braincon type 1381 histogram current meters moored on a taut wire. The meters were set at 2.0 m and 7.4 m below the surface. The total depth at station R-1A was 8.0 m. Measurement records at station R-1A began on March 23 and ended on April 14. A savonious rotor indicated speed from the total number of revolutions over a twenty-minute period. The longitudinal

Figure 8. Station R-1A location in the upper estuary channel during Operation HIFLO.

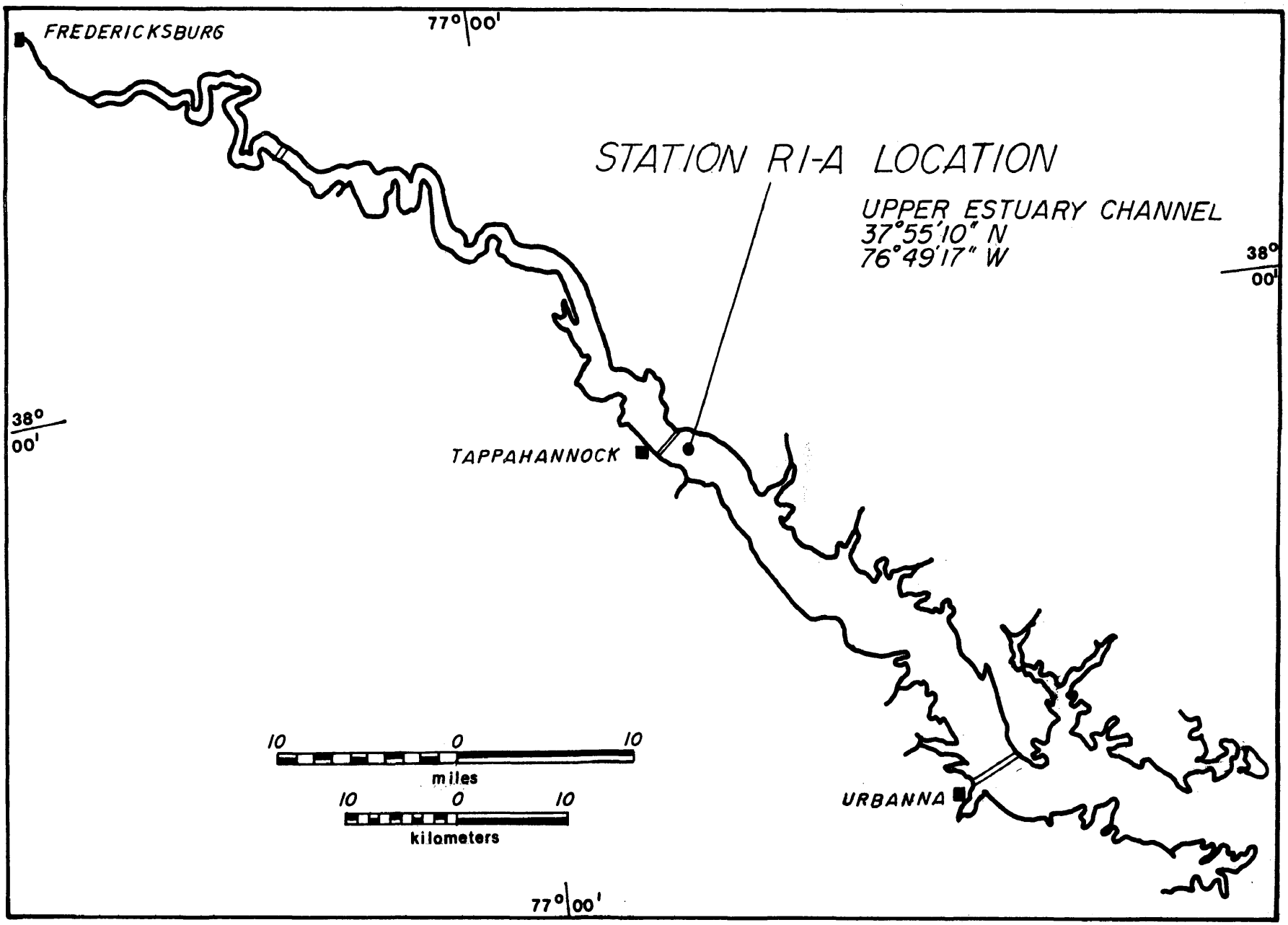
FREDERICKSBURG
77° 00'
STATION RI-A LOCATION
UPPER ESTUARY CHANNEL
37°55'10" N
76°49'17" W
38° 00'
38° 00'
TAPPAHANNOCK
10 0 10
miles
10 0 10
kilometers
URBANNA
77° 00'

component of velocity was calculated from digitized raw data for each twenty-minute interval.

Figure 9 displays the near-surface (2 m depth) time-velocity curve of current velocities recorded at station R1-A before and during high freshwater inflow. Before high inflow, March 24-25, the maximum flood current reached 70 cm/sec and a maximum ebb current of 55 cm/sec. During high freshwater inflow, March 27, the maximum flood current was 58 cm/sec and a maximum ebb current of 80 cm/sec. Also during high freshwater inflow, on March 27, the flood duration and amplitude was reduced by about 10% while the ebb duration was lengthened by about 15%. This corresponded with an increase in magnitude of the ebb-currents by approximately 20%.

Figure 10 displays the near-bottom (7.4 m depth) time velocity curve of current velocities recorded at station R-1A before and during high freshwater inflow. Before high inflow, March 23-24, the maximum flood current reached 48 cm/sec and a maximum ebb current of 44 cm/sec. During high freshwater inflow, March 27-30, maximum flood velocities reached 45 cm/sec and maximum ebb velocities reached 55 cm/sec.

In addition to this, the flood duration was shortened by about 5-10%. As a result, tidal amplitude was reduced by about 5%. Conversely, the ebb duration lengthened by about 10% associated with an increase in magnitude of about 10-15%.

At station R-1A before high inflow, March 23-25, the near-surface mean non-tidal velocity over 4 tidal cycles was 1.74 cm/sec, seaward. The near-bottom mean non-tidal velocity over four tidal cycles was 3.2 cm/sec, landward. Hence, indicating that a bidirectional flow regime existed at this point and time at the head of the estuary,

Figure 9. Time-velocity curves at station R-1A showing the change in magnitude and duration of near-surface flow, before and during high freshwater inflow.

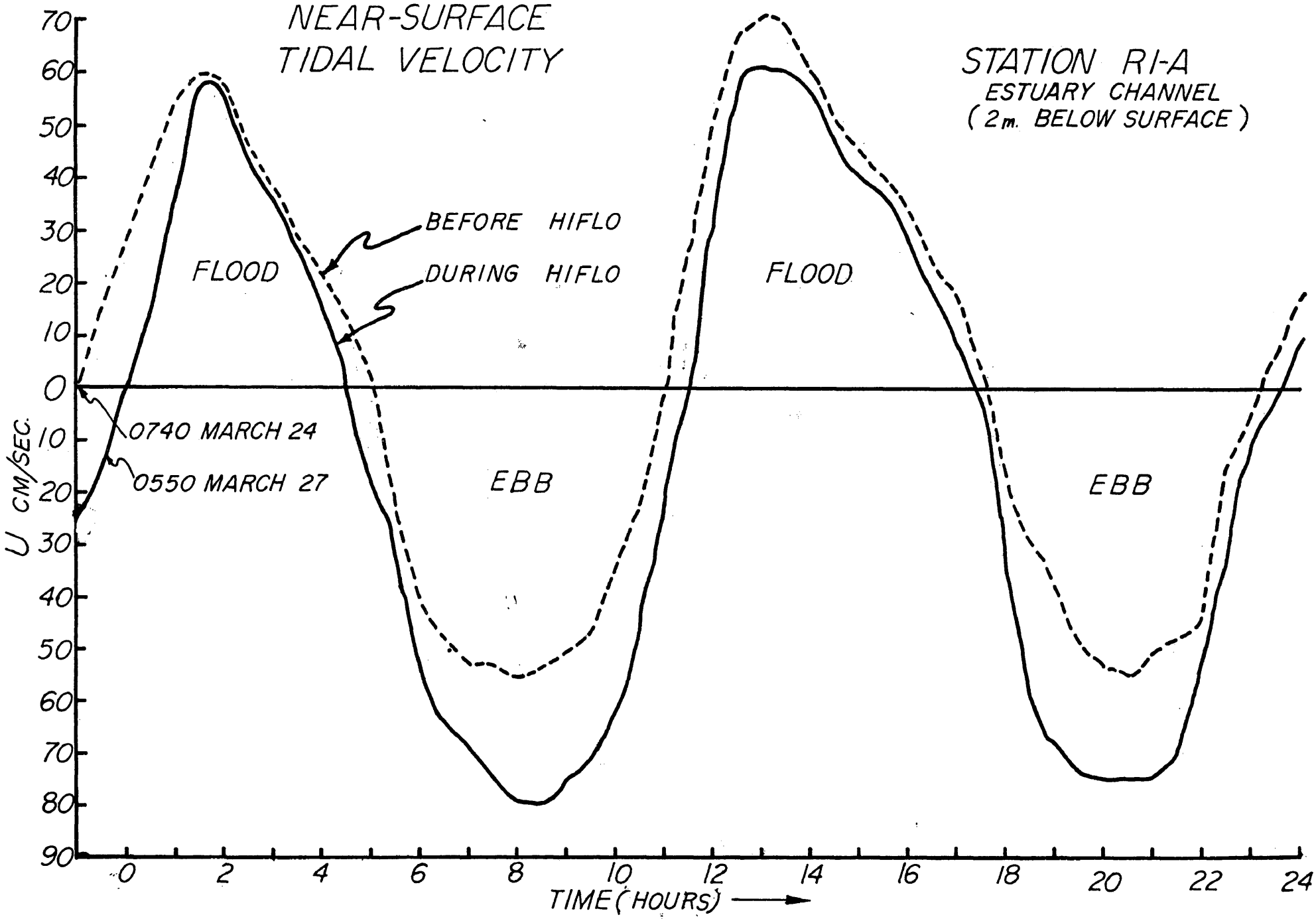
NEAR-SURFACE
TIDAL VELOCITY
STATION RI-A
ESTUARY CHANNEL
(2m. BELOW SURFACE)
BEFORE HIFLO
DURING HIFLO
FLOOD
FLOOD
EBB
EBB
0740 MARCH 24
0550 MARCH 27
U CM/SEC.
TIME (HOURS)
70
60
50
40
30
20
10
0
10
20
30
40
50
60
70
80
90
0
2
4
6
8
10
12
14
16
18
20
22
24

Figure 10. Time-velocity curves at station R-1A showing the change in magnitude and duration of near-bottom flow, before and during high freshwater inflow.

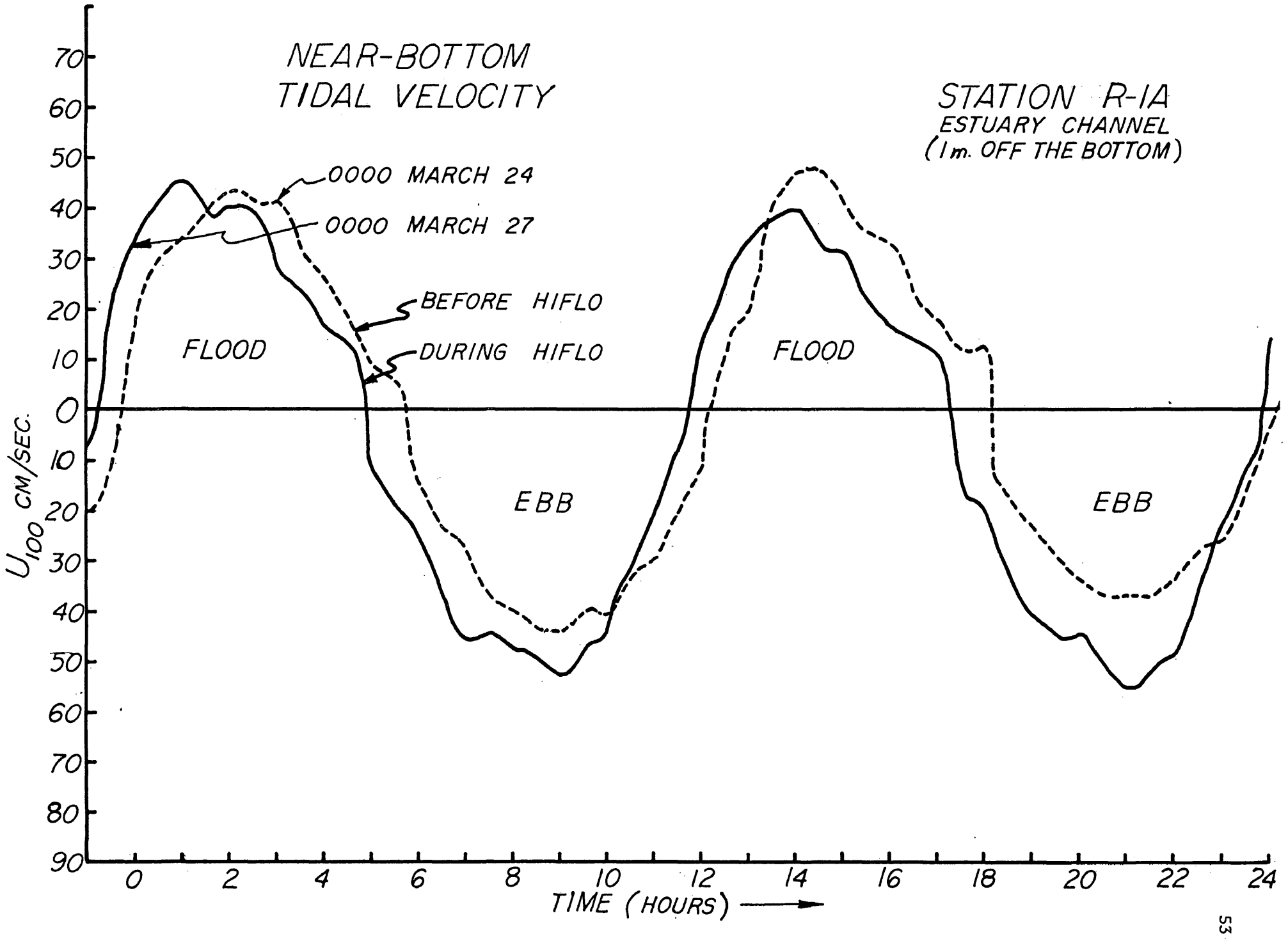
NEAR-BOTTOM
TIDAL VELOCITY
STATION R-1A
ESTUARY CHANNEL
(1m. OFF THE BOTTOM)
0000 MARCH 24
0000 MARCH 27
BEFORE HIFLO
DURING HIFLO
FLOOD
FLOOD
EBB
EBB
U_{100} CM/SEC.
TIME (HOURS)
70
60
50
40
30
20
10
0
10
20
30
40
50
60
70
80
90
0
2
4
6
8
10
12
14
16
18
20
22
24

with net-surface flow seaward and net-bottom flow landward. During high freshwater inflow to the estuary, March 26-30, the near surface mean net non-tidal velocity was 13.1 cm/sec seaward with a maximum net velocity of 26.9 cm/sec seaward occurring on March 27-28. The near bottom mean net non-tidal velocity was 5.9 cm/sec seaward with a maximum net-velocity of 14.16 cm/sec occurring on March 27-28. Thus, indicating that a strong net-seaward flow continued during the four days of high freshwater inflow in both the near-surface and near-bottom waters at the head of the estuary (station R-1A).

From the current velocity data on hand, it is difficult to discern the distance downstream that the net-seaward flow penetrated into the estuary, although one may equate the downstream penetration of this flow with the changes in the near-bottom salinity. From March 26 to March 29, near-bottom salinities dropped rapidly at Tappahannock (near station R-1A) from 1.2 ppt to 0.0 ppt. Near-bottom salinities at Tappahannock remained at 0 ppt until April 10, 1978. The salt intrusion was displaced 13 km (8 miles) seaward from its average position which is generally located around 72 km (near Tappahannock) from the mouth (Nichols, et al., 1981). Consequently, high freshwater inflow resulted in changing the circulation pattern in this zone (72 km-59 km from the mouth) from a two-layered estuarine circulation to a seaward river-type flow at all depths.

Estimating Boundary Shear Stress

It is generally accepted that the upper limit of boundary layer flow within a fully developed turbulent flow is .4 x total depth. Also, a depth of 1 m off the bed is considered the standard depth for

monitoring this type of boundary layer flow. At station R-1A, the near-bottom current meter was set at 60 cm (< 1 m) off the bed. Current velocity measurements within the boundary layer recorded during Operation HIFLO are examined in order to gain insight as to the relative magnitude of bottom shear stresses exerted on the bed. This is directly related to the fluids ability to erode bottom sediments within the estuary during the HIFLO event. Unfortunately, the existing bed-load transport equations that relate boundary shear stresses to critical or threshold erosion velocities, which relates the moving fluids ability to transport bed sediments, are not strictly applicable in this case. The state-of-the-art bed-load transport equations are based on experiments involving non-cohesive sediments. Consequently, the application of these equations for cohesive sediments, which are characteristic of the estuary, seems inappropriate in this case.

Since current velocity measurements within the estuary boundary layer at station R-1A consists of single point velocity measurements through time (Eularian description), a velocity profile of the boundary layer cannot be constructed. Although an approximation of boundary layer shear stress can be made from a single point velocity measurement taken at or close to 1 m off the bed, by using the quadratic shear stress equation in the form given by Sternberg (1972). This quantitative analysis should give a good indication of the relative magnitude of shear stresses exerted on the estuary bed during HIFLO. In addition, it can be judged whether or not the magnitude of these shear stresses are sufficient enough to erode and resuspend bottom sediment (i.e., exceed critical or threshold values for a particular bed type) within the upper estuary.

The quadratic shear stress law states that the Boundary Shear Stress (τ_o) is proportional to the fluid density (ρ) and the square of the mean velocity 100 cm off the bed times a proportionality constant (C_D) or drag coefficient. The drag coefficient relates the mean velocity near the bed to the force exerted by the fluid on the bed.

$$\tau_o = \rho \overline{U}_{100}^2 C_{D_{100}} \tag{1}$$

Sternberg (1968) has shown that for hydrodynamically rough flows, the drag coefficient assumes a constant value within the boundary layer and that this value is directly related to the bed configuration. Hence, given a representative value of $C_{D_{100}}$ for a given bed configuration, the relative shear stress may be approximated from a single measurement of mean velocity within the boundary layer.

Sternberg (1968) shows the relationship between $C_{D_{100}}$ and the Reynolds number for a variety of natural, non-cohesive bed configurations (Figure 11). The bed configurations are classified as rocky (A); gravelly (B); rippled sand (D, F); indistinctly roughened sand (E, C). The current velocities 1 m from the bed in these areas reached 40 cm/sec. Results indicate that at Reynolds' numbers greater than about 1.5×10^5 ($\overline{U}_{100}$ = 15 cm/sec), the magnitude of $C_{D_{100}}$ for each particular bed configuration is essentially constant. The value of $C_{D_{100}}$ for the various bed types ranges from about 2×10^{-3} to 4×10^{-3}. Sternberg (1972) proposes that although there appears to be a difference of a factor of two between the magnitude of $C_{D_{100}}$ for the various bed configurations, the difference is of the same order of magnitude. This fact, coupled with the notion that in most cases of field

measurements the bed configuration is not accurately known, suggests that all data should be grouped in order to present an average value of $C_{D_{100}}$ regardless of bed configuration. Table II shows the mean C_{100} and 95% confidence limits for all boundary layer data regardless of bed configuration (Sternberg, 1972).

The $C_{D_{100}}$ mean, upper limit and lower limit values in the "all data" column will be used to estimate boundary shear stresses at station R-1A during high freshwater inflow (March 26-29) to the head of the estuary. This decision is made since within the tidal current velocity durations of both flood and ebb phases during Operation HIFLO, the boundary-layer flow can transform from hydrodynamically smooth flow (near current slack; $R_e < 1.5 \times 10^5$) to hydrodynamically rough flow ($R_e > 1.5 \times 10^5$). Table III shows the range of estimated values of τ_o and u* at station R-1A (near-bottom) using Sternberg's (1968) $C_{D_{100}}$ mean, upper limit and lower limit values from March 26-29. The values of $\overline{U}_{100}$ are calculated for both the mean flood and mean ebb velocitites over one tidal cycle (semidiurnal) for each day of recorded high freshwater influx to the estuary head. The range of values (for τ_o and u*) $C_{D_{100}}$ appear to be well within reasonable range to infer that the magnitudes of these shear stresses are sufficient enough to erode and resuspend bottom sediment at this point in the estuary. This is presumed based on the fact that current velocities recorded during March 26-29 by far exceed the estimated values of u* associated with τ_o within the range of limits of $C_{D_{100}}$ values.

The writer has chosen Sternberg's (1968) mean value of 3.1×10^{-3} for $C_{D_{100}}$ to apply to station R-1A current velocity data. Sternberg (1968) has determined that this mean value is consistent within his

Figure 11. Drag coefficient ($C_{D_{100}}$) as related to the Reynolds number for all data (after Sternberg, 1968).

Table II. Mean C_{100} and 95% confidence limits for all boundary-layer data regardless of bed configuration (after Sternberg, 1968).

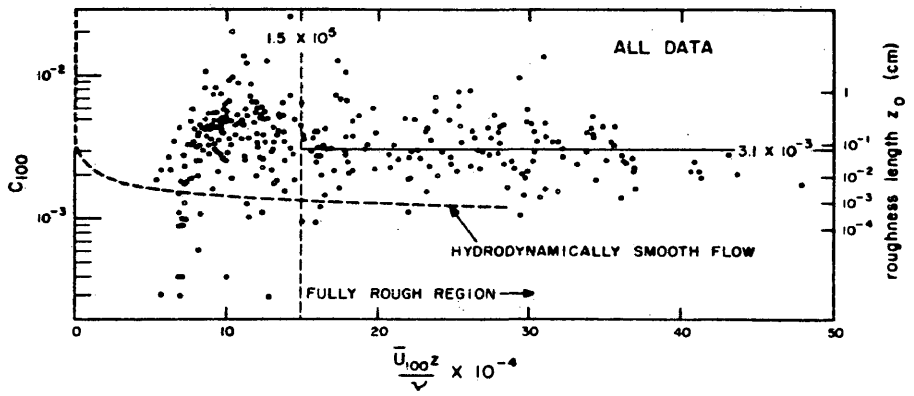

Figure 11.

Drag coefficient (C_{100}) as related to the Reynolds number for all data. Here $\bar{U}_{100}$ is the mean velocity one meter from the bed, z equals 100 cm, ν is the kinematic viscosity. Equivalent values of roughness length (z_0) can be determined by using the right-hand vertical axis. (After Sternberg, 1968.)

Table II.

Mean C_{100} and 95% Confidence Limits for All Boundary-Layer Data Regardless of Bed Configuration[a]

	All data	Re<1.5 X 10⁵	Re>1.5 X 10⁵
C_{100}	3.1 X 10⁻³	3.2 X 10⁻³	3.0 X 10⁻³
Upper limit	1.1 X 10⁻²	1.6 X 10⁻²	7.8 X 10⁻³
Lower limit	8.7 X 10⁻⁴	6.6 X 10⁻⁴	1.1 X 10⁻³

[a]After Sternberg, 1968.

TABLE III

MEAN $C_{D_{100}}$ FOR ALL BOUNDARY-LAYER DATA REGARDLESS OF BED CONFIGURATION (STERNBERG, 1972)

C_{100} MEAN = 3.1×10^{-3} (for both hydrodynamically smooth and rough flow)
UPPER LIMIT = 1.1×10^{-2}
LOWER LIMIT = 8.7×10^{-4}

τ_o and u* values for: Station R-1A near-bottom mean velocities for both flood and ebb at 100 cm off the bed from March 26-29, 1978 (Operation HIFLO)

$$\tau_o = \rho \overline{U}_{100}^2 C_{D_{100}}$$

$$u^* = C_D^{\frac{1}{2}} \overline{U}_{100}$$

DATE	$C_{D_{100}}$	FLOOD τ_o dynes/cm^2	FLOOD u* cm/sec	EBB τ_o dynes/cm^2	EBB u* cm/sec	$\overline{U}_{100}$ (cm/sec) Flood	$\overline{U}_{100}$ (cm/sec) Ebb
						(1 Tidal Cycle)	
Mar. 26	3.1×10^{-3}	2.48	1.57	2.93	1.71	28.31	30.75
	1.1×10^{-2}	8.81	2.96	10.40	3.22		
	8.7×10^{-4}	.697	.835	.822	.906		
Mar. 27	3.1×10^{-3}	2.40	1.54	3.78	1.94	27.83	34.92
	1.1×10^{-2}	8.51	2.91	13.41	3.66		
	8.7×10^{-4}	.024	.820	1.06	1.02		
Mar. 28	3.1×10^{-3}	2.08	1.44	3.85	1.96	25.91	35.26
	1.1×10^{-2}	7.38	2.71	13.67	3.69		
	8.7×10^{-4}	.584	.764	1.08	1.04		
Mar. 29	3.1×10^{-3}	1.71	1.31	3.61	1.90	23.55	34.13
	1.1×10^{-2}	6.10	2.46	12.81	3.57		
	8.7×10^{-4}	.482	.694	1.01	1.00		

data analysis for estimating τ_o via the quadratic shear stress law, regardless of the bed configuration. At this point, it is noteworthy to state that the quadratic shear stress law is employed under the reasonable assumption that a logarithmic type velocity distribution does exist. Although Sternberg (1972) found that in the various tidal channels used in his experiments, logarithmic velocity profiles occurred from 62% to 100% of the time, averaging about 85%. It must also be mentioned that little experimental evidence exists in determining drag coefficients for cohesive sediments. Some studies have been attempted, but up to this point have yielded inconclusive results (Aluruanadan, et al., 1980). Applying a mean value of 3.1×10^{-3} will at least give the reader some type of quantitative feel for the magnitude of shear stresses exerted on the estuary bed during high freshwater influx. This will also allow a basis for intuitive reasoning as to whether bottom sediment may be eroded and resuspended during an event of this nature.

Figure 12 shows the distribution of estimated shear stresses (τ_o) within the boundary layer at station R-1A using $C_D = 3.1 \times 10^{-3}$ over one tidal cycle before and during the HIFLO event. The distribution of the estimated boundary shear stresses basically resembles that of the current velocity distributions (Figures 10 and 11). Highest values of τ_o correspond with maximum current velocities over the duration of flood and ebb phases. Before the effects of high freshwater inflow reached station R-1A (March 23-24), a net-residual shear stress of .34 dynes/cm^2 existed within the boundary layer in the flood (landward) direction through time (one tidal cycle). During peak high freshwater inflow to the estuary head (March 26-27) at station R-1A,

Figure 12. Distribution of estimated boundary shear stress (τ_o) at station R-1A using $C_{D_{100}} = 3.1 \times 10^{-3}$ over one tidal cycle during peak high freshwater inflow to the head of the estuary (March 26-27, 1978).

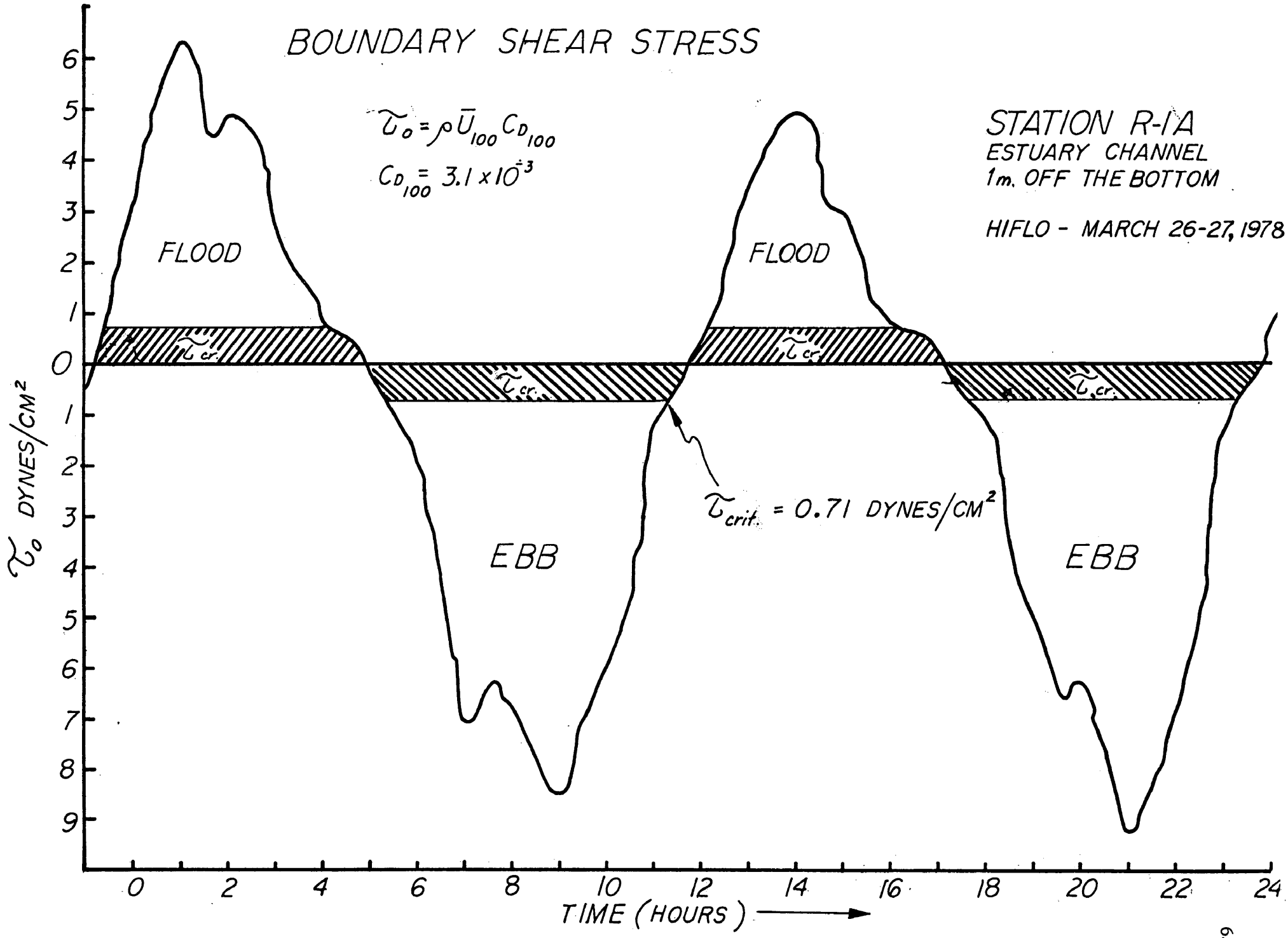
BOUNDARY SHEAR STRESS
$\tau_o = \rho \bar{U}_{100} C_{D_{100}}$
$C_{D_{100}} = 3.1 \times 10^{-3}$
STATION R-1A
ESTUARY CHANNEL
1m. OFF THE BOTTOM
HIFLO - MARCH 26-27, 1978
FLOOD
FLOOD
EBB
EBB
$\tau_{cr.}$
$\tau_{crit.} = 0.71$ DYNES/CM^2
τ_o DYNES/CM^2
TIME (HOURS)
0 2 4 6 8 10 12 14 16 18 20 22 24
6 5 4 3 2 1 0 1 2 3 4 5 6 7 8 9

a net-residual shear stress of 2.58 dynes/cm^2 existed within the boundary layer in the ebb (seaward) direction through time (one tidal cycle). Also, the magnitudes of shear stresses during high inflow were approximately reduced by 10-15% during the flood and increased by 15-20% during the ebb as compared to the distribution of the magnitude of shear stresses before high inflow.

Now that reasonable quantitative estimates of the magnitude of shear stresses exerted on the estuary bed have been determined, the question arises as to what is the relative estimate of a critical or threshold shear stress which will set the bed sediment in motion. First, the textural composition of the bottom sediment must be taken into account. Since estuarine sediments characteristically tend to be cohesive (Nichols, 1977; Krone, 1972; Meade, 1972), applications of experiments and equations predicting threshold or incipient motion for non-cohesive sediments are inappropriate. Many laboratory experiments studying the erosion of cohesive sediments have been made (Partheniades, 1965, 1970; Mignot, 1968; Graf, 1971; Metha and Partheniades, 1975; Young and Southard, 1978; Aruluanadan, et al., 1980). From this work, semi-quantitative models have been developed describing the erosion, transport and deposition of cohesive sediments. The inherent assumption of these models is that the behavior of cohesive sediments in the laboratory is representative of the behavior of cohesive sediments in situ. Some of these laboratory, as well as in situ experiments, on the erosion of cohesive sediments may be applicable to the Rappahannock Estuary sediments. These experiments are discussed so that reasonable quantitative and intuitive comparisons can be made in relation to the present research investigation.

Partheniades and Paaswell (1970) examined the erodibility of channels with cohesive boundaries and stated that many variables effect the erodibility of a cohesive sediment such as degree of packing, type and quantity of a clay mineral, concentration in the fluid, the temperature and pH of the fluid and the soil's structural geometry. Textural analysis reveals that channel bottom sediment samples at station R-1A in the Rappahannock Estuary are characterized as sandy clay (RP131) with 24% sand, 18% silt, and 58% clay (by weight). Other channel bottom samples in the immediate vicinity of R-1A are characterized as silty clay (RP146:4.3% sand, 30% silt, and 65.7% clay; RP057:4.2% sand, 27% silt and 68% clay). Water content of these samples was estimated at approximately 20-50% by weight with increasing water content corresponding with an increase in the percentage of clay. Nelson (1970) examined the clay mineralogy of bottom sediments in the Rappahannock and determined the clay mineral assemblages of samples within the vicinity of station R-1A (upper estuary) consist of kaolinite, illite, vermiculite, unorganized illite, 12.4 Å montmorillonite and 14.2 Å montmorillonite. Neither feldspar nor chlorite was detected in this area. Nelson (1970) found that no consistent mineralogical variations with depth occur in any part of the Rappahannock River or Estuary. Nelson (1972) has also determined the typical chemical properties in the low salinity sediments from the upper estuary with a pH ranging from 6.6-7.0 and Eh - 50 millivolts. Within the middle estuary, the pH increases to 7.0-7.3 and Eh to -100 millivolts.

Experimental Values of Critical Shear Stresses for Cohesive Sediments

Partheniades (1970) performed experimental investigations on the scouring of soft clay deposits using sediment that was similar in texture to the sediment occupying the estuary channel at station R-1A; namely, samples from San Francisco Bay (commonly known as bay mud) which contained equal amounts of silt and clay with traces of sand and some organic material. It was found that the minimum scouring shear stress (τ_o) was on the order of .47 dynes/cm^2 (0.0010 psf). Erosion took place by removal of individual clay particles and small clay clusters (termed surface erosion). Erosion rates depended strongly on the increase of average bed shear stress pass this threshold value.

Krone (1972) examined clay particle flocculation processes in the Savannah Harbor Estuary and their effects on estuarial shoaling processes. The textural composition of the cohesive bottom sediments here had an average clay size particle content (< 2μm) of 58% (range 52-65%); most of the remainder was silt size particles and a few percent of fine sand. The clay mineral composition was also similar to that of bottom sediments at station R-1A. The predominant clay mineral types were: kaolinite, montmorillonite and vermiculite. In this study, critical shear stresses for the cohesive estuarine bottom sediments were on the order of magnitude of approximately .62 dynes/cm^2.

Young and Southard (1978) obtained estimates of threshold erosion velocities both in the field and in the laboratory for marine muds relatively rich in organic matter and having an active infauna. A sea-floor flume was used to erode undisturbed cohesive bottom sediments

on the sea floor at Buzzards Bay, Massachusetts. In addition, a laboratory flume was used to study the effects of erosion resistance of the same cohesive muds redeposited in the flume. The purpose of this experiment was to compare the erosion resistance behavior of undisturbed muddy sediments with the erosion resistance behavior of the same sediments after redeposition in the laboratory.

Comparisons of the textural characteristics of Young and Southard's (1978) muddy sediments and the channel-bottom sediments at and near station R-1A in the Rappahannock Estuary are listed in Table IV. The textural compositions of the two sets of samples correspond fairly well with each other in that they have nearly similar percentages of sand, silt and clay, although Rappahannock samples have a slightly higher clay content. In addition, the Rappahannock sediments can also be considered partially consolidated, cohesive, biologically reworked sediments.

Results of sea flume erosion experiments are listed in Table V. The experimental values of threshold shear stresses for the undisturbed cohesive bottom sediments (in situ) ranged from 0.10 dynes/cm^2 to .71 dynes/cm^2. Corresponding threshold shear velocities (u*) ranged from .35 cm/sec to .81 cm/sec. Threshold velocities (u_{100}) at 100 cm above the bed ranged from 7.5 cm/sec to 22.3 cm/sec. The range of laboratory threshold values for unreworked beds reported in Young and Southard's (1977) experiments are generally greater than the values determined in situ and of similar estuarine and shelf muds as reported by others (Partheniades, 1965, 1970; Krone, 1972; Mignot, 1968). It is also noteworthy that the results of Young and Southard's experiments show that u^*_{cr} for the cohesive, bioturbated Buzzards Bay muds is less,

TABLE IV

COMPARISONS OF THE TEXTURAL CHARACTERISTICS OF YOUNG AND SOUTHARD'S (1978) MUDDY SEDIMENTS AND THE CHANNEL BOTTOM SEDIMENTS LOCATED AT STATION R-1A

Young and Southard (1978)

			(% wt)				
Cruise Date	Sampling Scheme	Depth Interval	SAND > 62μm	← SILT → 62-16μm	16-2μm	CLAY < 2μm	Water Content
AST 74-4 3-1-74	20 cores 100 m trans	0.1-1.0 (cm)	7±2	27±6	20±2	46±5	~55% (by wt)

NATALE RAPPAHANNOCK ESTUARY CHANNEL - VICINITY OF R-1A

		(% wt)			
		SAND > 62u	SILT < 62μs > 4μ	CLAY < 4μ	
RP-36	Jones Point - Channel	24	18.2	57.6	~20%
GRAB 107	Tappahannock	4.36	29.2	65.61	~50%
RP-14	3/4 mi. downriver from Tappahannock	4.2	27.0	68.6	

TABLE V

RESULTS OF SEA FLUME EXPERIMENTS (in situ)

Young and Southard (1978)

Cruise Date	EXPERIMENT	Threshold Shear Stress τ_o dynes/cm^2	Threshold Velocity (100 cm above bed) u^*_{100} cm/s
AST 74-17 8-15-74	Erosion Around Biogenic Tracks and Trails	.12	8.6
AST 74-18 8-20-74	Erosion Around Biogenic Tracks and Trails	.12	8.6
AST 74-18 8-20-74	Erosion of Flat Parts of Bed	.24	12.4
AST 74-21 9-19-74	Erosion of Flat Parts of Bed	.41	14.3
AST 74-24 10-30-74	Erosion of Flat Parts of Bed	.71	22.3
AST 75-1 2-4-75	Erosion of Flat Parts of Bed	.10	7.5

rather than more, than u^*_{cr} for non-cohesive fine sands. This is contrary to the results of Hjulström (1955) who predicted that u^*_{cr} for muds is greater than u^*_{cr} for fine sand for partially consolidated muds.

Figure 12 shows the distribution of boundary layer shear stresses versus time over one tidal cycle during peak high freshwater inflow to the Rappahannock Estuary (March 26-27). The maximum estimated value of critical or threshold shear stress, .71 dynes/cm^2 (as determined by Young and Southard, 1977), is greater than any value determined from the previously presented experiments of Partheniades (1970) and Krone (1972), is plotted against the shear stress curve. It is readily apparent from Figure 12 that the distribution of the magnitudes of shear stress exerted on the estuary bottom sediments at station R-1A during high freshwater inflow (March 26-27) greatly exceed the experimentally determined maximum threshold shear stress of .71 dynes/cm^2 for cohesive sediments of similar textural composition. The distribution of the magnitudes of shear stress from March 26-27 are also representative of the magnitude of shear stress from March 28-29 during high freshwater inflow. The threshold value of .71 dynes/cm^2 is exceeded in both the flood and ebb phases over the four days of flooding of which a corresponding net-residual shear stress of 2.58 dynes/cm^2 in the ebb (seaward) direction occurred.

Based upon the evidence presented, it certainly seems plausible that during the four days of high freshwater inflow (March 26-29) to the estuary head, channel bottom sediments in the vicinity of station R-1A could have very well been eroded, resuspended and transported in a net seaward direction farther down into the estuary. Further evidence supplied from the United States Geological Survey stream

gaging stations at Fredericksburg indicates that of the suspended sediment concentrations moving downriver with the mainstream influx delivered to the estuary head, 11% of this suspended sediment load was greater than 62μm (sand). In addition, if one examines Figures 10 and 11, time-velocity curves at station R-1A during Operation HIFLO (March 26-27), which is representative of tidal current velocities over four days of high freshwater inflow to the estuary (March 26-29). Because of their large amplitudes, these tidal currents are responsible for mixing fresh and saltwater, which creates excess turbulence that is responsible for resuspending much sediment from the bed (as much as 4.5 times greater than under normal conditions).

It certainly appears evident that sand-sized sediment can indeed move into the estuarine sediment regime during high freshwater inflow to the estuary. River-borne sand can be transported into the estuary either as part of the suspended load moving downriver with the flood waters or eroded and resuspended from the bottom as a result of boundary flow shear at the bed or by turbulent mixing of fresh and saltwater. How far the river-borne sand moves into the estuary may be dependent upon the magnitude of freshwater discharge to the estuary and the relative distance that the resultant net-seaward flow at all depths displaces the inner limit of salt intrusion (in a seaward direction).

Once the estuary recovers and the salt intrusion resumes its average position along with the reestablishment of its bi-directional flow regime in this area, river-borne sand delivered to the estuary may settle out and become a resident of the estuarine sediment regime. It is noteworthy at this point to state that the HIFLO event was one

of five similar high runoff events in 1978. Flooding events on the order of magnitude of Operation HIFLO have an average rate of occurrence of once a year. Therefore, if events of this nature are considered capable of transporting river-borne sand-sized sediment into the Rappahannock's estuarine sediment regime, they can do so on a relatively periodic basis. Consequently, the short-term effects of periodic flooding events upon sediment transport patterns may disrupt and produce a change in the long-term sediment dispersal patterns in a particular estuary.

IV. METHODS FOR INFERRING SEDIMENT MOVEMENT AND LOCAL SEDIMENT SOURCES WITH THE RAPPAHANNOCK RIVER-ESTUARY SYSTEM

Traditional Methods for Tracing Sand Movement

In the past, many methods have been employed to trace the movement of sand under hydraulic transport. The particular method used to trace sand movement is usually dictated by the needs of a particular experiment. This could vary between a simple desire to know the general direction of sediment movement to a full fledged sand-budget analysis, including volume rates. For the purposes of this experiment, it is intended to quantitatively determine whether river-borne sand, originating in the upper reaches of the Rappahannock as well as any other potential sand source within the riverine zone, is found within the estuarine sediment regime. Three relevant traditional techniques which might supply this quantitative information on sand-sized sediment within the Rappahannock River-Estuary System are:

1.) Fluorescent dye marking and irradiation of quartz particles (artificial tracers).

2.) Particle grain-size distributions.

3.) Particle grain-shape characteristics.

Each of these methods possesses certain strengths and weaknesses with regard to specific applications to the previously outlined objectives of this research project. A brief discussion follows regarding the intended applications of each method to the present study.

1.) Artificial Tracers - Fluorescent dye marking and irradiation of quartz particles

The primary prerequisite of any grains used to trace sediment movement is that they must be physically similar to the natural grains at the study site, regardless of the tracing medium employed. This is usually accomplished by extracting grains from the actual test site, marking and then reintroducing the grains to the site. Fluorescent tracer coatings via fluorescent dyes on sand particles has proved to be a useful method of tracing sand movement. This method has been employed in many field and laboratory experiments since the middle 1950's. Different methods of dyeing and their techniques have been described in the literature (Bruun, 1962; Wright, 1962; Yasso, 1962). Artificially induced radioactivity on quartz sand particles has also been employed as a method of tracing sand movement. Inman and Chamberlain (1959) labeled sand particles to investigate the transport of beach sand under the influence of wave action. Similar experiments using irradiated quartz particles were preformed by Gilbert and Cordeiro (1964) on beaches of Povoa do Varzim Harbor, Portugal.

In terms of useful application of artificial tracers in the present study, logical and practical hindrances arise. Tracer material must be released directly on the sand surface. Any grains released in water may be carried away in the flow until settling takes place. Enormously large amounts of sand particles would have to be marked in order to be detected any significant distance (60-70 km) from the injection point since the bulk of the tagged material is likely to be rapidly diluted through mixing with native material or else buried

and selectively removed from the zone of active transport. In addition, the time and expense of correctly monitoring this type of experiment was not available to the researcher.

2.) Particle Grain-Size Distributions

Grain-size distributions have proven useful in determining depositional environments of neritic and coastal sediments where size distribution gradients are related to various transport regimes. Bascom (1959) examined the relationship between sand size and beach face slope on selected Pacific Coast beaches of the United States. It was shown that the beach-face slope is principally controlled by two factors: (1) size of the sand, and (2) intensity of wave action. Miller and Zeigler (1958) presented a theoretical model for the expected patterns of sediment-size sorting in the region of shoaling wave, breaker and beach foreshore. The data from this study was compared with detailed observations in natural situations of sediment size and sorting patterns which resulted in a good agreement with the model. Klovan (1966) employed factor analysis to determine depositional environments from grain-size distributions of sediments collected from Barataria Bay, Louisiana. Klovan determined that three factors (as a result of the factor analysis) adequately describe the grain-size variations in the samples. Each of the three factors represented three basic kinds of energy responsible for the deposition of sediments: wind-wave energy, current energy and gravitational energy. Based on the evidence presented, Klovan suggested that the grain-size distributions are related to the relative amounts of the three types of energy active at the depositional sites.

A grain-size distribution analysis presents certain merits with respect to its application in the Rappahannock System. Of the sand samples that were sieved at whole phi (ϕ) intervals in the Rappahannock, certain trends are evident. Sand near Fredericksburg contains a larger percentage (about 50-70%) of coarser sand sizes (-1ϕ to 2ϕ); this percentage seems to gradually decrease downstream to approximately 20-30% near Port Royal. This may be a result of selective size-sorting within the fluvial reaches. At Horse Head Point and Fones Cliffs, higher percentages (70-90%) of finer sand sizes (2ϕ-3ϕ) contained within bottom sediments are more pronounced. This may be attributed to the constant denudation of these sand-sizes from the bluffs into the active transport system. As the estuary is approached, the sand-size distribution is almost exclusively finer than 2ϕ (.25 mm) except along the estuary shoals where coarser sizes (0ϕ-2ϕ) occurred close to the fastland flanks of the estuary. Although a more complete detailed analysis of grain-size distributions may give some indications of the transport of sand within the system with respect to local source material, it still eludes the question of identifying river-borne sands within the estuarine sediment regime. This type of analysis would not be able to answer this question based solely on the trends or gradients in the grain-size distributions.

3.) Particle Grain-Shape Characteristics

In the past, quartz sand particle shape morphology has been used to associate a particular quartz sand shape with a particular sand provenance or sedimentary process history. Traditionally, more elementary semi-quantitative descriptions of quartz sand particle shapes

have been employed to investigate various questions relating the sand-particle shape morphology to its depositional environment or its transport history. Wadell (1935) introduced a method of indexing sand (quartz) particle shapes by measuring the roundness (the average radius of curvature of all the corners divided by the radius of the largest inscribed circle) and sphericity (ratio of the lengths of the major and minor particle axes). Powers (1953) developed a semi-quantitative roundness scale which roundness values are obtained by comparison with photographic charts for sand grains where a perfect ball has a roundness of 1.0. Use of the Powers' roundness images for sand grains was further facilitated by a logarithmic scale (ρ) in which the limits of very angular classes are taken as 0.0-1.0 up to very round 5.0-6.0ρ (Folk, 1974).

Approximately a decade ago, Fourier grain-shape analysis was introduced as a more precise and less subjective numerical method for analyzing two-dimensional particle shapes. Schwarcz and Shane (1969) employed Fourier methods in redefining Wadell's (1935) measure of roundness in quartz particles. Ehrlich and Weinberg (1970) suggested that the use of Fourier harmonic amplitudes as a new measure of describing the total shape of a quartz particle. Ehrlich and others have applied this technique in field studies to demonstrate that quartz grains, in selected size ranges, possess certain quantifiable shape characteristics contained in the distribution of harmonic amplitudes. They believe that these distributions reflect either the source origin locale or the process history of the grains (Przygoki, 1971; Yarus, 1976, 1978; Brown, 1978; Ehrlich, et al., 1980). More recently, Boon, et al. (1982, in press) employed Fourier methods to interpret grain-

shape information of computer digitized two-dimensional images. Boon (1982) employed bandwidth averaging of certain selected Fourier harmonics to describe "band-specific" elements of quartz particle shapes over a defined range of logarithmically transformed Fourier harmonic amplitude values.

As stated previously, particle shape, as a contrastable attribute, was examined in the quartz fraction of the sediments sampled in the Rappahannock system. On the basis of this sampling, it was found that these attributes, in multivariate form (class intervals of harmonic amplitude) serves to differentiate the sand-sized sediment according to three fundamental types (end-members). It is the distribution of these types that will allow quantitative inferences to be made about identifiable sand provenances within the riverine zone and their contribution to the Rappahannock River-Estuary sedimentary system. Therefore, Fourier grain-shape analysis appears to be well suited for the objectives of this investigation in that it can attempt to quantitatively determine whether or not river-borne sand shape attributes are present within the estuarine sediment regime.

V. INTRODUCTION TO FOURIER ANALYSIS

The purpose of this section is to describe the basic concepts involved in the Fourier method as employed in this investigation. For further detailed information on this method, the reader is referred to Boon, et al. (1982, in press).

Fourier grain shape analysis allows a quantitative description of highly complex grain shapes by means of a Fourier series in a closed form. The procedure may be compared with conventional time-series analysis of a continuous periodic function $S(t) = S(t + T)$. Figure 13 shows that the same may be done for a function $R(\Theta)$ which describes the two-dimensional shape of a particle in polar coordinates where $R(\Theta) = R(\Theta + 2\pi)$. Hence, the approximation of the Fourier series is expressed as:

$$R(\Theta) = R_o \sum_{n=1}^{n-1} R_n \cos(n\Theta - \phi_n) + \tfrac{1}{2} R_n \cos(N\Theta) \qquad (2)$$

where:

$R(\Theta)$ = true particle shape expressed as a continuous function of polar angle.

R_o = mean radius from the origin (grain centroid) to the edge of the particle.

Θ = polar angles measured from an arbitrary reference line at equal increments (3.75^o) through 2π radians.

Figure 13. Two dimensional sand grain image shown in x - y coordinate (a) and polar coordinate (b) form.

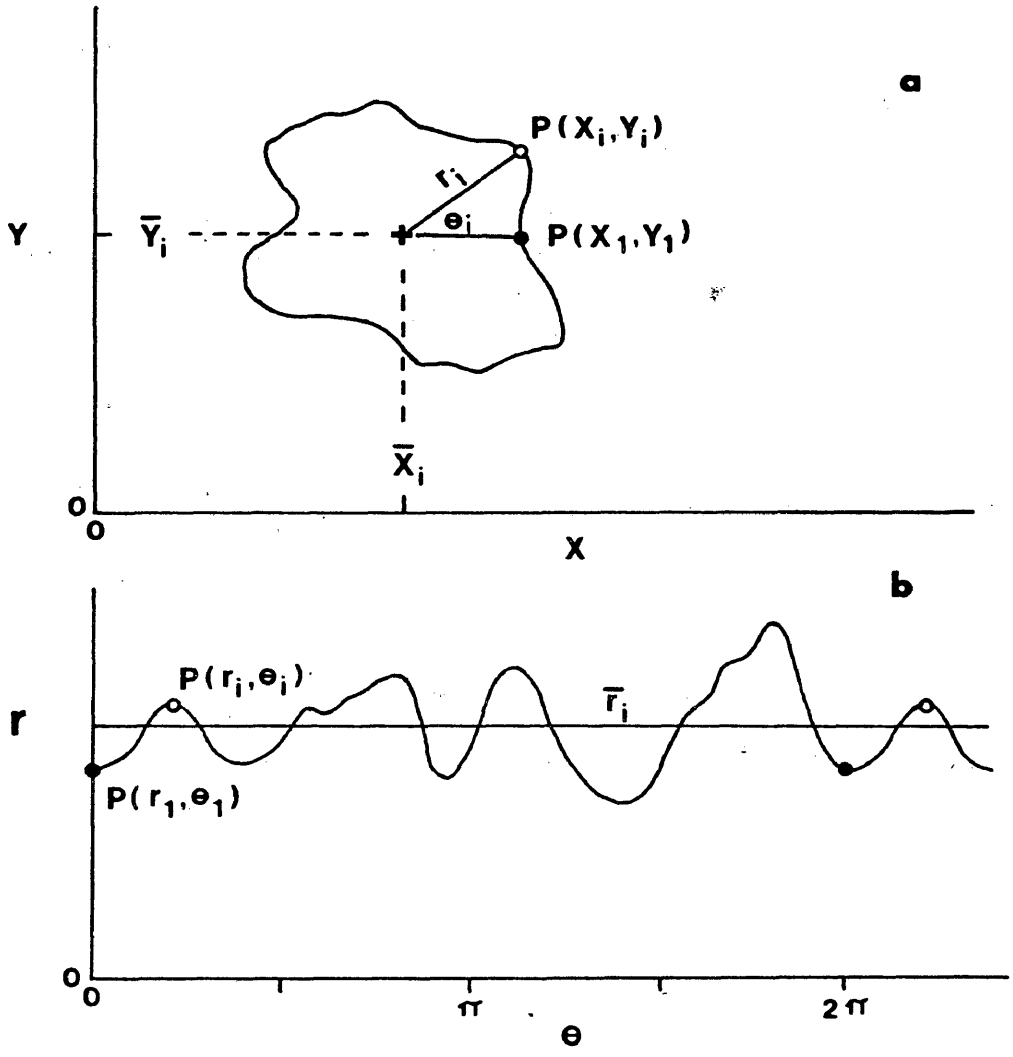
a
P(Xi,Yi)
ri
ei
P(X1,Y1)
Y
Ȳi
X̄i
0
0
X
b
P(ri,ei)
r̄i
r
P(r1,e1)
0
0
π
2π
θ

$R_n\phi_n$ = the amplitude and phase angle, respectively, of the nth harmonic term.

N = sufficient number of harmonic terms of which the approximation can be made to fit the particle shape as closely as required.

In Equation (2), the nth, or highest Fourier harmonic number, cannot exceed one-half the number of discrete data points obtained during measurement of the grain boundary (this is sometimes referred to as the Nyquist frequency). Currently, the highest harmonic of practical use is harmonic 24. The ultimate fit to the function $R(\Theta)$ is assured by the fundamental angular period (2π radians) belonging to any closed two-dimensional shape in polar coordinates, i.e., the outline of the grain boundary must repeat exactly each 2π radians and is therefore completely periodic. The central information supplied by the Fourier analysis and subsequently used to contrast quartz particles with "different" shapes is the number value of the 24 harmonic amplitudes given in dimensionless form after division by the mean radius (zeroth harmonic) in each grain. In a sample in which 400 grain shapes are analyzed, there are then 400 normalized amplitudes at each harmonic, and it is the statistical distribution of these items (at, for example, the 18th harmonic) that is used to characterize the shape properties of the grain population from which the sample is drawn. Following the practice of Boon, et al. (1982, in press), a shape "window" is utilized consisting of the RMS average of the 18th, 19th, 20th and 21st harmonic amplitudes from each grain analyzed. The latter authors have presented evidence suggesting this as a standard bandwidth in the

higher harmonic range where maximum contrastable shape information between samples is likely to be found for quartz particles in the size range of fine sand (2-3ϕ; .25 mm - .125 mm).

VI. FOURIER GRAIN-SHAPE ANALYSIS RESULTS

Fourier grain-shape analysis is performed on ninety-four selected sand samples from the Rappahannock River and Estuary as well as sand samples from sedimentary material composing the fastland bluffs directly flanking certain portions of the river. The ninety-four samples are selected on the basis of sample location. Thirty-eight of the samples are located within the river zone (Fredericksburg to Port Royal) consisting of samples from both the river channel and channel bars. Twenty-four samples are located within the river-estuary transition zone (Port Royal to Tappahannock) consisting of samples from the river channel and flanking shoals. Twenty-four samples are located within the estuary zone (Tappahannock to Windmill Point) consisting of samples from the estuary central channel and flanking shoals with emphasis on samples from within the estuary channel. The ten remaining samples came from sedimentary material composing the fastland bluffs directly flanking the river and estuary at Rock Creek Turn, Horse Head Point, Fones Cliffs and Jones Point. These samples were taken directly from the bluff material as well as from the beach material at the base of the bluffs.

Performing Fourier grain-shape analysis on these ninety-four samples should yield a fairly detailed description of the spatial distribution of any identifiable quartz particle shape populations within the Rappahannock River-Estuary System. The meaningful grain-

shape information will then be further facilitated by the use of Q-mode factor analysis. This type of multivariate analysis will attempt to show any discernible trend-gradients in the distribution of sand-shape characteristics throughout the river-estuary system. A discussion of Q-mode analysis will be presented in a later section.

Sample Preparation

The ninety-four selected sand samples from the Rappahannock River-Estuary are first dry-sieved (via Ro-Tap) to separate the 2-3ϕ (.25-.125 mm; 250-125μm) fine sand size fraction. This particular size fraction is chosen for shape analysis for three reasons: (1) this size fraction is within the mobile sand-size range as predicted by Hjulström (1935) and that of Sundborg (1956); (2) using this size fraction maintains a consistency of size-shape analysis throughout the river-estuary system; (3) use of this size fraction would also enable quartz particle shape data from the Rappahannock System to be compared with other grain-shape analysis data of the same size range but of different sedimentary provenances.

Once the 2-3ϕ size fraction is separated, the sand sample is immersed in dilute HCl (1:1) to remove any particle surface coatings and dissolve organic material. Stannous chloride ($Sn\,Cl_2$) is used to catalyze the reaction. If excess amounts of organic material are present, the sample is first immersed in 30% hydrogen peroxide for approximately one hour and then immersed in dilute hydrochloric acid for approximately one-half hour. After this process, the sample is rinsed and ready for etching of the feldspars. In order to distinguish the quartz particles from the feldspars, the sample is immersed

in hydrofluoric acid (HF) for three minutes. This process etches the feldspars so that they appear pitted (Swiss cheese like) under magnification. The sample is then rerinsed and dried. From this finished product, approximately a 500 grain subsample is drawn and is randomly and evenly dispersed atop of a clean glass microscope slide. The prepared sample is then mounted for view under a lietz compound microscope which has a video projection device coupled to its occular. The quartz sand particle shapes are now ready to be digitized.

Computerized, Two-Dimensional Digitization of Quartz Sand Particle Shapes

The quartz sand particles under magnification are directly projected onto a video image display via the video projection device. At this point, the quartz particles are readily distinguished from feldspar, mica, heavy minerals or any foreign matter present within the sample. In addition, the quartz grains may also be viewed through the eyepiece of the compound microscope to further ensure that only quartz sand particles will be digitized. The video image used to display the two-dimensional quartz particle shapes, aided by the use of a light pen, then automatically "digitizes" or draws each quartz particle grain boundary through the use of an x-y array or grid of serial ordered dots which comprise the video digitized image (Boon, et al., 1982, in press). A minimum of 400 quartz grains are digitized per sample which may take from 1.5 to 2 hours to complete. The quartz grain shape data generated during the digitization process is automatically transferred to a microcomputer which then stores this information on microcomputer storage disks for future retrieval.

Fourier Grain-Shape Data Composition and Graphical Output

Figure 14 shows that the two forms of grain-shape data output are generated for each of the ninety-four sand samples analyzed: (a) amplitude frequency table and (b) a histogram of the distribution of Fourier harmonic amplitudes over a chosen range of Fourier harmonics (bandwidth). The grain-shape data for each sample is first tabulated in the form of its arithmetic mean and standard deviation of the samples range of Fourier harmonic amplitudes for harmonics two through twenty-four (Figure 14a). These values are then logarithmically transformed to the $-\log_{10}$ scale. This is analogous to the phi (ϕ) scale log transformation in relation to particle grain-sizes, where the grain-size, expressed in millimeters, is converted into units of phi (ϕ) by $-\log_2$ transformation. From this data an amplitude-frequency table is generated (Figure 14a). This table displays the number frequency at which the quartz particle shapes, from the total number of grains within the sample, fell into a particular log transformed Fourier harmonic amplitude value (abscissa) for each of the two through twenty-four Fourier harmonics (ordinate). Henceforth, the abscissa values, $-\log_{10}$ of Fourier harmonic amplitudes, will be designated as Q_n where Q_n = -log amplitude of R_n.

Once the amplitude-frequency table has been generated, a grain-shape histogram is constructed (Figure 14b). This histogram represents the distribution of the grain-shape attributes of a particular sample over a defined range of Q_n values averaged for the 18th ... 21st harmonics (bandwidth averaging). A sample mean and standard deviation of its distribution over the range of Q_n values for the 18th ... 21st harmonics is given for each sample. For the present study, Q_n ranges

Figure 14. The two forms of grain-shape data graphical output: (a) amplitude-frequency table, (b) histogram form.

AMPLITUDE-FREQUENCY TABLE

RP11230A 415 GRAINS

2.	0	0	2	10	20	43	55	68	52	44	35	31	19	9	12	4	2	3	2	2	1	1	0	0	0	0	0	0	0	0	0	0	0	0
3.	0	0	0	0	5	12	36	60	69	69	63	27	17	22	8	10	6	3	3	2	1	0	2	0	0	0	0	0	0	0	0	0	0	0
4.	0	0	0	0	0	0	3	16	35	45	73	60	45	42	28	26	18	11	4	3	2	0	0	3	0	0	0	0	1	0	0	0	0	0
5.	0	0	0	0	0	0	0	3	5	27	45	61	63	62	60	31	15	19	10	8	3	1	0	2	0	0	0	0	0	0	0	0	0	0
6.	0	0	0	0	0	0	0	1	1	5	19	47	65	63	55	51	26	29	25	8	10	4	4	1	0	0	1	0	0	0	0	0	0	0
7.	0	0	0	0	0	0	0	0	0	4	3	25	43	58	64	58	48	35	31	21	12	6	4	1	2	0	0	0	0	0	0	0	0	0
8.	0	0	0	0	0	0	0	0	0	1	3	7	31	41	52	50	48	52	40	25	22	16	9	8	4	2	2	0	1	1	0	0	0	0
9.	0	0	0	0	0	0	0	0	0	0	0	3	9	28	45	55	61	65	51	29	25	15	8	9	4	4	0	2	0	0	1	0	0	0
10.	0	0	0	0	0	0	0	0	0	0	0	3	8	11	26	59	63	52	61	39	34	22	11	10	4	3	4	2	2	0	1	0	0	0
11.	0	0	0	0	0	0	0	0	0	0	0	0	1	5	16	36	53	61	64	49	43	27	22	20	10	3	3	0	0	0	0	1	0	0
12.	0	0	0	0	0	0	0	0	0	0	0	0	1	6	15	24	41	65	66	59	37	33	18	23	12	6	4	2	1	2	0	0	0	0
13.	0	0	0	0	0	0	0	0	0	0	0	1	1	1	4	20	30	54	52	65	48	45	23	21	20	11	6	5	5	2	1	0	0	0
14.	0	0	0	0	0	0	0	0	0	0	0	0	0	0	1	12	19	37	65	57	59	55	30	23	26	7	12	4	4	2	1	0	1	0
15.	0	0	0	0	0	0	0	0	0	0	0	0	1	1	2	5	22	30	49	67	59	42	46	29	20	14	11	9	3	1	1	0	1	1
16.	0	0	0	0	0	0	0	0	0	0	0	0	0	0	5	6	11	16	47	45	55	61	48	45	29	19	9	6	5	4	2	0	1	0
17.	0	0	0	0	0	0	0	0	0	0	0	0	0	0	1	2	6	16	39	53	53	63	45	43	41	22	9	9	5	2	2	0	1	1
18.	0	0	0	0	0	0	0	0	0	0	0	0	0	0	0	2	5	22	32	36	61	65	45	49	29	25	11	13	8	3	6	2	0	1
19.	0	0	0	0	0	0	0	0	0	0	0	0	0	0	0	3	5	5	25	44	53	64	54	51	35	29	16	11	7	3	4	3	1	1
20.	0	0	0	0	0	0	0	0	0	0	0	0	0	0	1	1	2	9	16	38	51	46	71	43	44	28	24	13	12	4	3	2	2	2
21.	0	0	0	0	0	0	0	0	0	0	0	0	0	0	0	1	1	1	6	18	36	46	54	52	57	43	29	20	25	8	10	3	3	2
22.	0	0	0	0	0	0	0	0	0	0	0	0	0	0	0	0	2	5	10	25	40	32	63	56	49	31	30	16	14	11	5	2	2	1
23.	0	0	0	0	0	0	0	0	0	0	0	0	0	0	0	1	1	6	10	18	44	51	51	62	47	49	22	22	13	9	3	4	0	1
24.	0	0	0	0	0	0	0	0	0	0	0	0	0	0	0	0	1	6	8	19	15	49	62	63	53	39	34	20	14	14	4	3	2	1
	8	.	.	.	.	.	.	.	.	8	.	.	.	.	.	.	.	.	8	.	.	.	.	.	.	.	8	.	.	.	.	8	.	.	.
	0									-1									-2								-3					-4		
	10									10									10								10					10		

a.

HARMONIC NUMBER	ARITHMETIC MEAN	S.D.	LOGARITHMIC MEAN	S.D.
2	0.16535	0.09896	0.87267	0.31052
3	0.12416	0.06598	0.98296	0.28990
4	0.07467	0.04216	1.20999	0.29642
5	0.05505	0.02994	1.32943	0.26397
6	0.04214	0.02407	1.45466	0.28303
7	0.03374	0.01925	1.54748	0.27181
8	0.02634	0.01685	1.67846	0.31777
9	0.02194	0.01241	1.74078	0.29573
10	0.01913	0.01190	1.80644	0.29977
11	0.01548	0.00885	1.89052	0.28900
12	0.01443	0.00864	1.92459	0.28875
13	0.01222	0.00799	2.00783	0.30894
14	0.01048	0.00612	2.06270	0.29100
15	0.01000	0.00650	2.09448	0.30956
16	0.00876	0.00609	2.15479	0.30690
17	0.00794	0.00496	2.18914	0.30073
18	0.00755	0.00482	2.21399	0.30700
19	0.00694	0.00449	2.25149	0.30635
20	0.00633	0.00421	2.29872	0.32312
21	0.00605	0.00393	2.31437	0.31084
22	0.00551	0.00350	2.35262	0.30983
23	0.00538	0.00354	2.35874	0.29234
24	0.00496	0.00333	2.41855	0.33415

RP11230A 415 GRAINS HARMONIC NUMBERS: 18 19 20 21
SAMPLE MEAN: 2.18496 SAMPLE STANDARD DEVIATION: 0.19580

b.

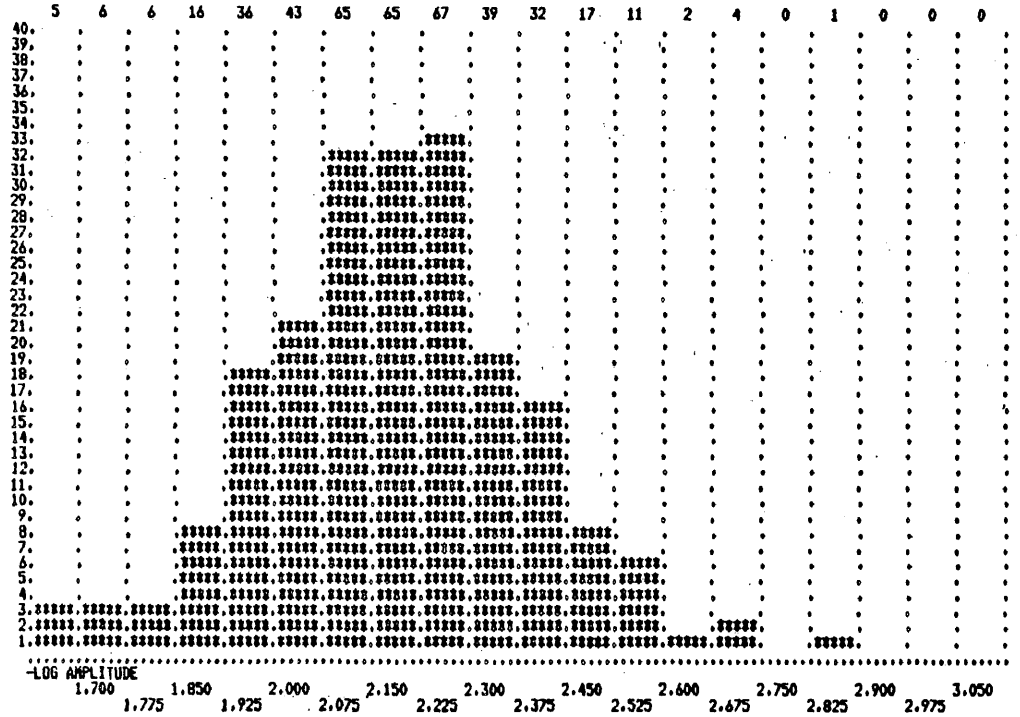

RP11230A 415 GRAINS CLASS FREQUENCIES IN PERCENT

1.20	1.45	1.45	3.86	8.67	10.36	15.66	15.66	16.14	9.40	7.71	4.10	2.65	0.48	0.96	0.00	0.24	0.00	0.00	0.00

from 1.7 to 3.0 which is subdivided into 16 equal class intervals. The number values at the bottom of Figure 14b represent the percentage that each Q_n class interval contributes to the total distribution for each particular sample. This data is generated for use in the Q-mode factor analysis so that sample to sample comparisons of grain-shape distributions can be made.

Representation of Quartz Grain-Shape Data in Histogram Form

Table VI lists thirty selected quartz grain-shape samples, depicted in Figures 15 through 17, which best illustrate the trend gradients of the distribution of Fourier harmonic amplitudes for the 18th ... 21st harmonics within the three hydrographic zones of the Rappahannock River-Estuary System.

River Zone

Figure 15 shows the distribution of Fourier harmonic amplitudes (Q_n) for ten selected sand samples which tend to best illustrate the distribution trends of Q_n within the river zone (from Fredericksburg to Port Royal). The general trend of quartz sand shapes within the river zone show Q_n sample means skewed towards lower Q_n values such as indicated by samples RP010, RP062, RP089, RP093, RP101, RP070 and RP076. The average Q_n mean of all 38 analyzed channel-bar-sands from the river zone is 2.25. The corresponding range of standard deviations for the thirty-eight samples is relatively narrow from 0.154 to 0.185 with an average standard deviation of 0.175. The narrow range of standard deviation along with a consistency of the distribution of Q_n values and Q_n means for these samples indicate that quartz sand particle shape distributions within the river zone are generally composed of

TABLE VI

LIST OF SELECTED QUARTZ PARTICLE-SHAPE HISTOGRAMS IN FIGURES 15-17, WHICH REPRESENT TRENDS IN THE DISTRIBUTION OF THE FOURIER HARMONIC AMPLITUDES FOR THE 18th...21st HARMONICS IN THE RAPPAHANNOCK RIVER-ESTUARY SYSTEM

SAMPLE	STATION	MEAN	STD. DEV.	LOCATION
		RIVER ZONE		
RP010	RK-01	2.26	.177	Fredericksburg Bar-South
RP062	RK-27	2.18	.169	Smithfield Bar-Channel
RP076	RK-23	2.26	.172	Moss Neck Bar-Channel
RP084	RK-21	2.23	.163	Morlean Reach-Channel
RP089	RK-20	2.28	.192	Hop Yard Bar-Channel
RP093	RK-19	2.24	.172	Lagrange Turn-Channel
RP098	RK-17	2.25	.204	Mount Bar-Channel
RP033	RK-07	2.31	.196	Rock Creek Turn-Channel
RP034	RK-07	2.37	.165	Rock Creek Turn-Bluff
RP101	RK-16	2.24	.184	D.R. from Cleve-Channel
		RIVER-ESTUARY TRANSITION ZONE		
RP036	RK-08	2.20	.171	Port Royal-Channel
RP112	RK-30	2.18	.195	Portobago Bay-Channel
RP115	RK-31	2.42	.188	Devils Elbow-South
RP042	RK-10	2.39	.185	Horse Head Point-Channel
RP-117	-	2.45	.163	Horse Head Point-Bluff
RP-142	GRAB 110	2.29	.185	Leedstown-Channel
RP-120	RK-33	2.30	.211	Smith Mount Lndg.-North
RP-123	-	2.46	.177	Fones Cliffs-Bluff Beach
RP-146	B.C. R-8	2.29	.174	Mulberry Point-Channel
RP-147	GRAB 107	2.30	.198	Tappahannock-Channel

TABLE VI (Continued)

ESTUARY ZONE

SAMPLE	STATION	MEAN	STD. DEV.	LOCATION
RP-056	RK-14	2.32	.193	Tappahannock-North
RP-058	RK-14	2.35	.204	Tappahannock-South
RP-148	B.C. R-7	2.29	.198	Lowery Point-Channel
RP-134	RK-37	2.30	.197	Wares Wharf-North
RP-150	B.C. R-6	2.27	.208	Neals Point Channel
RP-151	GRAB 105	2.35	.184	Sharps-Channel
RP-139	RIC 38	2.36	.197	Sharps-North
RP-154	B.C. R-8	2.35	.171	Greenvale Creek-Channel
RP-156	B.C. R-3	2.32	.199	Greys Point-Channel
RP-161	B.C. R-1	2.33	.216	Windmill Point-Channel

Figure 15. Grain-shape histograms of ten selected sand samples which are representative of the trends observed in the distribution of Fourier harmonic amplitude values for the river zone.

RIVER ZONE

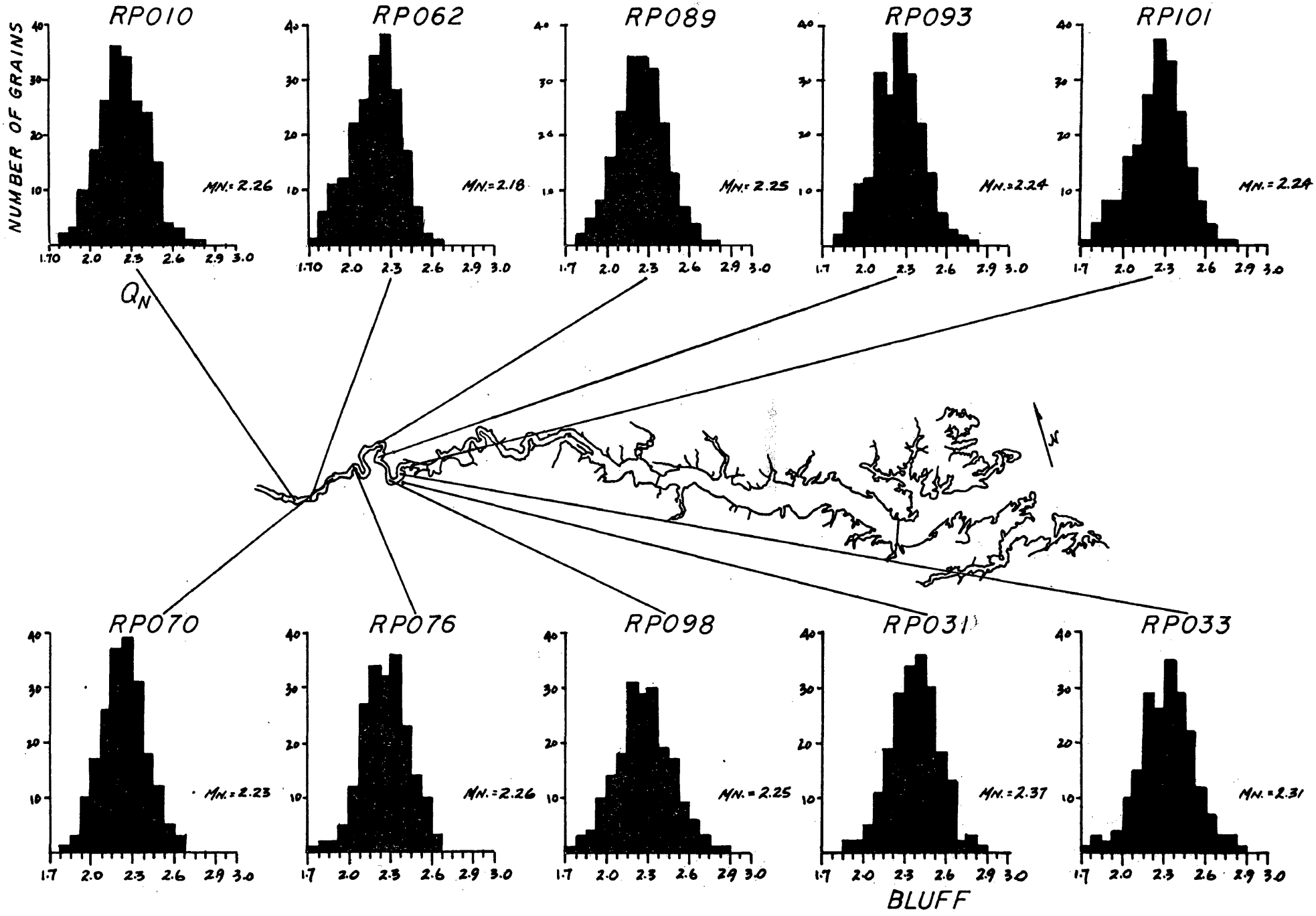
RP010
RP062
RP089
RP093
RP101
NUMBER OF GRAINS
MN.= 2.26
MN.= 2.18
MN.= 2.25
MN.= 2.24
MN.= 2.24
1.70 2.0 2.3 2.6 2.9 3.0
1.7 2.0 2.3 2.6 2.9 3.0
Q_N
RP070
RP076
RP098
RP031
RP033
MN.= 2.23
MN.= 2.26
MN.= 2.25
MN.= 2.37
MN.= 2.31
BLUFF

one sand-shape population, not a mixture of sand-shape populations. The distribution of Q_n values for these samples characterize the quartz grain-shapes in this zone as having very angular or "rough" quartz sand-shape patterns.

An interesting deviation from this trend occurs within the river zone in the proximity of Rock Creek Turn near Port Royal. Sample RP034 is a sand sample taken from a fastland bluff (Tertiary sedimentary material) which directly outcrops along the southwestern flank of the river at Rock Creek Turn. As one can see, the distribution of Q_n values and the Q_n sample mean are skewed towards the higher Q_n values (to the right). This is opposite of the distribution trends observed in the river sands. The sample mean of RP034 is 2.37 which is significantly higher than many of the sand samples occupying the river channel within this zone. The standard deviation of RP034 is narrow at 0.165. This also suggests that this sand shape population is unimodal. The high sample mean and narrow standard deviation statistically indicate that sample RP034 is not from the same population of some of the native sands occupying the river channel upriver from this point. In addition, the distribution of Q_n values for RP034 characterizes the quartz sand particles as having a more rounded or "smooth" shape pattern.

Sample RP033 is located within the river channel directly adjacent to the fastland outcrop at Rock Creek Turn. RP033 has a sample mean of 2.31 which is higher than any river channel sand sample up to this point in the river zone. RP033 standard deviation is 0.196 which is also the highest value of any river sample up to this point. This data suggests that a mixing of the two shape populations may be occurring in the immediate vicinity of Rock Creek Turn.

The question arises: Does the injection of fastland sand-sized sediment into the river's active transport system produce a localized mixing effect with the native sands occupying the river channel along this reach? Sample RP098 (upriver from Rock Creek Turn) and RP033 (downriver from Rock Creek Turn) indicate that this may be apparently so. RP098 (Mount Bar) is located 1 km upriver from Rock Creek Turn and has a sample mean of 2.25. This mean value is similar to the river samples upriver from Rock Creek Turn, yet the standard deviation of this sample is wide at 0.204. This is the largest value of standard deviation of any sand sample up to this point. The distribution of Q_n values in this sample indicates that "rough" sand shape patterns are dominant, yet there does appear to be a smaller contribution of "smooth" shape patterns. Sample RP101 is from the river channel approximately 7 km downstream from Rock Creek Turn. RP101 has a sample mean of 2.24 and a standard deviation of 0.184. The latter is a slightly higher observed value than the preceding river channel samples. Nonetheless, the distribution of Q_n values has reverted back towards the lower Q_n values (skewed left) that again is consistent with river zone sand samples except near Rock Creek Turn. This data suggests that the injection of sand-sized sediment from the bluffs at Rock Creek Turn produces a localized effect upon the distribution of sand-shape characteristics within the river-zone.

River-Estuary Transition Zone

Figure 16 shows the distribution of Fourier harmonic amplitudes (Q_n) for ten selected sand samples which tend to best illustrate the distribution gradients of Q_n values within the river-estuary transition

Figure 16. Grain-shape histograms of ten selected sand samples which are representative of the trends observed in the distribution of Fourier harmonic amplitude values for the river-estuary transition zone.

RIVER-ESTUARY TRANSITION ZONE

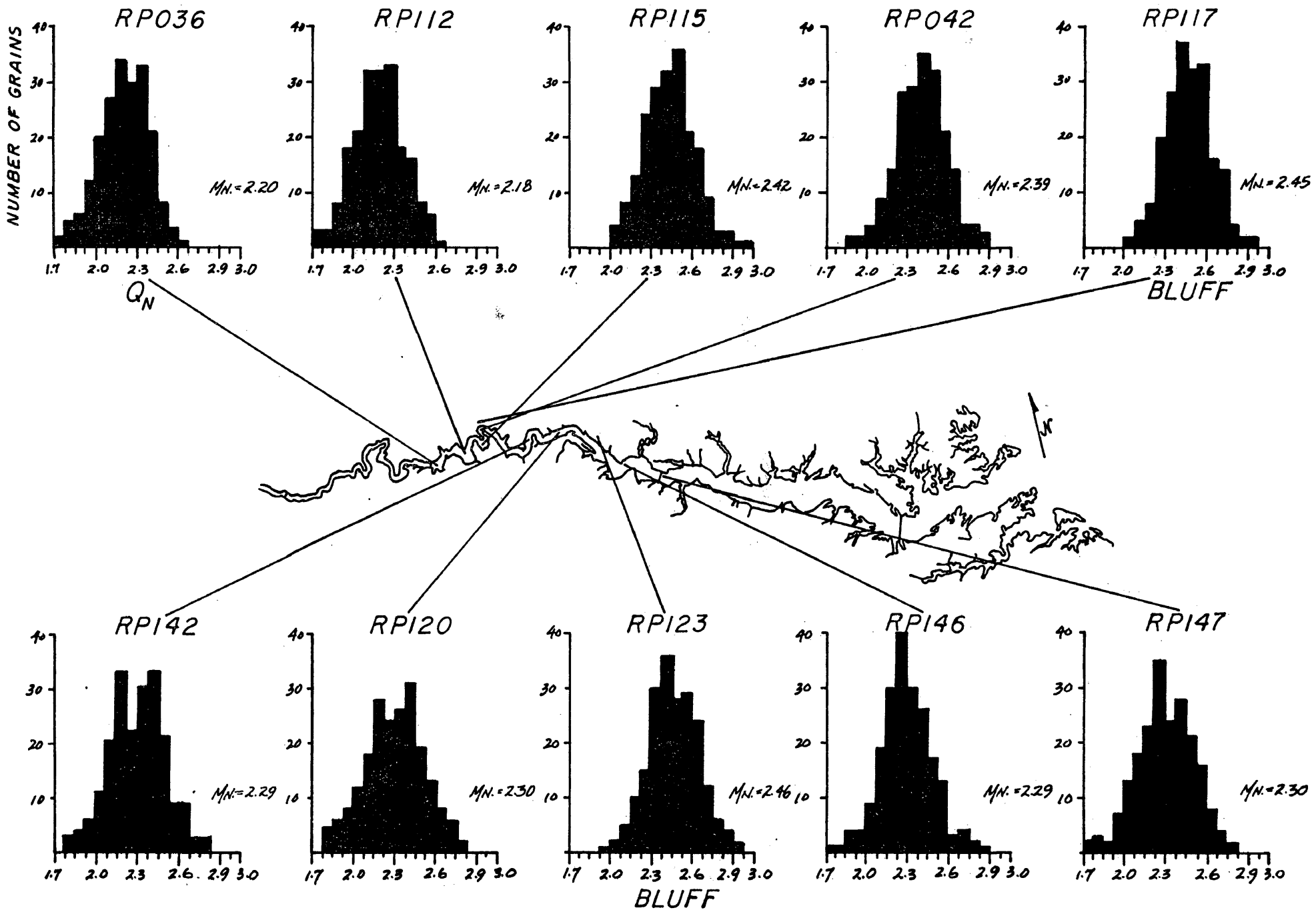

zone (from Port Royal to Tappahannock). The distribution of Q_n values for samples shown in Figure 16 reveals that very interesting trend gradients are evident in the river-estuary transition zone, particularly where fastland sedimentary material outcrops along the northeastern flanks of the river at Horse Head Point and along Fones Cliffs. Samples RP036 (Port Royal Channel) and RP112 (Portobago Bay Channel) display Q_n distributions that are consistent with the sand-shape distributions within the river zone; namely, sample means that are skewed to the lower Q_n values (RP036:2.20; RP112:2.18) which are representative of very angular or "rough" quartz sand particle-shape distributions. As the river approaches the fastland bluffs at Horse Head Point, an interesting trend gradient in the distribution of Q_n values begins to emerge. Sample RP115 is a sand sample taken approximately 1.5 km upriver from Horse Head Point. RP115 sample mean is 2.42, and it is readily apparent that the distribution of Q_n values are now skewed to the right. A possible explanation for this drastic shift in the sample mean to higher Q_n values may lie in the sand-shape characteristics of the Tertiary bluff sedimentary material being injected into the river's active transport system at Horse Head Point. RP117 is a sand sample taken from the bluff sedimentary material at Horse Head Point. The sample mean of RP117 is 2.45, the highest Q_n sample mean yet encountered within the river-estuary system. In addition, the standard deviation of sample RP117 is narrow at 0.163. This data indicates that the quartz sand particle shape population sampled from the bluffs at Horse Head Point is also unimodal and statistically non-similar to the native quartz sand-shape population occupying the river channel up to this point. Sample RP042 was taken directly in front of the Horse Head

Point bluffs from within the river channel. RP042 sample mean has a lower sample mean (2.39) and a wider standard deviation (0.185) in comparison to RP117. The wider distribution of Q_n values in RP042 may indicate a mixing of the two quartz sand shape populations within the river's active transport system. The aforementioned mixing hypothesis is further substantiated by the distribution of Q_n values of samples RP142 and RP120 which were sampled from the river channel (RP142) and northern shoal (RP120) approximately 13 km and 20 km, respectively, downriver from Horse Head Point. Both RP142 and RP120 have sample means around 2.30 which is within a range that is intermediate of the sample means of both the river sand-shape population and the fastland bluff sand-shape population. Moreover, the standard deviations of samples RP142 and RP120 are markedly wider at 0.185 and 0.211, respectively. RP120 has the widest range of standard deviation of any sample that has been analyzed within the river's active transport system up to this point. If one examines the distribition of Q_n values, there does appear to be some indication of bimodality with peaks occurring at both lower Q_n class intervals and higher Q_n class intervals.

As the river approaches the Fones Cliffs area where, again, fastland sedimentary material outcrops along the northeastern flank of the river, a similar sand-shape gradient analogous to what was encountered at Horse Head Point is evident. Sample RP123 is a sand sample taken from the sedimentary material composing the beach at the foot of the bluff at Fones Cliffs. The distribution of Q_n values for RP123 is closely similar to RP117 from Horse Head Point bluffs. RP123 has a sample mean of 2.46 (RP117:2.45) with a narrow standard

deviation of 0.177 (RP117:0.163) which again indicates that the sand-shape population comprising RP123 is statistically non-similar to the native sand-shape population occupying the upper reaches of the Rappahannock River. The mixing hypothesis is again substantiated by the distribution of Q_n values of samples RP146 (Mulberry Point) and RP147 (Tappahannock) which are sand samples taken from the river channel approximately 9 km and 17 km, respectively, downriver from Fones Cliffs. Again, similar to the sand-shape distributions encountered downriver from Horse Head Point, RP146 and RP147 have sample means around 2.30. These mean values are intermediate of the characteristic sample means of both sand-shape populations. In addition, the standard deviations of RP146 and RP147 are large at 0.174 and 0.198 respectively, and there also appears to be some indication of bimodality. Thus, the aforementioned distribution trend gradients within the river-estuary transition zone supplies quantitative evidence that the two identifiable sand-shape populations, derived from non-similar sand provenances landward of the estuary proper, are possibly being mixed together within the active transport system of the river-estuary transition zone. Consequently, it would follow that any sand-sized sediment transported downriver from these bluffed reaches would be comprised of a mixture of the two non-similar sand-shape populations; namely, the Piedmont-derived river sands and the fastland bluff sands, presuming that selective size of shape sorting is not an active process along these reaches.

Estuary Zone

Figure 17 shows the distribution of Fourier harmonic amplitudes (Q_n) for ten selected sand samples which tend to best illustrate the

Figure 17. Grain-shape histograms of ten selected sand samples which are representative of the trends observed in the distribution of Fourier harmonic amplitude values for the estuary zone.

ESTUARY ZONE

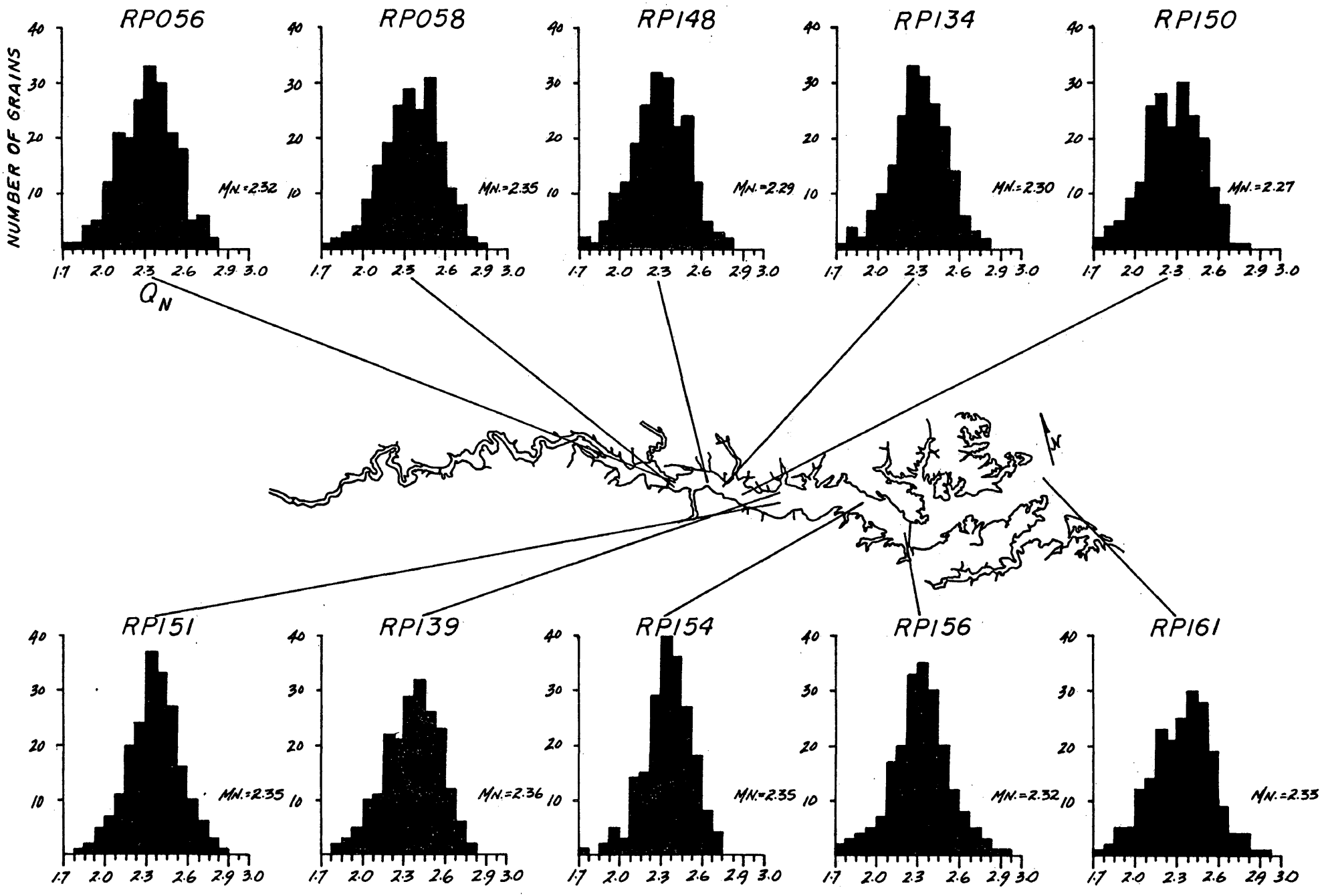

distribution gradients of Q_n values for the sand-shape populations within the estuary zone (from Tappahannock to Windmill Point). Sand-shape samples from within the estuary zone presents intriguing evidence which tends to support the mixing hypothesis of the two non-similar sand-shape populations; namely, the river zone sand-shape population and the fastland bluff sand-shape population.

At the head of the estuary (Tappahannock), a cross-sectional array of sand-shape samples RP147 (Figure 16), RP056 and RP058 support the mixing hypothesis. Sample RP056 is taken from the northeastern shoal flanking the estuary channel. RP056 has a sample mean of 2.32 and a standard deviation of 0.195. Sample RP058 is taken from the southwestern shoal flanking the estuary channel. RP058 has a sample mean of 2.35 and a standard deviation of 0.204. This again, indicates a wide distribution of Q_n values for this sand sample. Sample RP147 is taken from the estuary's central channel. RP147 has a sample mean of 2.30. This is somewhat lower than the samples adjacent to it on the flanking shoals, yet the standard deviation still remained large at 0.198. There is a similarity between the three samples at Tappahannock in that there appears to be a non-normal distribution of Q_n values over the range of class intervals. This trend might suggest that the shape populations along this cross-section are polymodal, consisting of a mixture of the two sand-shape populations at the head of the estuary not only within the estuary channel but on the flanking shoals as well.

Samples RP148 (Lowery Point) and RP150 (Neals Point) are located within the estuary's central channel approximately 5.5 km and 13 km respectively, down-estuary from Tappahannock. RP148 and RP150 have

sample means of 2.30 which are similar to the sand-shape distributions of samples within the channel of the river-estuary transition zone and at the head of the estuary at Tappahannock.

The range of standard deviations for RP148 and RP150 is large at 0.198 and 0.208 respectively. Sample RP134 is located on the north-eastern shoal at Wares Wharf, approximately 10 km downestuary from Tappahannock. The distribution of Q_n values of RP134 is also similar to that of the estuary channel with a sample mean of 2.30 and a standard deviation of 0.197. Thus, it appears evident that there is a consistency of sand-shape distributions within the channel as well as on the flanking shoals from the river-estuary transition zone down through the middle estuary. In addition, this consistency of sand-shape distribution, namely sample means around 2.30, large standard deviations (0.198-0.208) and non-normal distributions are supportive of the sand-shape mixing hypothesis of the two extreme shape populations (i.e., bluff sands and river sands).

In the middle and lower portions of the estuary, the samples remain distributed over a wide range of Q_n class intervals, although the Q_n sample means have shifted to slightly higher Q_n values. This may indicate that lateral erosion of the fastland banks flanking the middle and lower portions of the estuary are influencing the distribution of sand-shape characteristics of the sand-sized sediment within the estuary's active transport system. Evidence supporting this speculation is supplied by samples RP151 and RP139. These samples are located near Sharps (approximately 20 km downestuary from Tappahannock) in the estuary's central channel and northern shoal, respectively. RP151 has a Q_n sample mean of 2.35 and a standard

deviation of 0.184. RP151 sample mean is slightly higher than the previous samples located within the estuary's central channel up to this point, although the distribution appears to be nearly normal. In comparison, sample RP139 located adjacent to RP151 on the northeastern shoal has a higher sample mean of 2.36, a larger standard deviation of 0.197 and the distribution of Q_n values appears to be disproportionate about the mean. Since fastland bank erosion along this section of the estuary has been estimated at approximately .6 to 1.0 m/yr (Byrne and Anderson, 1976), it may be influencing the sand-shape distribution of the native sands occupying these reaches of the estuary, particularly along the shoaling areas which directly flank the fastland banks.

Sample RP154 is located within the estuary channel at Greenvale Creek (approximately 23 km downestuary from Tappahannock). RP154 has a sample mean of 2.35 and a standard deviation of 0.171. Further downestuary, sample RP156 located within the lower estuary's channel at Greys Point (approximately 24.5 km downestuary from Tappahannock, near Urbanna) has a sample mean of 2.32. RP156 sample mean is slightly lower than the previous channel sample (RP154).

The distribution of Q_n values of RP156 again suggests that this sample is composed of a mixture of the two extreme sand-shape populations. This trend appears to be consistent with other channel sand samples from the head of the estuary to the lower portions of the estuary. Sample RP161 is located outside the mouth of the Rappahannock River near Windmill Point. RP161 has a sample mean of 2.33 which again is a value that is intermediate of the two extreme sand-shape populations identified within the river and river-estuary transition zone, yet it has a standard deviation of 0.216 which is

larger than any sand sample analyzed from within the Rappahannock River-Estuary System. This data may again suggest a mixing of sand-shape populations which may be derived from either the river-estuary of the Chesapeake Bay or both.

The quantitative data presented by the distributions of Q_n values throughout the river-estuary system suggests that interesting trend gradients in the sand-shape populations are readily apparent and that two statistically non-similar sand-shape populations, that are potential sources of sand-sized sediment to the Rappahannock Estuary, clearly exist. It is further intended that Q-mode factor analysis will be able to distinguish the two non-similar shape populations and give some insight as to the relative contribution of these two distinct populations to the distribution of sand-sized sediment within the Rappahannock River-Estuary System. Q-mode factor methods and its applications in relation to this research project will be discussed in detail in a forthcoming section.

Cumulative Percent Distributions of Quartz Grain-Shape Samples Over the Range of Q_n Class Intervals

The grain-shape data generated in histogram form may also be presented in the form of cumulative percent distributions of the Q_n class intervals under the assumption that the distribution of Q_n values tends to be normally distributed over the range of the sixteen Q_n class intervals. This form of graphical presentation will allow many sand-shape samples from the Rappahannock River-Estuary System to be plotted in relation to each other on the same graph so that sample to sample comparisons can be made. In addition, this type of graphical representation would make the trend gradients of the distribution of Q_n values

Figure 18. Cumulative percent distributions of the sixteen class intervals of the Fourier harmonic amplitudes for the most extreme sand-shape samples: RP062, Smithfield Bar-River Channel; RP116, Fastland Bluff Sample from Horse Head Point.

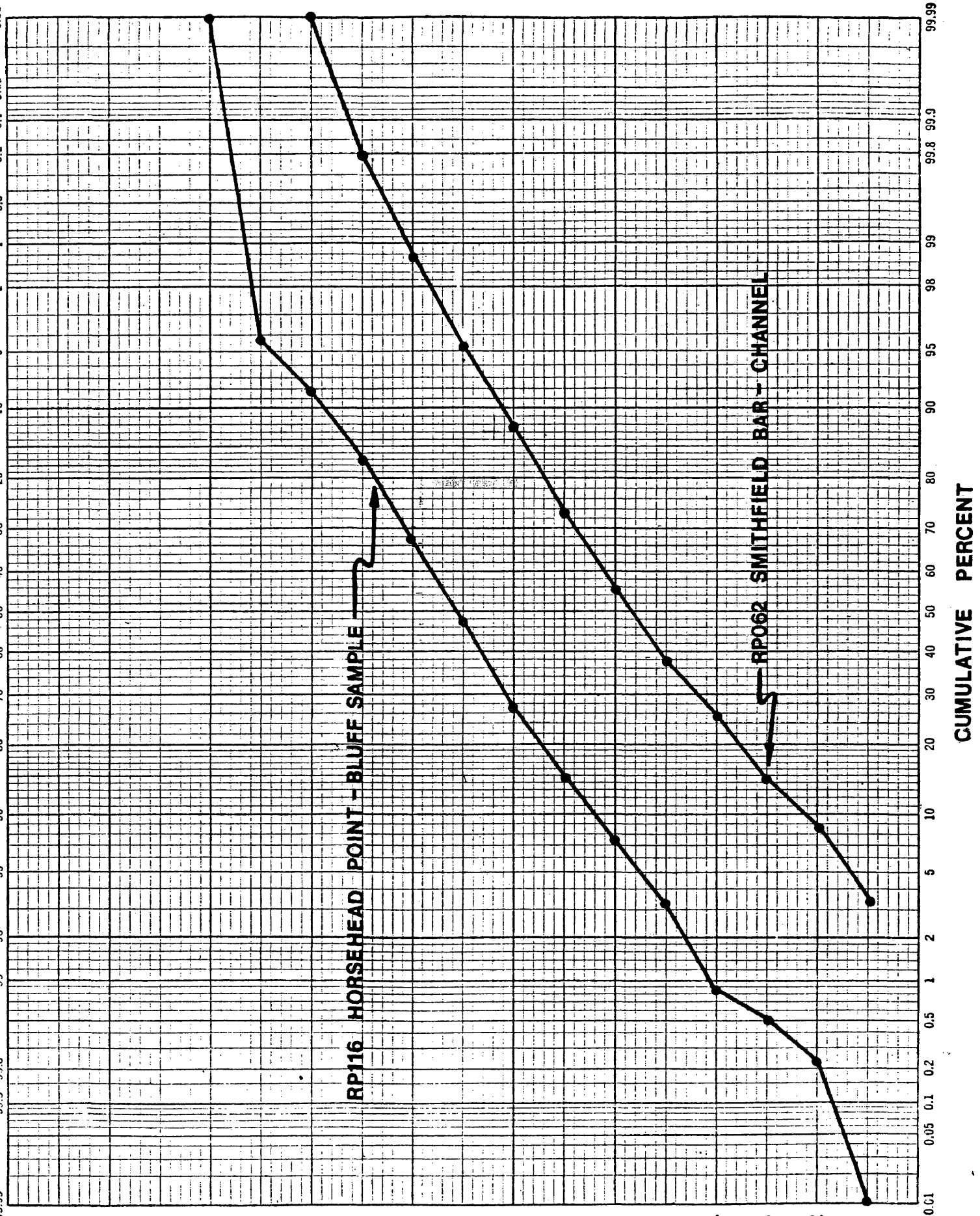
RP116 HORSEHEAD POINT - BLUFF SAMPLE
RP062 SMITHFIELD BAR - CHANNEL
- LOG AMPLITUDE CLASS INTERVALS
CUMULATIVE PERCENT

Figure 19. Trends observed in the cumulative percent distributions over the range of sixteen class intervals of the Fourier harmonic amplitudes for the river zone, river-estuary transition zone and estuary zone.

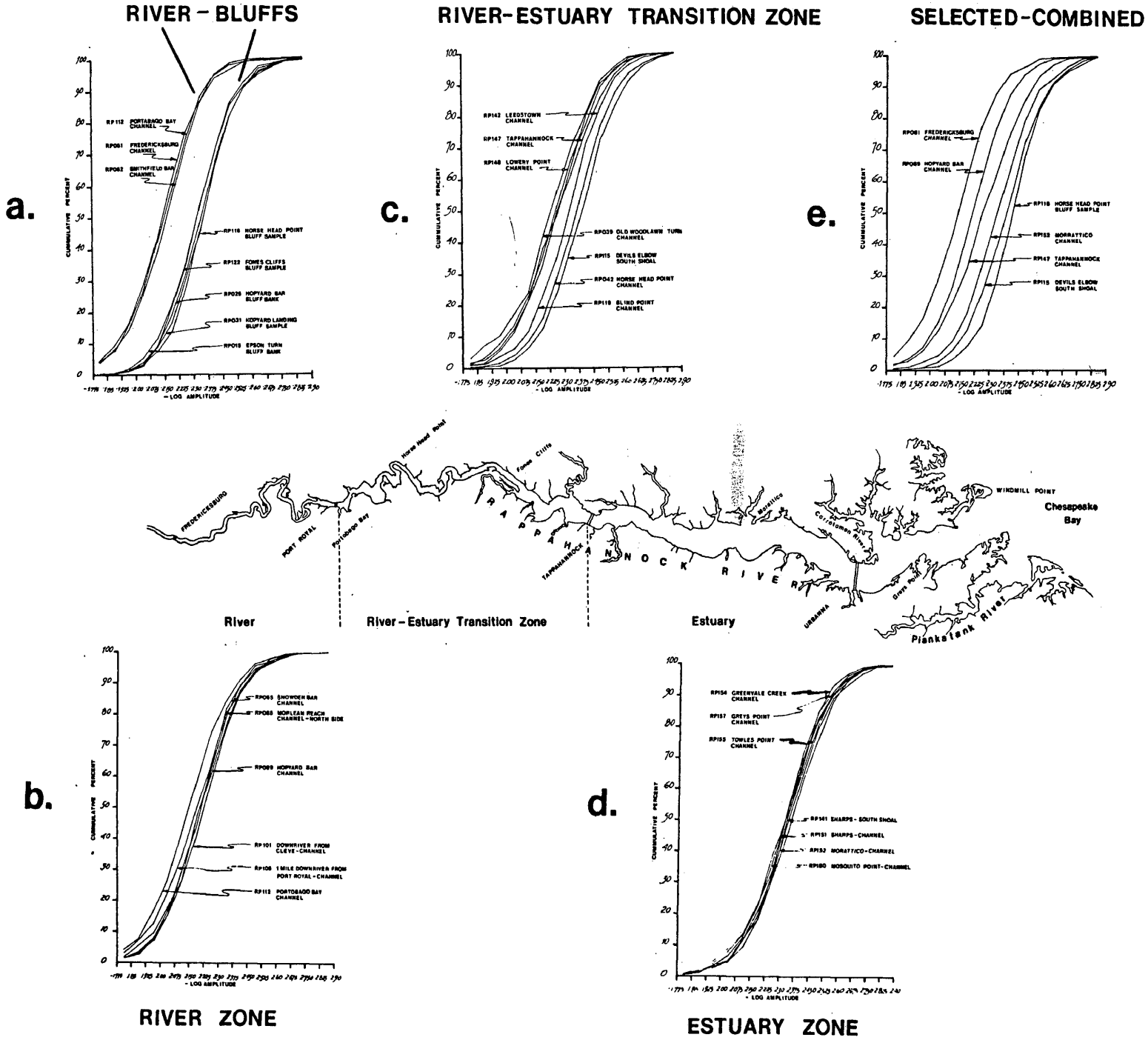
RIVER – BLUFFS
RIVER-ESTUARY TRANSITION ZONE
SELECTED-COMBINED
a.
c.
e.
b.
d.
CUMULATIVE PERCENT
LOG AMPLITUDE
RP112 PORTOBACCO BAY CHANNEL
RP081 FREDERICKSBURG CHANNEL
RP082 SMITHFIELD BAR CHANNEL
RP116 HORSE HEAD POINT BLUFF SAMPLE
RP122 FOWES CLIFFS BLUFF SAMPLE
RP029 HOPYARD BAR BLUFF BANK
RP031 HOPYARD LANDING BLUFF SAMPLE
RP013 EPSON TURN BLUFF BANK
RP142 LEEDSTOWN CHANNEL
RP147 TAPPAHANNOCK CHANNEL
RP148 LOWERY POINT CHANNEL
RP039 OLD WOODLAWN TURN CHANNEL
RP115 DEVILS ELBOW SOUTH SHOAL
RP042 HORSE HEAD POINT CHANNEL
RP118 BLIND POINT CHANNEL
RP081 FREDERICKSBURG CHANNEL
RP089 HOPYARD BAR CHANNEL
RP116 HORSE HEAD POINT BLUFF SAMPLE
RP152 MORRATTICO CHANNEL
RP147 TAPPAHANNOCK CHANNEL
RP115 DEVILS ELBOW SOUTH SHOAL
FREDERICKSBURG
PORT ROYAL
Portobago Bay
Horse Head Point
Fowes Cliffs
TAPPAHANNOCK
Morattico
Corrotoman River
WINDMILL POINT
Chesapeake Bay
Grays Point
URBANNA
Piankatank River
River
River-Estuary Transition Zone
Estuary
RP085 SNOWDEN BAR CHANNEL
RP088 NORLEAN REACH CHANNEL-NORTH SIDE
RP089 HOPYARD BAR CHANNEL
RP101 DOWNRIVER FROM CLEVE-CHANNEL
RP106 1 MILE DOWNRIVER FROM PORT ROYAL-CHANNEL
RP112 PORTOBACCO BAY CHANNEL
RP154 GREENVALE CREEK CHANNEL
RP157 GREYS POINT CHANNEL
RP155 TOWLES POINT CHANNEL
RP141 SHARPS-SOUTH SHOAL
RP151 SHARPS-CHANNEL
RP152 MORATTICO-CHANNEL
RP160 MOSQUITO POINT-CHANNEL
RIVER ZONE
ESTUARY ZONE

explained within the previous section more visually evident, particularly within each of the three hydrographical zones.

In order to determine whether the distribution of Q_n values of sand samples from within the Rappahannock River-Estuary System are normally distributed, the two most extreme sand-shape sample distributions, namely, RP062 (river sands) and RP116 (fastland bluff sands) are plotted upon statistical probability paper. If the two extreme samples plot in a nearly linear fashion, it is a good indication that the distribution of Q_n values of these samples tend to be normally distributed.

Figure 18 shows the cumulative percent of Q_n values versus the sixteen Q_n class intervals for samples RP062 and RP116. From the nearly linear plots of these samples, it appears evident that the distribution of Q_n values does indeed tend to be normally distributed. Therefore, presenting the sand-shape data in terms of its cumulative percent distributions would in fact be a valid representation of the quartz grain-shape data.

Figure 19 illustrates the trends in the cumulative percent distributions over the range of sixteen Q_n class intervals for the river zone, river-estuary transition zone, estuary zone, river-bluff comparison and selected sand-samples from each zone combined.

Figure 19a shows the clear differences between the cumulative percent distributions of the river sand-shape characteristics and the fastland bluff sand-shape characteristics. Based on the distribution of sand-shape characteristics of both the river and fastland bluff sands, it is readily apparent that sand samples from the river are statistically non-similar to the sand samples from the bluffs. This fact is also indicated by the histogram data. In addition, it is

noteworthy to state that sand samples from both populations are consistently distributed within a narrow range of Q_n values.

Figure 19b shows the cumulative percent distributions of sand samples within the river zone. It is apparent that the distributions of Q_n values for these samples remains consistent with the histogram data in that the river sand-shape population is characterized by higher percentages of Q_n values towards the lower Q_n class intervals. It is interesting to note that sample RP101 (downriver from Cleve Channel) is skewed towards higher Q_n class intervals. This sample is in close proximity of Rock Creek Turn where fastland bluff sediments directly outcrop along the southwestern flank of the river. The cumulative percent distribution of RP101 suggests that this sample may be influenced by the injection of more rounded sand shapes from the fastland bluff, upriver at Rock Creek Turn, into the river's active transport system. In addition, it displays how the shape analysis technique can objectively indicate subtle differences in the distribution of shape patterns within a particular sample group.

Figure 19c shows the cumulative percent distributions of sand samples within the river-estuary transition zone. The most noticeable trend within the cumulative percent distributions of these sand samples is the wide range of distribution among the Q_n class intervals depending on the location of a particular sample in relation to the eroding fastland bluffs at Horse Head Point and Fones Cliffs. RP039 (Old Woodlawn Turn) is located upriver from Horse Head Point. This sample shows higher percentages of Q_n values towards the lower Q_n class intervals which is consistent with the river sand-shape population. In comparison, cumulative percent distributions of

sand samples at Horse Head Point in both the river channel (RP042) and on the southern shoal (RP115), show a marked shift of larger percentages in the higher range of Q_n class intervals. Cumulative percent distributions of sand sample locations downriver from Horse Head Point, show a gradual shifting towards the lower Q_n class intervals within increasing distance downriver from Horse Head Point (RP119-Blind Point Channel; RP142-Leedstown Channel). This data suggests that a mixing of the two sand-shape populations is occurring. A similar situation occurs downriver along Fones Cliffs. Bluff sand-shape characteristics (cumulative percent distributions towards higher Q_n values) dominates along this reach. Further downriver from Fones Cliffs, the cumulative percent distributions again begin to shift back towards lower Q_n values characteristic of the river sand-shape patterns (RP147-Tappahannock, RP148-Lowery Point). Therefore, it is apparent that the cumulative percent distributions in the river-estuary transition zone indicate that the sand-shape characteristics of sand samples within this zone are composed of a mixture of the two shape populations (i.e., river and bluff sands). The relative amounts of each sand-shape population contained within these sand samples seems to be related to the sample's location, either upriver or downriver, from the fastland bluffs at Horse Head Point and Fones Cliffs.

Figure 19d shows the cumulative percent distributions of sand samples within the estuary zone. The interesting feature of this graph is that the distribution of cumulative percent data is consistent through the estuary in that the sand-shape populations within this zone are distributed over a wide range of Q_n values, yet they do not show a wide range of deviation in relation to each other as

did the sand samples from the river-estuary transition zone. The cumulative percent distribution of the estuary's sand samples suggests, as does the histogram data, that the sand-shape distributions within the estuary are composed of a mixture of the two sand-shape populations (i.e., river and bluff sands).

Figure 19e shows the cumulative percent distribution of selected-combined sand samples representative of each sample group which illustrates the trends in sand-shape characteristics throughout the river-estuary system.

VII. INTRODUCTION TO FACTOR ANALYSIS

Factor analysis is one of the most widely used multivariate statistical procedures. Its purpose is to reduce the overall complexity often found in multivariate data of which little insight into the underlying data structure is known. Factor analysis was first developed by psychologists in the 1930's and 1940's. Its original purpose was to extract fundamental measures of intellect from scores on intelligence tests and other tests of mental ability. Since then, factor analysis methods have attained wide-spread application in many disciplines that deal with different forms of multivariate data.

Factor analysis methods have been employed in various geological investigations. Klovan (1966) employed the use of factor analysis in determining depositional environments from grain-size distributions. Sayles (1965) used factor analysis for determining relationships between heavy mineral distributions in relation to coastal sedimentary environments along the coasts of Southern California. Oh (1980) employed factor analysis methods in grain-size analysis in the Eyre Delta. Results of this analysis were compared with the Gironde Estuary and the Salie Beach (France). More recently, Bopp and Biggs (1981) employed factor analysis to partition the variability of environmentally active metals in Delaware Bay sediments.

Factor analysis is a term used to describe a collection of numerical methods which are capable of reducing the overall

complexity of structured multivariate data by analyzing interrelationships within a set of variables or objects. The underlying object of factor analysis is to construct a few hypothetical variables or objects called factors, that contain the essential information in a larger set of original observations. As a result, a small number of factors will account for the same amount of information as the larger set of original observations. Therefore, factor analysis can be viewed as a multivariate method of data reduction.

Factor analysis is concerned with interpreting the structure of the variance-covariance matrix (R-mode) or the association matrix (Q-mode) obtained from a collection of multivariate observations. Initially, a data matrix, X , composed of a collection of multivariate observations is represented by N rows and p columns of data. The N rows represent objects and the p columns represent observations or variables measured on each object.

An example of such a matrix is shown in Table VII. These data illustrate how an object or a variable can be represented as a vector quantity (a directed line segment) defined as a matrix with only one row or column. Figure 20 is constructed using the first and second rows of Table VII. The diagram describes the eight objects (rock specimens) in terms of their composition based on two variables (the amount of quartz and hornblende). The variables form orthogonal coordinate axes and each object vector is said to be contained within the defined "variable space". The data from Table VII will also permit a three-dimensional variable space to be constructed in which each object vector can be plotted with respect to these mutually orthogonal variable axes. Although

Table VII. An example of a geological data matrix (from Jöreskog, et al., 1976).

Figure 20. Representation of the data in Table VII in vector (directed line segment) form.

TABLE VII. EXAMPLE OF A GEOLOGICAL DATA MATRIX (FROM JORESKOG, et al., 1976.)

ROCK SPECIMEN #	QUARTZ	HORNBLENDE
1	4.51	2.66
2	6.07	0.58
3	6.42	1.32
4	4.46	2.16
5	8.92	2.54
6	7.60	2.39
7	5.29	1.69
8	4.73	2.65

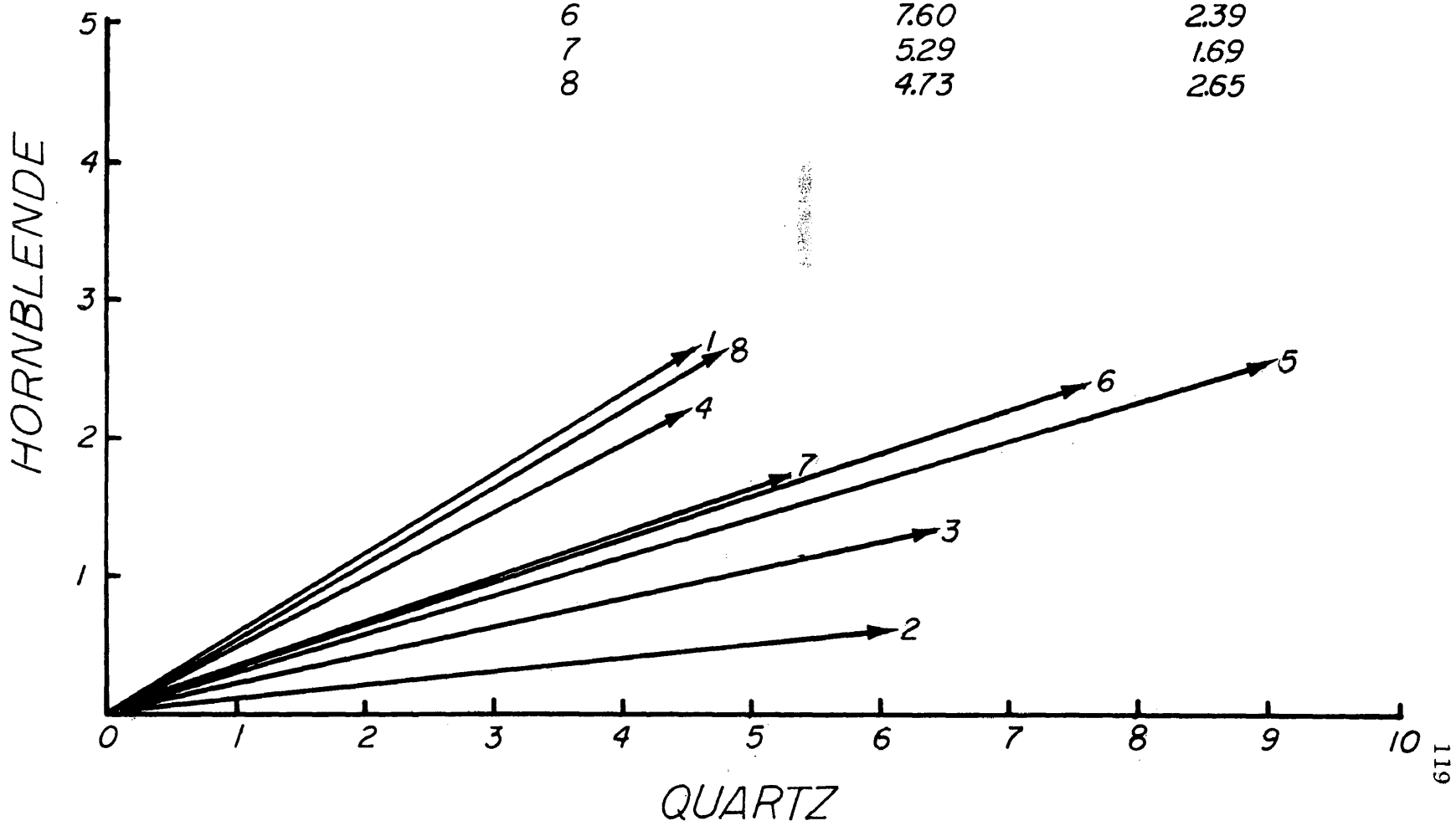

variable space of dimension greater than three cannot be visualized in a graphical sense, it is nevertheless possible to apply factor analysis to multivariate data of virtually any dimensional order using matrix algebra.

At this point, it should be mentioned that one can also represent the collection of variable data in what is referred to as "object space" and the purpose of the analysis would then be to examine the relationship between variables in this space. The latter task is undertaken through development of a matrix of variable correlations and forms the basis of R-mode factor analysis. This type of factor analysis has little application in studies which creates excess turbulence; that is compositional aspects (proportional mixing) of multivariate object data and will not be discussed here. The reader is referred to Davis (1973) for a description of R-mode methods.

Q-Mode Factor Methods

Q-mode analyses are designed to portray interrelationships between objects. The mainstay of Q-mode factor analysis lies with the definition of inter-object similarity. In studies, such as the present one, involving compositional aspects (proportional mixing) of multivariate data, it is the proportions of the constituents that are of major importance.

In order to construct a "similarity" or association matrix containing the degree of similarity between all possible pairs of N objects, a similarity coefficient must first be determined. This similarity coefficient defines the degree of similarity between two objects so that they may be evaluated in relation to the proportions of their constituents. Thus, for any two objects, n and m (row

vectors of the data matrix), the coefficient of proportional similarity, "cosine theta" computes the cosine of the angle between the two row vectors as situated in p dimensional space. The value of cos Θ ranges from +1.0 (for two collinear vectors) to 0 for two vectors 90^{o} apart.

A geometrical example of object "similarity" as measured by the cos Θ value is shown in Figure 21. Note that the objects 1 and 3 have constituents in the proportion of 2:1. The cos Θ_{13} value is equal to +1.0 (collinearity, hence, absolute similarity). In contrast, the cos Θ_{12} value determined by the proportions of the contained constituents is equal to 0.838 (non-collinearity, hence, non-similarity). It would then follow that if two object vectors were 90^{o} apart, the cos Θ value would be equal to 0; hence, absolute dissimilarity. In dealing with a set of N objects, cos Θ must be computed for each possible pair of objects. Thus, allowing the coefficients to be arranged in an N x N matrix of associations, or what is then termed the association matrix. When N is large, this matrix will contain many elements. The association matrix is then ranked by eigenanalysis. This will provide a means of adequately describing the objects in terms of fewer basic dimensions than original variables. For further detailed information on the practice and procedures of Q-mode factor analysis, the reader is referred to Jöreskog, Klovan and Reyment (1976).

Figure 21. A geometrical example of object "similarity" and "dissimilarity" as measured by the cos Θ value (from Jöreskog, et al., 1976).

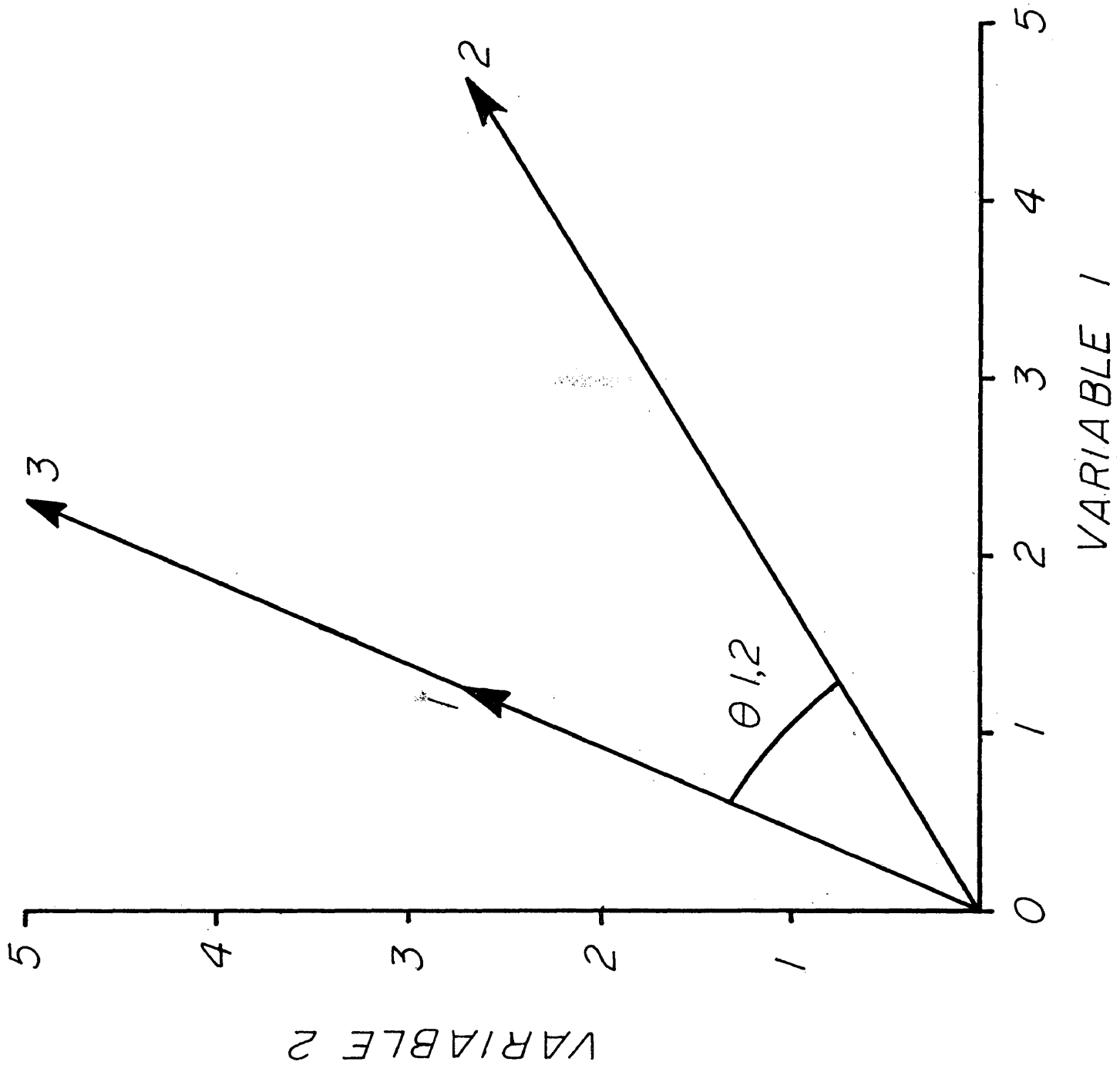
VARIABLE 2
VARIABLE 1
θ 1,2
1
2
3
0
1
2
3
4
5

VIII. Q-MODE FACTOR ANALYSIS RESULTS

Imbrie (1963) was one of the first geologists who expanded Q-mode factor analysis methods and published computer programs to show how factor analysis could be applied to common geological problems such as delineating lithofacies. Subsequently, these methods have been further expanded and successfully used in various sedimentalogical problems. Klovan and Miesch (1976) later developed the computer program, CABFAC, for Q-mode factor analysis of geologic data having constant row-sums. The latter authors have also developed another program, Q-MODEL, which reads the output file from CABFAC and can be used to develop a variety of Q-mode models. The underlying theme of these models is to serve to reproduce estimates of the original data rather than of the data in row-normalized form. It should also be mentioned that the CABFAC and Q-MODEL algorithms represent a satisfactory solution to analysis of empirical data considered to be mixtures of a finite number of end-members; if "pure" end-members are found within the data set; or, if the composition of "true" end-members are known a priori. More recently, Full, et al., 1981 have developed an algorithm termed EXTENDED Q-MODEL that defines feasible end-members which are "closest" to the data envelope. Thus, where neither of the previously aforementioned conditions are satisfied, the composition of "external" end-members can be deduced from the structure of the data.

In this investigation, the CABFAC Program of Klovan and Miesch (1976) is employed in order to gain further insight into the structure of the normalized data matrix. This algorithm determined that seven eigenvalues, derived from this matrix, can describe 99.54% of the total grain-shape variance of the ninety-four sand-shape samples from the Rappahannock. The normalized data matrix is constructed from the factor loadings matrix (94 sand-shape samples times 7 principal factors (eigenvalues) multiplied by the factor scores matrix (16 Q_n class intervals times 7 principle factors).

An oblique factor solution, one of three methods that the Q-MODEL algorithm uses to define end-members, is employed in the output file from CABFAC. An oblique solution which, by searching either the rotated factor space or variable space, locates extreme points or the most divergent samples as end-members. These points, representing real samples, become reference axes. Thus, the relative distances of all sample points about these references can be interpreted as mixing proportions.

The oblique factor rotation determined that three eigenvalues are sufficient to explain 98% of the variance in the data matrix and that these "significant" eigenvalues represent three compositionally distinct end-members. These end-members, or mutually orthogonal factors, are sufficient enough to encompass 98.5% of the total grain-shape variance. Factor I accounts for 50.85% of the total variance. Factor II accounts for 47.05% of the total variance. Factor III accounts for 0.58% of the total variance. Thus, the total grain-shape variance among the ninety-four sand shape samples is essentially described by a two factor (end-member) system; namely, factor I and

factor II. Although end-member (factor) III accounts for 0.58% of the total variance, this factor is included so as to increase the dimensionality of the object space. This enables a suitable "shape window" to be constructed which would tend to more accurately explain the distribution of object vectors within the rotated factor space. Therefore, each of the ninety-four object vectors (sand-shape samples) can now be described in terms of the three mutually orthogonal end-members.

Figure 22 shows the construction of a three factor plot of the grain-shape compositional data of the ninety-four sand-shape samples from the Rappahannock River-Estuary System. The object vectors (sand samples) are plotted on a triangular compositional diagram, so that the objects (samples) may be considered as various mixtures of end-members I, II, and III.

The number I normalized factor component is termed the "rough end-member" which is representative of the shape characteristics of the river sand-shape population found within the upper reaches of the Rappahannock River. The number II normalized factor component is termed the "smooth end-member" which is representative of the sand-shape population composing the fastland sedimentary material that outcrops along the flanks of the river at Rock Creek Turn, Horse Head Point and Fones Cliffs. The number III normalized factor component is termed the "intermediate end-member" which is the third mathematically derived end-member whose factor axes ensures that the relationships between all the object vectors are portrayed according to the entire spectrum of their grain-shape distribution. Hence, each object vector (sand sample) is composed of various percentages of the three end-members (factor components).

Figure 22. Construction of a three-factor triangular diagram illustrating the trend gradients observed in the distribution of the ninety-four sand-shape samples among the three end-members determined from Q-mode factor analysis.

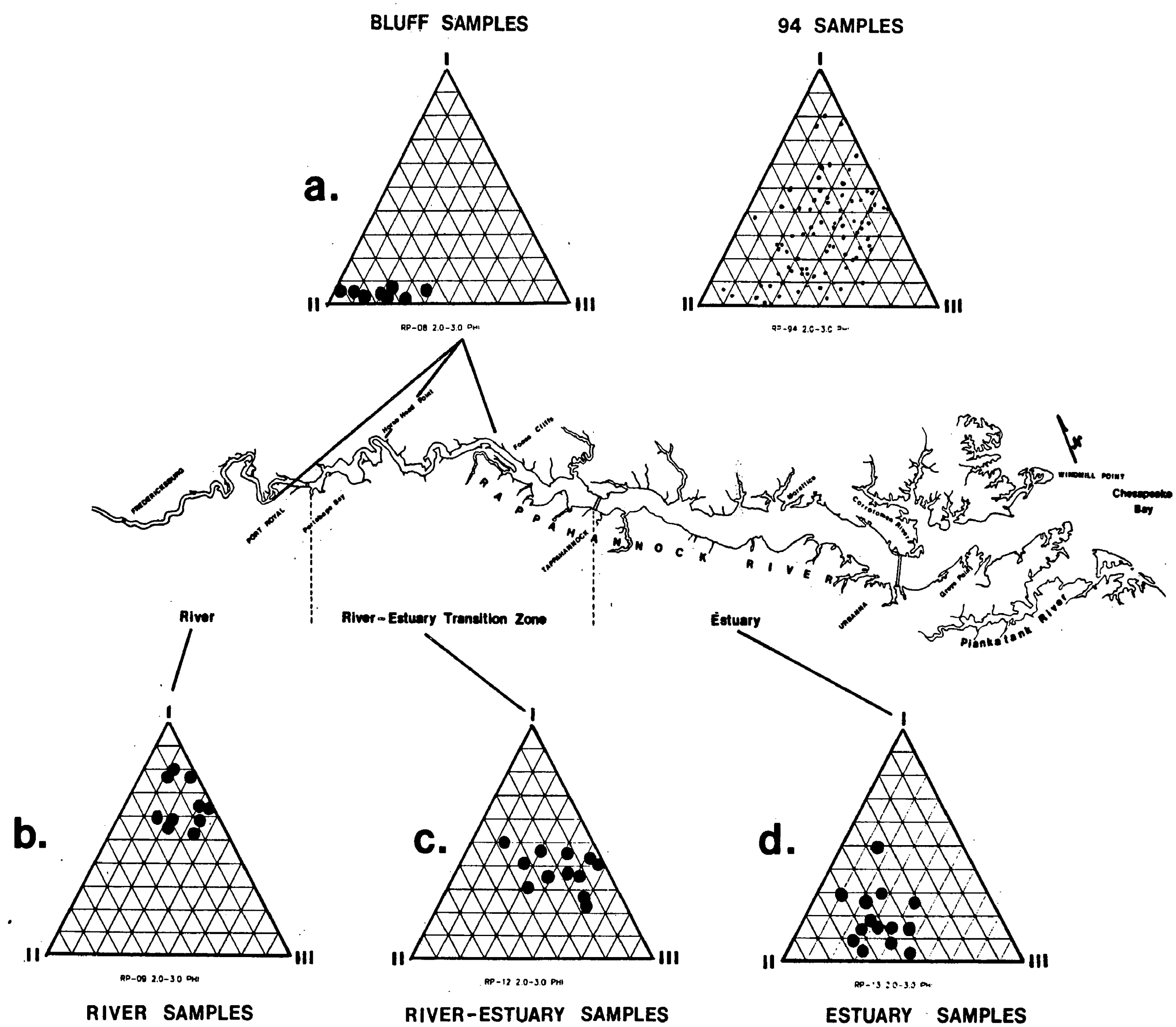
BLUFF SAMPLES
94 SAMPLES
a.
RP-08 2.0-3.0 PHI
FREDERICKSBURG
PORT ROYAL
Portobago Bay
Horse Head Point
Fones Cliffs
RAPPAHANNOCK RIVER
TAPPAHANNOCK
Morattico
Corrotoman River
URBANNA
Grey Point
Piankatank River
WINDMILL POINT
Chesapeake Bay
River
River-Estuary Transition Zone
Estuary
b.
c.
d.
RP-09 2.0-3.0 PHI
RP-12 2.0-3.0 PHI
RIVER SAMPLES
RIVER-ESTUARY SAMPLES
ESTUARY SAMPLES

Figure 22 clearly illustrates that trend gradients are evident among the distribution of object vectors contained within the object space defined by the three end-member (factor) components. The trend gradients observed within these triangular diagrams display the end-results of the (Q-mode) data reducing technique. The particular location of each sand-shape sample on the triangular diagrams are dictated by their percent composition of each of the respective three end-member (factor) components.

Figure 22a shows that it is readily apparent that sand samples from the fastland bluffs at Rock Creek Turn, Horse Head Point and Fones Cliffs cluster closely around the "smooth" end-member or the number II normalized factor component. Each of the fastland bluff sand-shape samples are comprised of at least 70% of the "smooth" end-member. Only negligible percentages of the "rough" and "intermediate" end-members (I and III) are contained within these samples.

Figure 22b shows the distribution gradient of sand samples representative of the Piedmont-derived river sand-shape population. It is clearly evident in this figure that the river sands cluster around the "rough" end-member or number I normalized factor component. This trend gradient is clearly divergent from the fastland bluff sands trend gradient. The river sand samples are comprised as as great as 90% and at least 52% of the "rough" end-member (factor I).

Figure 22c shows the distribution gradient of sand samples representative of the river-estuary transition zone. These sand samples tend to cluster in a zone that is an intermediate position between the "rough" and the "smooth" end-members. The sand-shape population contained within this zone is generally composed of 2-40% of the

"smooth" end-member and 30-50% of the "rough" end-member. The distribution gradient of sand samples indicates that the sand-shape population contained in this zone is comprised of a mixture of both the "rough" and "smooth" end-members. This supports the hypothesis that both the Piedmont-derived river sand-shape population and the fastland bluff sand-shape population are mixing together within the active transport system along these reaches.

Figure 22d shows the distribution gradient of sand samples representative of the estuary zone. These samples tend to cluster in a zone that is close to the "smooth" end-member (factor II). Some of the sand samples in this zone contain as much as 50% of the "rough" end-member (RP150), although the estuary samples generally contain from 10-20% of the "rough" end-member. Nonetheless, it must be stated that significant percentages of the "rough" end-member are consistently present within the sand samples from the estuary. A general trend towards the "smooth" end-member may suggest that more rounded sand sized sediment is being contributed to the estuarine sediment regime via lateral erosion of its fastland banks.

End-Member (Factor) Percentages

Table VIII lists a series of sand-shape samples contained within each hydrographic zone. These samples are representative of the observed trend gradients in the percent composition of each of the three end-member components. Figures 23 through 25 illustrate these observed trend gradients for each zone as well as trends observed along the entire length of the river-estuary system.

River Zone

Figure 23 illustrates the trend gradients observed in the end-member percent compositions of the sand-shape samples from the river zone. The most noticeable trend is that sand-shape samples from this zone are consistently comprised of high percentages of the "rough" end-member. This trend does deviate in the vicinity of Rock Creek Turn where fastland bluffs directly outcrop along the south side of the river. RP031 is a sand sample of this bluff material. It is clearly evident that the end-member percent composition of RP031 directly contrasts that of the percent compositions of the native river sands occupying the river channel up to this point. RP033 is a sand sample located within the river channel directly adjacent to Rock Creek Turn. In comparison with the percent composition of the fastland bluff sands, this sample contains nearly equal percentages of both the "rough" and "smooth" end-members. Sand samples taken both upriver (RP098) and downriver (RP101) from Rock Creek Turn contain significantly higher percentages of the "rough" end-member than does the sand samples from the river in the immediate vicinity of Rock Creek Turn. This evidence suggests that the injection of fastland bluff sands into the active transport system may produce more of a localized effect upon the distribution of sand-shape characteristics within the river zone. It should also be mentioned that the trends observed in the factor percent compositions in the river zone are also consistent with the trends observed in the histogram and cumulative percent grain-shape data.

TABLE VIII

LIST OF REPRESENTATIVE SAND-SHAPE SAMPLES AND THEIR PERCENT COMPOSITION OF THE THREE END-MEMBER (FACTORS I, II, AND III) COMPONENTS FOR EACH OF THE THREE HYDROGRAPHIC ZONES

RIVER ZONE

SAMPLE	MEAN	STD. DEV.	% of Factor I	II	III	LOCATION
RP010	2.26	.177	52	14	34	Fredericksburg Bar
RP061	2.17	.179	80	7	13	Bernard Bar-Channel
RP070	2.23	.154	49	5	46	Castle Ferry Bar-Channel
RP076	2.26	.172	40	16	44	Moss Neck Bar-Channel
RP089	2.25	.180	45	14	41	Hop Yard Bar-Channel
RP098	2.25	.204	50	25	25	Mount Bar-Channel
RP031	2.37	.165	5	57	38	Rock Creek Turn-Bluff
RP033	2.31	.196	31	37	32	Rock Creek Turn-Channel
RP101	2.24	.184	49	14	37	Cleve-Channel

RIVER-ESTUARY TRANSITION ZONE

RP037	2.24	.199	45	24	31	Port Royal-North
RP105	2.22	.207	55	23	22	Port Royal-Channel
RP106	2.22	.198	59	20	21	2.5 km D.R. from Port Royal-Channel
RP112	2.18	.195	76	12	12	Portobago Bay-Channel
RP115	2.42	.188	8	70	22	Devils Elbow-South
RP117	2.45	.163	4	84	12	Horse Head Point-Bluff
RP042	2.39	.185	9	61	30	Horse Head Point-Channel
RP142	2.29	.185	41	38	21	Leedstown-Channel
RP120	2.30	.211	42	44	14	Paynes Island-North
RP144	2.33	.202	30	51	19	Paynes Island-Channel
RP123	2.46	.177	6	87	7	Fones Cliffs-Bluff
RP055	2.29	.177	23	28	49	Mulberry Point-Channel

TABLE VIII (Continued)

			ESTUARY ZONE			
			% of Factor			
SAMPLE	MEAN	STD. DEV.	I	II	III	LOCATION
RP058	2.35	.204	26	54	20	Tappahannock-South
RP057	2.35	.194	23	52	25	Tappahannock-Channel
RP056	2.32	.193	30	42	28	Tappahannock-North
RP134	2.30	.197	26	33	41	Wares Wharf-North
RP137	2.35	.186	26	53	21	Wares Wharf-South
RP150	2.27	.208	50	37	13	Neals Point-Channel
RP139	2.36	.197	29	61	10	Sharps-North
RP151	2.35	.184	14	50	36	Sharps-Channel
RP141	2.38	.188	14	60	26	Sharps-South
RP152	2.38	.188	8	52	40	Morattico-Channel
RP157	2.35	.192	17	54	29	Greys Point-South
RP155	2.37	.179	15	54	31	Towles Point-Channel
RP160	2.35	.196	14	38	48	Mosquito Point-Channel
RP161	2.33	.216	37	58	5	Windmill Point

Figure 23. Illustration of the trend gradients observed in the end-member percent compositions representative of sand-shape samples from the river zone.

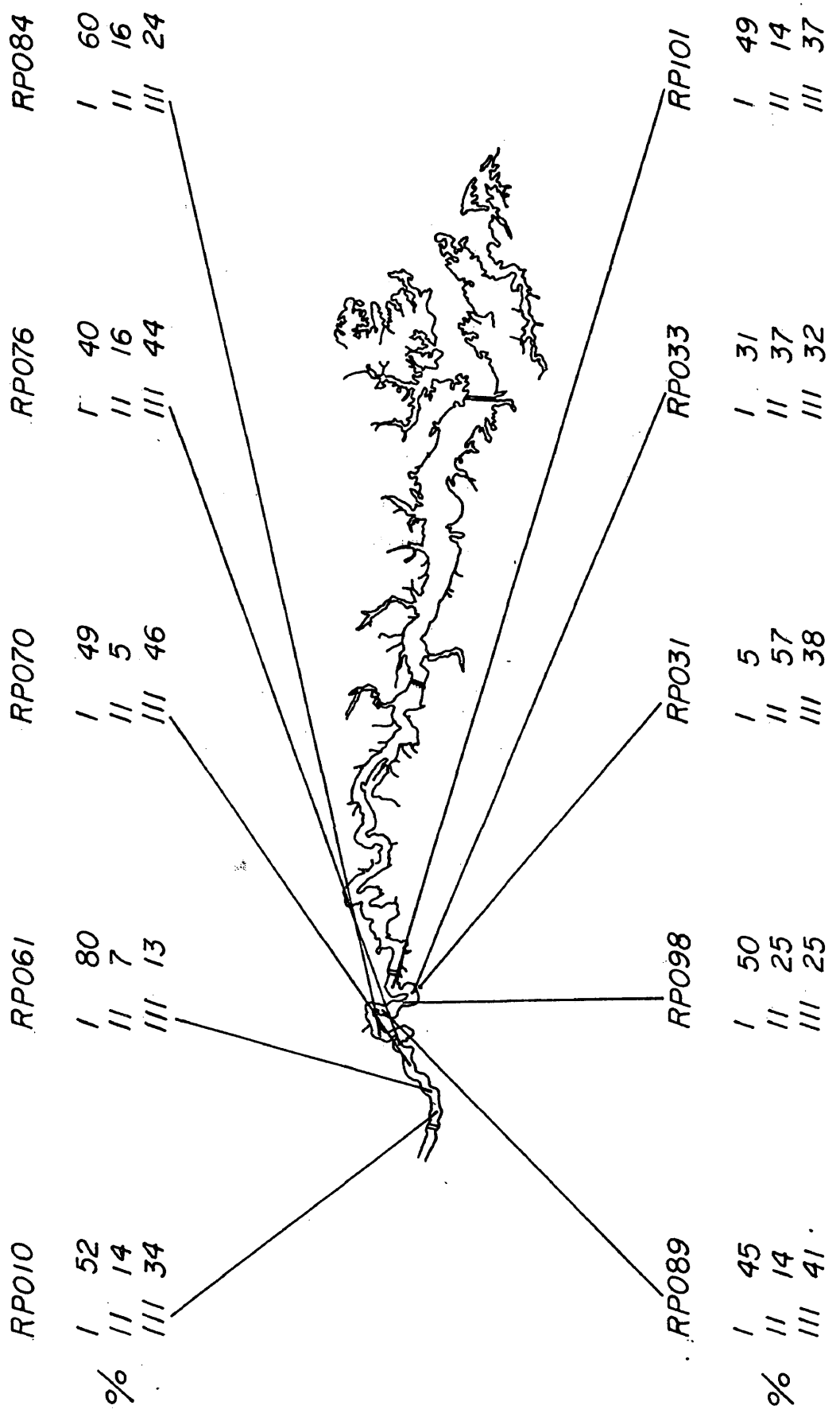
RP084
I 60
II 16
III 24
RP076
I 40
II 16
III 44
RP070
I 49
II 5
III 46
RP061
I 80
II 7
III 13
RP010
I 52
II 14
III 34
RP101
I 49
II 14
III 37
RP033
I 31
II 37
III 32
RP031
I 5
II 57
III 38
RP098
I 50
II 25
III 25
RP089
I 45
II 14
III 41
%
%
BLUFF
RIVER ZONE

River-Estuary Transition Zone

Figure 24 illustrates the trend gradients observed in the end-member percent compositions of the sand samples from the river-estuary transition zone. From Port Royal downriver to Portobago Bay, sand-shape samples are still clearly dominated by the "rough" end-member representative of the Piedmont-derived river sand-shape population. Sand samples from the river channel as well as along the flanking shoals of this reach contain high percentages of the "rough" end-member.

As the river approaches Horse Head Point, where fastland bluffs directly outcrop along the northern side of the river, the predominant influence of the "rough" end-member markedly decreases within the river channel from 76% at Portobago Bay to 9% at Horse Head Point. In the immediate vicinity of Horse Head Point, factor II, the "smooth" end-member now clearly dominates the sand-shape characteristics contained within the sand-sized sediment occupying this reach (61% factor II and 9% factor I). The bluff sample at Horse Head Point contains 84% of the "smooth" end-member and a negligible amount (4%) of the "rough" end-member. This data strongly suggests that sand-sized sediment derived from the fastland bluffs at Horse Head Point is being contributed to the river's active transport system along this reach.

Moving downriver from Horse Head Point, the strong influence of the "smooth" end-member begins to gradually diminish. This corresponds with a relative increase in the percentages of the "rough" end-member. In particular, at Leedstown (approximately 6 km downriver from Horse Head Point) RP142 contains a nearly even percentage of

Figure 24. Illustration of the trend gradients observed in the end-member percent compositions representative of sand-shape samples from the river-estuary transition zone.

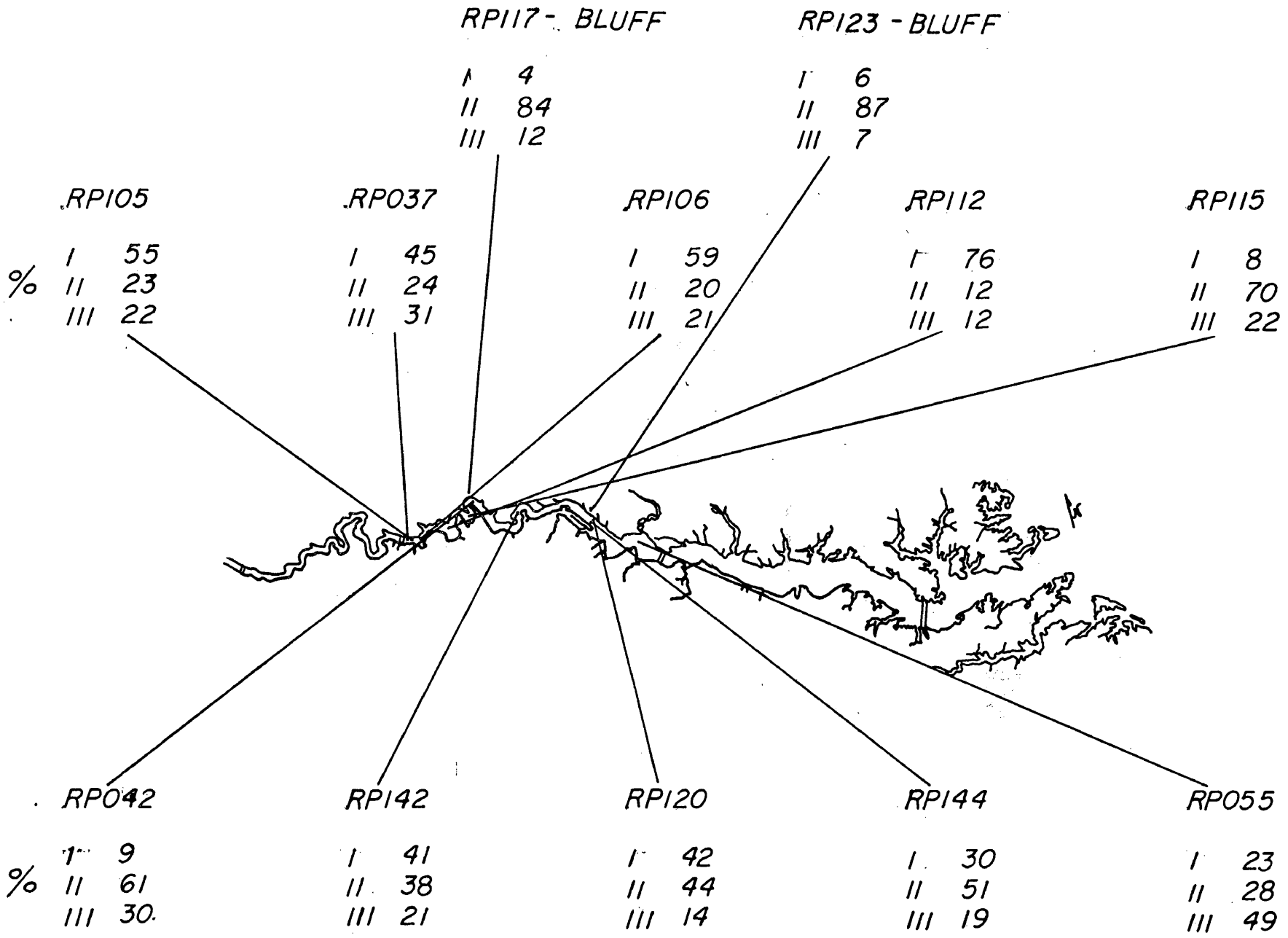

RIVER-ESTUARY TRANSITION ZONE

both the "rough" (41%) and "smooth" (38%) end-members. This again suggests that a mixture of both sand-shape populations is being actively transported downriver from Horse Head Point towards the head of the estuary.

At Fones Cliffs (downriver from Leedstown) fastland bluff sediments again directly outcrop along the northern side of the river. Here a similar trend exists in the sand-shape distributions analogous to Horse Head Point. The sand-sized sediment contained within the Fones Cliffs bluffs contains 87% of the "smooth" end-member. Sand samples from the river channel as well as along the flanking shoals in the immediate vicinity of Fones Cliffs contain nearly even percentages of both the "rough" and "smooth" end-members. This evidence is consistent with that of the trends observed upriver near Horse Head Point in that both sand-shape populations are mixing together within active transport along this reach.

Approaching the head of the estuary (downriver from Fones Cliffs) sand samples from the channel and shoals contain nearly even percentages of both sand-shape populations. This trend is in consistent agreement with the histogram and cumulative percent data for this reach. Therefore, based on the evidence presented, it appears that both the Piedmont-derived river sand-shape population as well as the fastland bluff sand-shape population are present within the bottom sediments at the head of the estuary.

Estuary Zone

Figure 25 illustrates the trend gradients observed in the end-member percent compositions of the sand samples from the estuary zone.

Figure 25. Illustration of the trend gradients observed in the end-member percent compositions representative of sand-shape samples from the estuary zone.

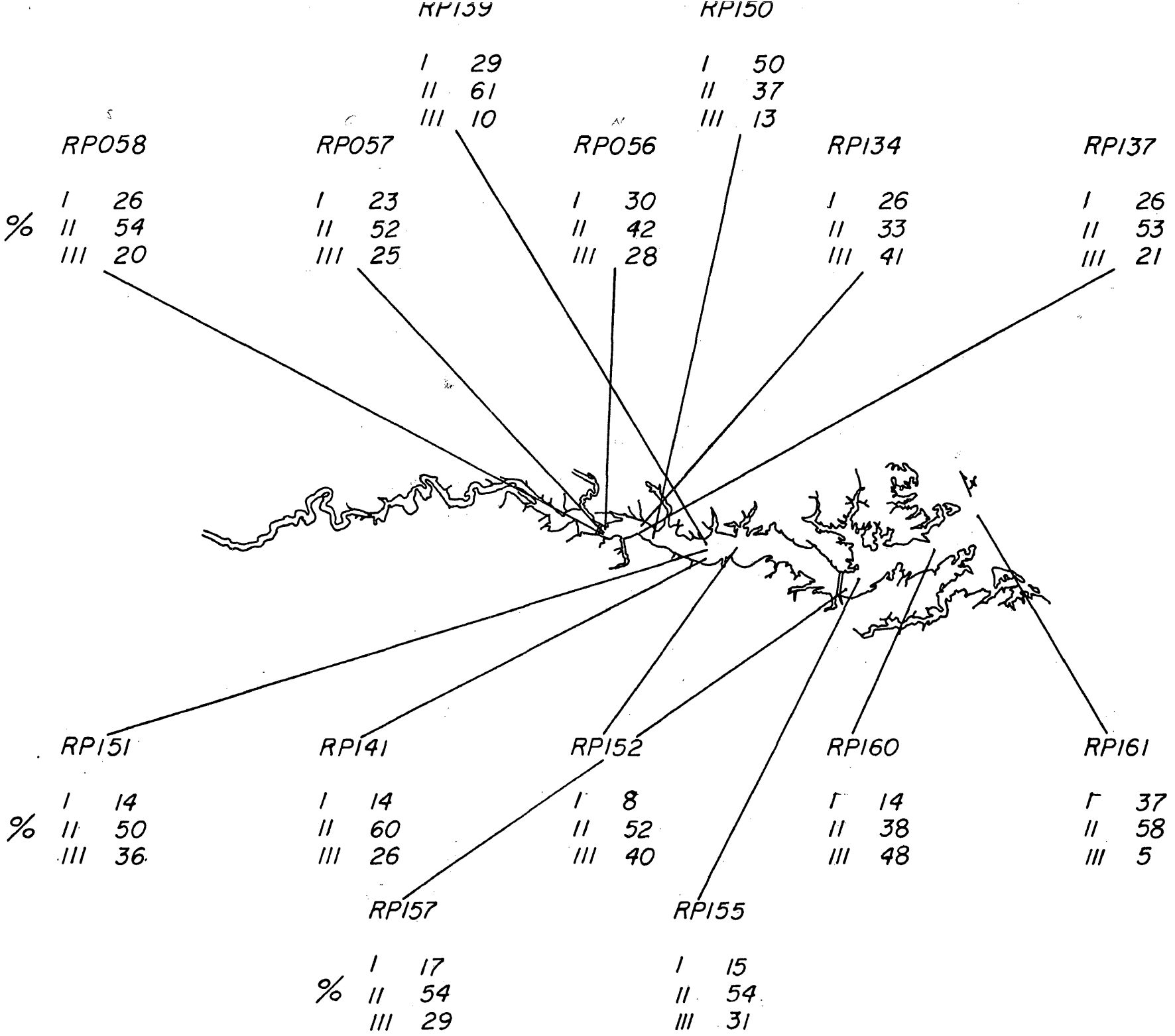

ESTUARY ZONE

The most noticeable trend gradient in this zone is that higher percentages of the "rough" end-member are contained within the channel and flanking shoals of the upper estuary reaches than in the middle and lower estuary reaches. Sand samples from Tappahannock downestuary to Sharps contain from 20-50% of the "rough" end-member associated with varying percentages of the "smooth" end-member.

The trend-gradient observed within the middle and lower portions of the estuary show that the percent composition of the "rough" end-member tends to gradually diminish down to around 15% corresponding with a gradual increase in the "smooth" end-member percentages. This trend is observed within the central channel as well as along the flanking shoals. Another interesting trend gradient is observed along the shoaling areas of the middle estuary. Higher percentages of the "smooth" end-member occur within the sand-sized sediments contained on the southern shoaling areas than along the northern shoaling areas. This could be attributed to the higher rates of erosion along the southern flanks of the estuary as compared to the northern flanks. Consequently, larger amounts of more rounded sand-sized sediment, derived from fastland erosion, may be contributed to the southern shoal sediment regime than that of the northern shoaling areas flanking the estuary's central channnel. Another intriguing piece of evidence within the lower estuary is that the sand sample taken just outside the estuary mouth contains 37% of the "rough" end-member. This is a higher percentage of factor I than any sand sample contained within the sediments of the estuary proper.

IX. DISCUSSION AND INTERPRETATION OF RESULTS

Up to this point, quantitative investigations concentrating on the transport of sand-sized sediment within Atlantic Coastal Plain estuaries has received minimal attention, for it is well known that sediments within these estuaries tend to be mainly comprised of muds (silts and clays) and organic matter with lesser percentages of sand. This is attributed to the thought that average bi-directional flow pattern in partly mixed estuaries creates an essentially closed system in terms of suspended sediment transport processes (see Figure 1, Krone, 1972). Consequently, it is believed that river-borne sand-sized sediment is inhibited from down-river transport into the estuarine sediment regime pass the landward limit of salt intrusion.

The research objective of this investigation is to attempt to gain quantitative insight into the question as to whether river-borne sand-sized sediment originating in the upper reaches of the Rappahannock River is ultimately transported into the estuarine sediment regime. In addition, evaluate plausible transport mechanisms which may provide the opportunity for river-borne sands to move into the Rappahannock Estuary.

Based upon the spatial distribution of sand-sized sediment within the Rappahannock River-Estuary System, as determined by bottom sediment textural analysis, the two major landward sources of sand-sized sediment to the Rappahannock Estuary are the Piedmont-derived river sands and the fastland bluff sands. Bottom sediment textural analysis shows that

sand is the major constituent of sediment samples from the river zone, particularly within the river channel. The river channel from Fredericksburg to Port Royal consistently contains high percentages of sand. The channel-bars within the river zone contain varying percentages of sand. The textural trends observed on these depositional features indicates that higher percentages of sand are contained on the channel-bars located near the fall line in the proximity of Fredericksburg. The high percentage of sand on these bars tends to gradually decrease moving downriver towards Port Royal and the textural trends seem to be dictated by the meander morphology.

In the river-estuary transition zone, the general trend is that higher percentages of sand are contained within the river channel than along the flanking shoals, although the opposite of this trend occurs near Port Royal. An interesting trend occurs along the shoaling areas of this zone where fastland bluffs directly outcrop along the flanks of the river. The percentage of sand increases dramatically in the vicinity of the bluffed reaches along Horse Head Point and Fones Cliffs. In addition, the percentage of sand contained along the northern shoal in this zone closely corresponds with the percentage of sand contained along the southern shoal. This textural data is a good indication that the constant denudation of fastland bluff sediments is contributing significant percentages of sand-sized sediment to the river's active transport system along these reaches.

In the Rappahannock Estuary, higher percentages of sand occur close to the shoreline on shoaling areas flanking the estuary's central channel. The percentage of sand generally decreases or grades outward towards the estuary channel. Lower percentages of sand occur within

the estuary channel relative to the flanking shoals. The trend of higher percentages of sand along the shoals than within the estuary channel would seem to suggest that lateral erosion of the fastland flanks of the estuary may be contributing sand to the estuary's active transport system. Alternatively, this may also suggest the possibility that the flanking shoals are a potential pathway for river-borne sand-sized sediment to be transported into the estuary, since a net-landward bottom flow does not usually exist along the shoals.

Thus, the quantitative evidence supplied by sediment textural analysis not only provides information on the spatial distribution of sand-sized sediment within the river-estuary system but also shows that certain trends in the distribution are evident. These trends present evidence that is supportive of the statement that the two major landward sources of sand to the estuary are the Piedmont-derived river sands and the fastland bluff sands. More importantly, textural evidence shows that sand is consistently present in various degrees within the estuarine sediment regime.

Fourier grain-shape analysis provides the most compelling quantitative evidence that is supportive of the hypothesis that river-borne sands are present within the Rappahannock's estuarine sediment regime. Based on the distribution of Fourier harmonic amplitudes, grain-shape analysis is successful in identifying two statistically non-similar sand-shape populations; namely, the Piedmont-derived river sands, occupying the upper reaches of the Rappahannock River and the fastland bluff sands. Geologically, each of these two sand-shape populations were deposited during different geological time settings as well as different depositional environments. Sand-sized sediment occupying

the upper reaches of the Rappahannock River is derived from Piedmont Quaternary fluvial terrace deposits which flank the upper reaches of the river above the fall line at Fredericksburg. Sand-sized sediment contained within the fastland bluff sedimentary material at Rock Creek Turn, Horse Head Point and Fones Cliffs is Tertiary in age and deposited in marine, near-shore marine and fluvial depositional environments.

It is, in a sense, fortuitous that the two major landward sources of sand-sized sediment to the Rappahannock Estuary (river sands and fastland bluff sands) possess quantifiably distinct sand-shape attributes. Hence, it appears that Fourier grain-shape analysis is well suited to address the research objectives as a quantitative means of determining the distribution of the two non-similar sand-shape populations within the Rappahannock River-Estuary's active transport system. More importantly, this type of analysis will also allow quantitative inferences to be made on whether the Piedmont-derived river sand-shape attributes are present within the estuarine sediment regime.

The quantitative grain-shape data is generated by the distribution of Fourier harmonic amplitudes of ninety-four grain-shape samples over a defined range of Fourier harmonic amplitude values. This data presents interesting trend gradients within the Rappahannock River-Estuary system corresponding to the grain-shape (signatures) characteristics and spatial distribution of the two non-similar shape populations. These trend gradients also correspond well with the spatial distribution (percent sand by weight) of sand-sized sediment throughout the bottom sediments of the river-estuary system. The histogram and cumulative percent distributions clearly illustrate the non-similarity

of the two grain-shape populations as well as readily apparent trends in the spatial distributions of these populations within the Rappahannock River-Estuary's active transport system.

Histogram data objectively characterizes the quantitative grain-shape attributes of the two grain-shape populations. The Piedmont-derived river sands are represented by an average sample mean of 2.25 ($Q_n = -\log_{10} R_n$) and standard deviation of 0.175. These river sands are characterized as having "rough" or angular grain shapes. The fastland bluff sands are represented by an average sample mean of 2.43 and standard deviation of 0.165. Fastland bluff grain-shapes are characterized as having "smooth" or rounded grain-shapes. The non-similarity of the grain-shape attributes of the two populations can be related to each of the population's depositional environments. Intuitively, one would expect Piedmont-derived Quaternary fluvial sands to be very angular in shape due to its relative immaturity within transporting environments. Conversely, one would expect Tertiary fastland bluff sands, deposited in marine and fluvial environments, to have a more rounded shape since these sediments may have been subjected to various higher energy transport environments over longer periods of time.

The distribution of histogram data of the grain-shape samples throughout the river-estuary system present a strong indication of trend gradients occurring among the distribution of the two sand-shape populations within the active transport system. The distribution of histogram data in the river-zone shows a consistent trend, in that the grain-shape population occupying this zone has sample means skewed to the lower Q_n values (average 2.25) indicating "rough" or angular shape patterns. The river sand-shape population is present in both the

present within the estuarine sediment regime both in the estuary channel as well as along its flanking shoals.

On the basis of multiple sample comparisons, cumulative percent plots of the distribution of Fourier harmonic amplitudes presents trends which reflect an internal consistency that is also present within the histogram data. Figure 19a clearly shows the non-similarity between the cumulative percent distributions of the river sands and the fastland bluff sands over the range of Fourier harmonic amplitude values. There is an apparent internal consistency in the cumulative percent distributions of both sand-shape populations in that there is a very small range of deviation among the distribution of sand samples from each population. This suggests that there is an overall consistency in the sand-shape characteristics of the sand-sized sediments occupying these zones. This small range of deviation among the sample distributions occurs within the river zone and estuary zone (Figure 19c). The river-estuary transition zone shows a trend that is opposite to that observed in the river and estuary zones. In this zone, the cumulative percent distributions of grain-shape samples displays a wide range of deviation. The trend in this zone shows that in areas where fastland bluffs outcrop along the river (Horse Head Point and Fones Cliffs), the cumulative percent plots shift markedly from the lower Q_n values to higher Q_n values (which are characteristic of the fastland bluff grain-shape distributions). Moving downriver away from the bluffed reaches and towards the estuary, the cumulative percent distributions begin to gradually shift back to the lower Q_n values. This trend gradient suggests that fastland bluff sand-shape characteristics are present within the river's active transport system along these reaches. The fact that the cumulative percent

river channel and on the depositional meander bars. In the river-estuary transition zone, the river sand-shape population still dominates pass Port Royal down to Portobago Bay. Downriver from Portobago Bay, another trend gradient develops in the vicinity of bluffed reaches at Horse Head Point and further downriver at Fones Cliffs. Based on the distribution of histogram data, the sand-sized sediment within active transport along these reaches are composed of various mixtures of the two sand-shape populations. This is indicated by grain-shape sample means that are intermediate of river and fastland bluff sand-shape population means, a wider range of standard deviations and indications of bimodal or polymodal grain-shape distributions.

In the Rappahannock Estuary, trends observed in the distribution of histogram data also suggest that sand-sized sediment within the estuary regime is comprised of various mixtures of the two sand-shape populations found landward of the estuary. This, again, is indicated by sample means that are intermediate to the extreme sand-shape samples, a wider range of standard deviations and polymodal distributions. Grain-shape distributions of samples occupying the upper estuary's central channel and flanking shoals tend to resemble that of the river-sand shape population with sample means skewed towards the lower Q_n values. Grain-shape distributions occupying the middle and lower estuary on both the flanking shoals and channel show a gradual trend towards "smoother" shape attributes, yet wide ranges of standard deviations as well as polymodal distributions, are evident in these samples. Thus, the histogram data provides first-hand quantitative evidence which supports the hypothesis that river-borne sands are

distributions shift markedly from lower Q_n values towards higher Q_n values along the bluffed reaches and then gradually shifts back towards lower Q_n values approaching the estuary, suggests that the injection of fastland bluff sands produces a localized effect upon the distribution of sand-shape characteristics in this zone. The cumulative percent distributions are also supportive of the hypothesis that the river and bluff sand-shape populations are mixing together within the active transport system and that various mixtures of these two sand-shape populations are present within the estuary's central channel as well as along the flanking shoals.

Results of the Q-mode factor analysis provide the quantitative mainstay for the hypothesis that river-borne sand-sized sediment is present within the estuarine sediment regime of the Rappahannock River-Estuary system. The Q-mode factor analysis applied to grain-shape data is based on the percentage frequency distributions over the sixteen Q_n class intervals for the analyzed ninety-four sand samples. Q-mode analysis is successful in determining three compositionally distinct end-members (factor components), obtained from the normalized data matrix, that are sufficient to encompass 98.5% of the total grain-shape variation within the ninety-four sand samples. End-members (factors) I and II represent 98.0% of total variance. These end-members are representative of the river sand-shape population and the fastland bluff sand-shape population. This indicates that the three end-member (factor) components are sufficient enough to explain virtually all of the total grain-shape variance within the sand samples. More importantly, Q-mode analysis shows that most of the variability among the sand-shape samples from the river-estuary's

active transport system, occurs between the river sand-shape population (factor I) and the fastland bluff sand-shape population (factor II). This, of course, correlates well with the trends observed in the histogram and cumulative percent grain-shape data.

The three-factor (triangular) diagram (Figure 22) depicts obvious trends in the distribution of sand-shape samples among the three end-member components. Figure 22 clearly shows how the Q-mode factor analysis serves to differentiate the river sand-shape population and the fastland bluff sand-shape population. The river sand-shape population tends to cluster around end-member I, while the fastland bluff sand-shape population clusters around end-member II. Grain-shape samples from the river-estuary transition zone and estuary zone are composed of various percentages of the river and fastland bluff sand-shape populations. The river zone sand samples tend to be composed of high percentages of end-member I. Sand-samples from the river-estuary transition zone tend to cluster in an area within the middle of the diagram. The distribution of these sand samples show that sand-shape characteristics in this zone tend to be composed of intermediate percentages of the "rough" end-member I and the "smooth" end-member II. The point that sand-samples within this zone contain nearly even percentages of end-member I and end-member II suggests that sand-sized sediment within active transport is composed of various mixtures of the Piedmont-derived river sands and the fastland bluff-derived sands.

In the estuary zone, sand samples tend to cluster in an area that is closer to end-member II than end-member I. This infers that the sand-shape characteristics of sand within the estuary tends to be of

a more rounded nature, yet evidence of "rough" sand grain-shapes is still consistently present within the estuarine sediments.

The end-member percentage diagrams (Figures 22-24) present a more clear representation of Q-mode factor analysis results in that they display the lateral and longitudinal trends of the end-member percentages for each hydrographic zone. The most striking trends observed in these diagrams is that high percentages of end-member I, representative of the Piedmont-derived river sand-shape population, are present within the river's channel and bar sands from Fredericksburg to Portobago Bay. When the river comes in contact with the Horse Head Point fastland bluff sediments, the percent composition of end-member I within the channel sand samples dramatically decreases from 76% at Portobago Bay to 9% at Horse Head Point. This corresponds with a dramatic increase in the percent composition of end-member II from 12% at Portobago Bay to 61% in the river channel at Horse Head Point. End-member III accounts for the remaining 30%. Moving downriver from Horse Head Point, away from the influence of the fastland bluffs, the percent composition of end-member I and end-member II even out, both within the river channel as well as along the flanking shoals. When the river comes in contact with Fones Cliffs, a similar trend is again evident. The fastland bluff sands at Fones Cliffs are comprised of 87% of end-member II, while sand-sized sediment within active transport directly adjacent to the bluffs in both the river channel and flanking shoals show nearly even percentages of end-member I and end-member II. This quantitative evidence strongly supports the hypothesis that the river sands and bluff sands are involved in some sort of mixing process within active transport at the injection points of the fastland

bluff sands (Horse Head Point and Fones Cliffs). More importantly, this data shows that a fairly even mixture of both sand-shape populations is present within the river channel as well as the flanking shoals moving downriver towards the head of the estuary at Tappahannock. Thus, it would certainly seem plausible that river-borne sand-sized sediment that is eventually transported downriver into the estuarine sediment regime via the central channel or its flanking shoals would tend to be composed of a mixture of both the river and fastland bluffs sand-shape populations.

The trend gradients observed within the estuary zone are also supportive of the mixing hypothesis. This is particularly evident within the upper estuary. In both the estuary's central channel as well as its flanking shoals, end-member I comprises 30-50% of the sand-samples, while end-member II generally comprises 40-60%. It is also evident that in the upper estuary, higher percentages of end-member I are present within the estuary channel than on its flanking shoals. This suggests that the Piedmont-derived river sands may move more readily into the estuary via the central channel than along its flanking shoals. Alternatively, lower percentages of end-member I occurring along the estuary's shoaling areas suggests that Piedmont-derived river sands may be transported into the estuary along the flanking shoals and then may become reworked and transported from the shoals into the estuary channel. It is also a possibility that lateral erosion of the estuary's flanks is contributing more rounded sand sediment shapes to the estuarine sediment regime, particularly along shoaling areas close to the shoreline.

In the middle and lower estuary, the percent composition of end-member I gradually diminishes within the estuary's central channel as well as along its flanking shoals. This could be attributed to a relative increase in the rate of lateral erosion of fastland material flanking the reaches of the middle and lower estuary. A resulting increased input of more rounded sand-sized sediment to the estuary's active transport system may create a masking effect upon the Piedmont-derived river sands present within the channel and shoal sands along these reaches. In other words, the presence of Piedmont River sands within the middle and lower estuary may be subdued by the increased deposition of more rounded sand-sized sediments that may be locally derived from shoreline erosion of the fastland. In addition, fairly rapid rates of sediment deposition within the lower estuary channel may also produce a masking effect upon the presence of Piedmont-derived river sands along these reaches. Another possibility may be that lesser amounts of Piedmont-derived river sands are actually transported as far down as the lower estuary. This would correlate well with the gradually decrease in end-member I percentages in both the estuary channel as well as the flanking shoals from the upper estuary down into the lower estuary.

Another intriguing piece of evidence provided by the Q-mode analysis is that the sand sample taken in the channel outside the mouth of the Rappahannock River contained 37% of end-member I. This suggests that the shape characteristics of the Piedmont-derived river sands are also present within the sediments outside the river mouth. It also implies that river-borne sand-sized sediment may eventually become transported out of the river-estuary system, hence, becoming

a part of the Chesapeake Bay sediment regime. Although one can only speculate on the basis of one sample outside the mouth of the Rappahannock River, the fact that this sample contains 37% of end-member I does present interesting implications. This would seem to suggest that river-borne sand-sized sediment is not only transported into the estuarine sediment regime, but may also eventually be transported outside the mouth and begin to interact with the Chesapeake Bay's active transport system. At this point, it is interesting to note that previous studies of the Chesapeake Bay bottom sediments (Environmental Protection Agency's baseline sediment study) indicate that these sediments contain appreciable amounts of sand-sized sediment. A portion of the total percentage of sand-sized sediment within the Chesapeake Bay is held unaccountable in terms of the potential sand sources within the Bay. Therefore, the fact that Fourier grain-shape analysis presents evidence that Piedmont-derived river sands are present in the sediments outside the mouth of the Rappahannock Estuary, suggests that this sub-tributary to the Chesapeake Bay may also be included as a potential source of sand-sized sediment to the Chesapeake Bay's bottom sediment regime.

An alternative hypothesis for the high percentage of Piedmont-derived river sands located outside the mouth of the estuary may be that Piedmont-derived fluvial sands were deposited outside the mouth of the river during lower stands of sea level. Associated with the subsequent gradual rise in sea level, present day transport processes outside the estuary mouth may be reworking past deposits in this area. Consequently, these reworked deposits may become transported into the lower estuary sediment regime. This hypothesis would be

supported by the high percentage (37%) of the "rough" end-member I contained within the sand sample taken outside the mouth of the estuary. In addition, the trend of higher percentages of end-member I in the lower estuary than in the middle estuary may bear some relation to this alternate hypothesis.

Since Fourier grain-shape analysis provides the most convincing quantitative evidence that Piedmont-derived river sands are present within the estuarine sediment regime, the question then arises; what transport mechanisms can account for this? It is the writer's belief that periodic high freshwater inflows to the Rappahannock Estuary, caused by river flooding events, provides the transport mechanism that is capable of transporting river-borne sand-sized sediment into the estuarine sediment regime. Events of this nature can disrupt the average estuarine circulation patterns by lowering the salinity and increasing haline stratification in the estuary. As a result of high freshwater inflow to the head of the estuary, the inner limit of salty water shifts towards a more seaward position, downstream of its position prior to high inflow. This, in effect, would create a net-seaward flow at all depths where a net-landward bottom flow existed prior to high freshwater inflow. Depending upon the magnitude of the freshwater inflow, the estuary may either retain its salt intrusion through all stages of high inflow or the salt intrusion can be displaced outside the estuary mouth. The most important sedimentological effect of high freshwater inflow is that large amounts of river-borne sediments are transported into the estuarine sediment regime as well as resuspension of existing bottom sediments within affected portions of the estuary.

The purpose of Operation HIFLO was to learn how the Rappahannock Estuary responds to high river inflow and influx of sediment. Periodic river-flooding events and resulting high freshwater inflow to an estuary produce changes in the hydrodynamic conditions. Consequently, this results in a disruption of estuarine sediment transport patterns. Important aspects of flooding events that produce these changes are: the frequency of occurrence, the time-duration of the event, the magnitude of river discharge rates and the ability to disrupt average estuarine circulation patterns.

The HIFLO event, although not a major flood, was one of five high runoff events in the Rappahannock River during 1977-1978. "HIFLO" discharge was one that occurs frequently, once a year on the average. The storm period lasted for four days from March 26-March 29, 1978. The HIFLO event had a peak river discharge of 358 m/sec. A runoff event of this magnitude is seven times the annual average discharge. Flooding events of larger magnitudes, such as tropical storm "Agnes", have a recurrence interval of once every twenty-five years. In the Rappahannock, "Agnes" had a peak discharge rate of 1,296 m/sec which is almost four times greater in magnitude than the "HIFLO" event and twenty-five times the annual average discharge rate.

The HIFLO event was successful in disrupting the average partially-mixed estuarine circulation pattern in the Rappahannock Estuary. By March 28, one day after high freshwater inflow at Fredericksburg, the inner limit of salty water shifted to its most seaward position, 12.8 km downstream of its position prior to high inflow. In addition, high river inflow increased stratification and caused a slight freshening throughout the estuary. The estuary retained its salt intrusion as

well as its partially-mixed flow regime through all stages of high inflow (Nichols, et al., 1981).

The mainstream influx produced high suspended sediment loads in the upper estuary that extended 60 km downstream from Fredericksburg. Suspended sediment influx over the fall line reached a rate of 12,300 tons per day over the four days of flooding. This rate is 6.5 times greater than the annual rate of suspended sediment discharge for 1978. During this time of high freshwater inflow, eighty-nine percent of the total suspended sediment load moving downriver from Fredericksburg towards the head of the estuary was finer than 62μ and eleven percent was greater than 62μ (sand). Suspended sediment concentration measurements in the sampled zone were depth integrated from the water surface to a point approximately 9 cm (0.3 ft) above the bed. These measurements did not include bed-load discharges.

This evidence shows that river-borne sand-sized sediment is actively transported downriver towards the head of the estuary via suspended load during the HIFLO event. It would then seem intuitively obvious that river-borne sand-sized sediment is also moving downriver via bedload transport, although no quantitative data substantiates this. Therefore, it is evident that river-borne sand is actively transported downriver towards the estuary during "HIFLO". Consequently, this sand has the potential of becoming transported into the estuarine sediment regime.

In addition to a mainstream influx of river-borne sands transported downriver towards the estuary via suspended load, another viable alternative for the transport of sand into the estuarine sediment regime is the resuspension and consequent net-seaward transport of

pre-existing bottom sediments within the upper estuary by tidal currents. Current velocity observations taken within the upper estuary's central channel (station R-1A) during the HIFLO event show that a strong net-seaward flow existed during the four days of high freshwater inflow in both the near-surface and near-bottom waters. This resulted in a seaward displacement of the salt intrusion some 13 km downstream of its position prior to high freshwater inflow.

Estimates of shear stresses exerted on the bed within the boundary layer of the upper estuary's central channel during the four days of flooding indicate that the relative magnitude of boundary shear stresses exceed the critical threshold values. This implies that the magnitude of boundary shear stresses exerted on the bottom sediments of the upper estuary channel are sufficient enough to erode and resuspend bottom sediments. This, coupled with net-seaward current velocities through depth, results in the transport of resuspended bottom sediments in a net-seaward direction into the estuarine sediment regime.

If one also examines the time-velocity curves (Figures 9 and 10) at station R-1A during Operation HIFLO (March 26-27, 1978), another possible transport mechanism is evident. Because of the large amplitudes, these tidal currents are responsible for mixing fresh and saltwater which in turn generates turbulence that can also erode and resuspend bottom sediments within the upper estuary. As a result of this turbulence, mixing is fast and suspended sediment dilution is high. Hence, excess turbulence created by fresh-saltwater mixing can create a transport mechanism whereby sand-sized sediment may become eroded and resuspended off the bottom. Depending upon the relative

position of the resuspended sand within the water column, it may either settle out quickly or become transported further down estuary by tidal current action.

Therefore, it certainly seems plausible that river-borne sand-sized sediment can indeed move into the estuarine sediment regime during high freshwater inflows to the estuary. River-borne sands can be transported into the estuary either as part of the mainstream suspended load moving downriver with the flood waters, or eroded and resuspended from the bottom as a result of boundary flow shear at the bed or by turbulent mixing of fresh and saltwater. How far the river-borne sands move into the estuary via the central channel or along flanking shoals may be dependent upon the magnitude of freshwater discharge into the estuary and the relative distance that the resultant net-seaward flow displaces the inner limit of salt intrusion in a seaward direction. Once the estuary recovers and the salt intrusion resumes its average position, along with the re-establishment of its bi-directional flow regime, river-borne sand-sized sediment delivered to the estuary may settle out and become a resident of the estuarine sediment regime.

The quantitative evidence previously discussed strongly supports the hypothesis that river-borne sand-sized sediment is present within the Rappahannock's estuarine sediment regime and that extreme hydrological events, such as periodic river flooding, may provide the transport mechanism for this sediment to move into the estuary. The next logical argument that presents itself is what are the potential pathways for the river-borne sands to move into the estuarine sediment regime. In light of this argument, a list of all the possible scenarios regarding the transport of river-borne sand-sized sediment

down to the lower estuary are presented for discussion in order to evaluate and determine whether the quantitative evidence accumulated favors one of these mutually exclusive alternatives over the other.

Generally, there are four possible scenarios regarding the transport of river-borne sands into the lower Rappahannock Estuary:

1.) Piedmont-derived river sands only reaching the lower estuary.

2.) Fastland bluff sands only reaching the lower estuary.

3.) River and bluff sand together reaching the lower estuary.

4.) No sand, except the locally derived from shoreline erosion or landward transport of bottom sands from the Chesapeake Bay.

The first two scenarios, that either Piedmont-derived river sands of fastland bluff sands only reach the lower Rappahannock Estuary, would seem improbable since it is inconsistent with the quantitative data presented. Fourier grain-shape analysis identifies two non-similar sand-shape populations landward of the Rappahannock Estuary, namely, the Piedmont-derived river sands and the fastland bluff sands. Q-mode factor analysis indicates that both of these shape populations are present within the river's active transport system landward of the estuary. Since both sand-shape populations are present within the river channel as well as along the flanking shoals, one would expect that if sand from these reaches eventually becomes transported into the estuarine sediment regime, it would be comprised of both sand-shape populations. The only reasonable explanation of finding only river sands or fastland bluff sands within the sediments of the lower estuary would be if there is selective shape-sorting involved in the transport

processes. This is not found to be true since varying percentages of both sand-shape populations are present within the estuary channel as well as along the flanking shoals.

The third scenario that both river sands and fastland bluff sands reach the lower estuary presents the most plausible arguement and is consistent with the quantitative data presented. This scenario is in agreement with the fact that both sand-shape populations are present within the channel of the lower estuary. Q-mode factor analysis shows that high percentages of the river sand-shape population as well as the fastland bluff sand-shape population are present within the upper estuary channel and along the flanking shoals.

Higher percentages of the fastland bluff sands are present along the flanking shoals of the upper estuary than within the channel, particularly along the northern shoal. A possible explanation for this may be that fastland bluffs mainly outcrop along the northern flank of the river. Once sand from these bluffs enters the active transport system, it may tend to remain on the shoals as it moves into the estuarine sediment regime. In addition, there may be a further input of fastland bluff sands to the shoals as a result of accelerated lateral erosion of the fastland banks flanking the estuarine reaches. This situation would tend to mask the presence of the river sand-shape population along the shoaling areas.

High percentages of the Piedmont-derived river sand-shape population occurring within the upper estuary channel than on the shoals may be attributed to the fact that higher percentages of this sand-shape population occur within the channel than along the shoals in the river-estuary transition zone. Piedmont-derived river sands within

the channel of this zone may then become transported into the estuary channel during flooding events when the salt intrusion is displaced in a seaward direction. Piedmont-derived river sands as well as fastland bluff sands deposited along the shoaling areas of the upper estuary may also become resuspended by wave and current action. Consequently, these sands may move into the estuarine channel, settle out and become incorporated into the channel bottom sediments.

Lower percentages of Piedmont-derived river sands occurring within the channel and flanking shoals of the middle and lower estuary may be a result of increased sedimentation rates within these portions of the estuary. In addition, the availability of more rounded sand-sized sediment to the estuarine sediment regime from lateral erosion of the fastland flanks would have a stronger influence over the far-field distribution of Piedmont-derived river sands within the lower portions of the estuary. Alternatively, the shoaling areas of the estuary may provide a more plausible transport pathway for Piedmont-derived river sands to the lower estuary than in the channel since a net-seaward bottom transport usually exists along these areas. Here again, it is also a possibility that Piedmont-derived river sands contained within the sediments of the shoaling areas can become resuspended by wave and current action. Consequently, these sands may then move into the estuary channel and settle out into the channel bottom sediments. This, in effect, would account for the presence of Piedmont river sands in the lower estuary channel.

The fourth scenario; no sand, except that locally derived from shoreline erosion or landward transport of bottom sands from the Chesapeake Bay is contained within the estuarine sediment regime

presents an interesting alternate hypothesis. The sand-shape sample (RP161) from outside the mouth of the Rappahannock Estuary contains a high percentage of the Piedmont-derived sand-shape population as well as the fastland bluff sand-shape population. Piedmont River sands may have been deposited outside the mouth of the Rappahannock River during lower stands of sea level. A subsequent gradual rise in sea level in turn may rework these deposits and consequently transport these Piedmont sands back into the mouth of the drowned river valley. With the onset of a net-landward bottom flow caused by estuarine circulation patterns, these sands may move progressively upestuary within the estuary channel, hence, accounting for the presence of Piedmont-derived river sands within the lower portions of the estuary. This type of situation may be augmented during extreme hydrological events by meterological forcing from the Chesapeake Bay into the Rappahannock Estuary mouth.

With this concept in mind, the presence of Piedmont-derived river sands within the Rappahannock estuarine sediment regime may be a result of compounded transport processes. River-borne sands may move into the estuary via the flanking shoals and consequently redistributed into the estuary channel by wave and current action during average flow conditions. These sands may also move into the estuary with the mainstream influx river-borne sediments during flooding events and become deposited in the upper portions of the estuary. This is supported by higher percentages of Piedmont River sands in the upper estuary reaches as opposed to lower percentages of these sands contained within the middle and lower reaches of the estuary. Lastly, the presence of Piedmont sands within the lower estuary may be a result of the reworking of past deposits of these sands outside the

mouth and consequent landward transport of sand from the Chesapeake Bay into the estuary mouth as a result of rising sea levels.

Although the quantitative evidence presented shows that Piedmont-derived river-borne sands are present within the Rappahannock estuarine sediment regime, a reasonable amount of speculation still remains as to how these sands got there. The merits presented as a result of this research investigation lie in its contribution to the understanding of the dynamics of sediment transport processes in coastal plain estuaries. In attempting to gain this understanding, utilization of new state-of-the-art quantitative techniques such as Fourier grain-shape analysis helps to gain further insight into questions pertaining to sediment transport and dispersal within estuaries which still remains incompletely understood.

X. CONCLUSIONS

The quantitative evidence supplied by bottom sediment textural analysis, Fourier grain-shape analysis and Q-mode factor analysis support the hypothesis that river-borne sand-sized sediment is present within the Rappahannock estuarine sediment regime. Suspended sediment measurements, as well as analysis of current velocity observations within the estuary during Operation Hiflo, indicate that extreme hydrological events, such as periodic river flooding, provide a plausible transport mechanism to move river-borne sands into the estuarine sediment regime. Events of this nature can disrupt average bi-directional circulation patterns by displacing the salt intrusion to a more seaward position, increase stratification and consequently increase the magnitude of sediment dispersal within the estuary. High freshwater inflows to the estuary on the order of magnitude of the "Hiflo" event can have a frequency of occurrence of up to five times per year in the Rappahannock system. Thus, significant percentages of river-borne sands can become incorporated into the estuarine sediment regime on a relatively periodic basis. These sands may eventually become reworked and redistributed over the long term within the estuarine sediment transport system.

Based on the spatial distribution of sand-sized sediment within the Rappahannock system, the two major landward sources of sand to the Rappahannock Estuary are the Piedmont-derived river sands and fastland

bluff sands which directly outcrop along certain portions of the river flanks. Sand-sized sediment is found to be consistently present within the bottom sediments comprising the estuary's central channel as well as along its flanking shoals. Higher percentages of sand occur within the bottom sediments comprising the shoaling areas of the estuary in relation to the percentage of sand contained within the channel. A general trend in the distribution of sand within the estuary is that the percentage of sand decreases, or grades outward, from the shoreline flanks into the estuarine channel. This indicates that lateral erosion of the estuary flanks (up to 0.6 meter (2.0 ft) per year) may also be contributing sand-sized sediment to the estuarine sediment regime. Alternatively, this may also indicate that river-borne sands move into the estuary via the flanking shoals since a net-landward bottom flow does not usually exist along these areas.

Fourier grain-shape analysis is successful in objectively identifying two statistically non-similar sand-shape populations within the Rappahannock system; namely, the Piedmont-derived river sands and the fastland bluff sands. It is, in a sense, fortuitous that these two non-similar sand-shape populations represent the two major landward sources of sand to the Rappahannock Estuary. The Piedmont-derived river sands are characterized as having angular or "rough" sand-shape attributes. The fastland-bluff sands are characterized as having rounded or "smooth" sand-shape characteristics. The readily contrastable shape attributes of these two populations can be related to the sand-sized sediment provenance's depositional environments as well as their geological time setting. The Piedmont River sands are derived from Quaternary fluvial terrace deposits flanking the upper reaches of the Rappahannock River

above the fall line at Fredericksburg. The fastland bluff sands are derived from Tertiary marine, near-shore and fluvial deposits. Intuitively, one would expect the Tertiary bluff sands to be more rounded since these sediments are relatively mature in terms of the sedimentary cycle.

Q-mode factor analysis, a multivariate statistical technique, is employed on the grain-shape data generated from ninety-four analyzed sand samples from the Rappahannock River-Estuary's active transport system. On the basis of sand-sized sediment sampling throughout the river-estuary system, Q-mode factor analysis serves to differentiate the two sand-shape populations by providing quantitative information on the distribution of these populations within the river-estuary's active transport system. Factor analysis is successful in determining three significant end-member (factor) components which are sufficient enough to encompass 98.5% of the total grain-shape variance among the ninety-four sand samples analyzed. End-member I, representative of the Piedmont-derived river sand-shape population encompasses 50.8% of the total variance. End-member II, representative of the fastland bluff sand-shape population, encompasses 47% of the total variance. End-member III accounts for the remaining 0.5% of the total variance. Thus, one may consider the sand-shape populations in the Rappahannock system to be essentially represented as a two end-member system, yet a third end-member is included to increase the dimensionality of the "shape window" of which the factor analysis uses in order to quantitatively describe the original set of grain-shape observations.

Q-mode factor analysis clearly indicates that trend gradients within the distribution of end-member types are evident within the

river-estuaries active transport system. The grain-shape attributes contained within sand samples from the river zone are almost exclusively dominated by end-member I, the "rough" end-member. In the river-estuary transition zone where fastland bluff sediments directly outcrop along the flanks of the river, both sand-shape populations mix together within the active transport system. High percentages of end-member II, the "smooth" end-member, as well as end-member I, occur within the river channel and flanking shoals in the immediate vicinity of these bluffed reaches. Sand-sized sediment occupying the reaches downriver from the bluffs, approaching the estuary, contain nearly even percentages of both the river sands and fastland bluff sands. The northern shoal shows slightly higher percentages of end-member II, which suggests that a certain amount of bluff-derived sands remain on the shoals and moves downriver towards the estuary. Thus, a mixture of both sand-shape populations are present within the channel and shoaling areas near the head of the estuary.

Sand-sized sediment contained within the channel and flanking shoals of the upper estuary display the same trend as upriver. Varying percentages of both end-member occur within areas, although higher percentages of end-member II occur along the flanking shoals than within the upper estuary channel. This trend indicates that lateral erosion of the estuary flanks is contributing more rounded sand-sized sediment to the estuary's active transport system and that this sediment tends to remain on the shoaling areas.

In the middle estuary, lower percentages of end-member I occur in both the channel as well as along the flanking shoals in relation to end-member II. This is attributed to low rates of sedimentation along

these reaches due to the possibility of sediment bypassing in the middle estuary reaches (Luken, 1982 Personal Communication). It is also possible that locally derived sand from lateral erosion has an increasing influence upon the far-field effects of the distribution of Piedmont-derived river sands within these reaches. Nonetheless, Piedmont river sand-shape characteristics are still present within the bottom sediments of the middle estuary.

In the lower estuary, slightly higher percentages of end-member I are present within the bottom sediments contained within the estuary channel and on the shoals in relation to percentages contained within these areas in the middle estuary. In addition, a sand-sample taken outside the estuary mouth shows a marked increase in percent composition of end-member I in relation to the percentages found within the middle and lower reaches of the estuary. This trend may be interpreted in two ways; higher percentages of end-member I in the lower estuary than in the middle estuary channel can be attributed to higher rates of deposition within the lower estuary than in the middle reaches (Luken, 1982 Personal Communication). Thus, river sands moving down the estuary along the shoals or perhaps within the channel may bypass the middle estuary and settle out within the lower estuary. Another interpretation is that Piedmont-derived river sands may have been deposited outside the river mouth during lower stands of sea level. With the subsequent gradual rise in sea level and the development of estuarine circulation patterns, these deposits are reworked into suspension and may move back into the lower estuary mouth via a net-landward bottom transport.

Thus, the aforementioned trends in the distribution of river-borne sands within the Rappahannock estuarine sediment regime may be a result of both long-term and short-term sediment transport processes. Short-term processes such as periodic river flooding can erode and resuspend sand-sized sediment within the riverine reaches of the Rappahannock and consequently deliver these sediments into the upper estuary sediment regime. Long-term processes such as typical bi-directional estuarine circulation patterns, as well as any deviations from these patterns induced by meterological forcing, etc., can erode and redistribute river-borne sands within the estuarine sediment regime, hence accounting for its presence within the bottom sediments throughout the river-estuary system.

XI. BIBLIOGRAPHY

Arulanandan, A., Gillogley, E., and Tully, R., 1980. Development of a Quantitative Method to Predict Critical Shear Stress and Rate of Erosion of Natural Undisturbed Cohesive Soils. U.S. Army Corps of Engineers, Tech. Report GL-80-5, p. 99.

Bascom, W.H., 1951. The Relationship Between Sand Size and Beach Face Slopes. Trans. Am. Geophys. Union, v. 32, pp. 866-874.

Boon, J.D., III, Evans, D.A., and Hennigar, H.F., 1982. Interpretation of Grain Shape Information from Fourier Analysis of Digitized Two-Dimensional Images. Mathematical Geology (in press).

Bopp, F.K., III, and Biggs, R.B., 1981. Metals in Estuarine Sediments: Factor Analysis and Its Environmental Significance. Science, v. 214, October, 1981, pp. 441-443.

Brown, P.J., 1978. Origin and Hydrodynamic History of Quartz Sand on the Southeastern United States Continental Shelf - Fourier Grain Shape Analysis. Ph.D. Dissertation, Dept. of Geology, University of South Carolina.

Bruun, P., 1962. Tracing of Material Movement on Seashores. Shore Beach, v. 30, pp. 10-15.

Byrne, R.J., and Anderson, G.L., 1977. Shoreline Erosion in Tidewater Virginia. Special Report in Applied Marine Science and Ocean Engineering No. 111 of the Virginia Institute of Marine Science, Gloucester Point, Va.

David, J.C., 1973. Statistics and Data Analysis in Geology. John Wiley and Sons, Inc.

Ehrlich, R., and Weinberg, B., 1970. An Exact Method for the Characterization of Grain Shape. Jour. Sed. Pet., v. 40, pp. 205-212.

Ehrlich, R., Brown, P.J., and Colquhoun, D., 1980. Origin of Patterns of Quartz Sand Types on the Southeastern United States Continental Shelf and Its Implication on Contemporary Shelf Sedimentation - Fourier Grain Shape Analysis. Jour. Sed. Pet., v. 50, no. 2, pp. 1095-1110.

Elliot, A.J., 1978. Observations of Meterological Induced Circulation in the Potomac Estuary. Estuarine and Coastal Marine Science, v. 6, pp. 285-299.

Folk, R.J., 1974. Petrology of Sedimentary Rocks. The University of Texas, Geology 370k, Hemphill Publishing Co., Drawer M., Univ. Station, Austin, Texas 78712.

Full, W.E., Ehrlich, R., and Klovan, J.E., 1981. Extended QMODEL - Objective Definition of External End-Members in the Analysis of Mixtures. Mathematical Geology, v. 13, no. 4, pp. 331-334.

Gilbert, A., and Cordeiro, S., 1964. A General Method for Sand Labelling with Radioactive Nuclides. Laboratorio Nacional de Engenharia Civil, Technical paper no. 225.

Graf, W.H., 1971. Hydraulics of Sediment Transport. McGraw-Hill Book Co., New York, p. 513.

Hardaway, C.S., and Anderson, C.L., 1981. Shoreline Erosion in Virginia. Sea Grant Program, Marine Advisory Service, Virginia Institute of Marine Science, Gloucester Point, Va.

Hicks, S.D., 1964. Tidal Wave Characteristics of Chesapeake Bay. Chesapeake Science, v. 5, no. 3, pp. 103-113.

Hjulström, F., 1935. Studies of the Morphological Activity of Rivers as Illustrated by the River Fyris. Bull. Geol. Inst. Uppsala, v. 25, pp. 221-527.

Hjulström, F., 1955. Transportation of Detritus by Moving Water. In "Recent Marine Sediments, A Symposium, Society of Economic Paleontologists and Mineralogists" (Parker D. Trask, ed.), Special Publication No. 4, Tulsa, Oklahoma.

Imbrie, J., 1963. Factor and Vector Analysis Programs for Analyzing Geologic Data. O.N.R., Geogr. Brance, Tech. Rep. 6, p. 83.

Inglis, C., and Allen, F.H., 1957. The Regimen of the Thames Estuary as Affected by Currents, Salinities and River Flow. Proc. Inst. of Civil Engineers, v. 7, pp. 827-878.

Inman, D.L., and Chamberlain, T.K., 1959. Tracing Beach Sand Movement with Irradiated Quartz. Jour. Geophys. Res., v. 64, no. 1, pp. 41-47.

Jöreskog, K.G., Klovan, J.E., and Reyment, R.A., 1976. Geological Factor Analysis, Methods in Geomathematics 1. Elsevier Scientific Publishing Company, N.Y.

Klovan, J.E., 1966. The Use of Factor Analysis in Determining Depositional Environments from Grain Size Distributions. Jour. Sed. Pet., v. 36, no. 1, pp. 115-125.

Klovan, J.E., and Miesch, A.T., 1976. Extended CABFAC and QMODEL Computer Programs for Q-Mode Factor Analysis of Compositional Data. Computers and Geosciences, v. 1, pp. 161-178.

Krone, R.B., 1972. A Field Study of Flocculation as a Factor in Estuarial Shoaling Processes. U.S. Army Corps of Engineers Tech. Bull. No. 19.

Meade, R.H., 1969. Landward Transport of Bottom Sediments in Estuaries of the Atlantic Coastal Plain. Jour. Sed. Pet., v. 39, pp. 222-234.

Meade, R.H., 1972. Transport and Deposition of Sediments in Estuaries. In "Environmental Framework of Coastal Plain Estuaries", Geol. Soc. Am. Memoir 133, pp. 91-120.

Mehta, A.J., and Partheniades, E., 1975. An Investigation of the Depositional Properties of Flocculated Fine Sediments. Jour. of Hydraulic Res., v. 13, no. 4, pp. 361-381.

Mignot, C., 1968. A Study of the Physical Properties of Various Very Fine Sediments and their Behavior Under Hydrodynamic Action. La Houille Blanche, v. 23, no. 7, pp. 591-620.

Miller, R.L., and Zeigler, J.M., 1958. A Model Relating Dynamics and Sediment Patterns in Equilibrium in the Region of Shoaling Waves, Breaker Zone, and Foreshore. Jour. Geology, v. 66, no. 4, pp. 417-441.

National Ocean Survey, 1982. Tide Tables. East Coast of North America, p. 285.

Nelson, B.W., 1970. Clay Mineralogy of the Bottom Sediments, Rappahannock River, Virginia. Proc. 7th Nat. Confr. on Clays and Clay Minerals, pp. 135-147.

Nelson, B.W., 1972. Biogeochemical Variables in Bottom Sediments of the Rappahannock River Estuary. In "Environmental Framework of Coastal Plain Estuaries", Geol. Soc. Am. Memoir 133, pp. 417-451.

Newell, W., and Rader, E., 1982. Tectonic Control of Cyclic Sediments in the Chesapeake Group of Virginia and Maryland. G.S.A. Guidebook, North-South East Section Meeting, Washington, D.C., American Geological Institute.

Nichols, M.M., 1974. Development of the Turbidity Maximum in the Rappahannock Estuary, Summary. Mem. Inst. Geol. Bassin Aquiteine, no. 7, pp. 19-25.

Nichols, M.M., 1977. Response and Recovery of an Estuary Following a River Flood. Jour. Sed. Pet., v. 47, no. 3, pp. 1171-1186.

Nichols, M.M., et al., 1981. Response of Freshwater Inflow in the Rappahannock Estuary, Virginia, Operation HIFLO '78. Chesapeake Research Consortium, Incorporated, Publication No. 95.

Oh, J.K., 1980. Application of Factor Analysis to Grain Size Analysis in Eyre Delta and Its Comparison with the Gironde Estuary and the Salie Beach (France). Bull. of KORDI, v. 2, pp. 63-67.

Partheniades, E., 1965. Erosion and Deposition of Cohesive Soils. Jour. Hydr. Div., Proc. ASCE, v. 91, no. HY1, Proc. Paper 4204, pp. 105-139.

Partheniades, E., and Paaswell, R.E., 1970. Erodibility of Channels with Cohesive Boundary. Jour. Hydr. Div., Proc. ASCE, v. 114, no. HY3, Proc. Paper 7156, pp. 755-771.

Powers, M., 1953. A Roundness Scale for Quartz Particles. Jour. Sed. Pet., v. 23, pp. 117-119.

Pritchard, D.W., 1954. A Study of Salt Balance in a Coastal Plain Estuary. Jour. Marine Research, v. 13, pp. 133-144.

Pritchard, D.W., 1967. Observations of Circulation in Coastal Plain Estuaries. In "Estuaries" (G. Lauff, ed.), American Association of the Advancement of Science, v. 83, pp. 37-44.

Przygocki, R.S., 1976. Identification of Sediment Sources in a Fluvial Network - North Carolina Blue Ridge - Fourier Grain Shape Analysis. M. Sc. thesis, University of South Carolina, Columbia, S.C.

Sayles, F.L., 1965. Coastal Sedimentation: Point San Pedro to Miramontes Point, California. University of California Hydraulic Engineering Laboratory, Technical Report HEL-2-15.

Schwarcz, H.P., and Shane, K.C., 1969. Measurement of Particle Shape by Fourier Analysis. Sedimentology, v. 13, pp. 213-231.

Simmons, H.B., 1955. Some Effects of Upland Discharge on Estuarine Hydraulics. Proc. A.S.C.E., Hydraulics Div., v. 81, Separate No. 792.

Sternberg, R.W., 1968. Friction Factors in Tidal Channels with Differing Bed Roughness. Marine Geology, v. 6, pp. 243-260.

Sternberg, R.W., 1972. Predicting Initial Motion and Bedload Transport of Sediment Particles in the Shallow Marine Environment. In "Shelf Sediment Transport: Process and Pattern" (Swift, D.J., et al., eds.), Hutchinson and Ross, Inc., pp. 61-82.

Sundborg, A., 1956. The River Klarälven: A Study in Fluvial Processes. Geog. Ann., Stockholm, v. 38, pp. 125-316.

U.S. Geological Survey, 1977; 1978; 1979; 1980. Water Resources Data for Virginia. U.S.G.S. Data Repts. VA-77-80-1.

Wadell, H., 1935. Volume, Shape, and Roundness of Quartz Particles. Jour. Geology, v. 43, pp. 250-279.

Wright, F.F., 1962. The Development and Application of a Fluorescent Marking Techniques for Tracing Sand Movement on Beaches. Columbia Univ., Dept. of Geology, Tech. Rept. 2.

Yarus, J.M., 1978. Shape Variation of Sand Sized Quartz in the Eastern Gulf of Alaska and Its Hydrodynamic Interpretation-Fourier Grain Shape Analysis. Ph.D. Dissertation, University of South Carolina, Columbia, S.C.

Yasso, W.E., 1962. Fluorescent Coatings on Coarse Sediments in an Integrated System. Columbia Univ., Dept. of Geology, Tech. Rept. 1.

Young, R.N., and Southard, J.B., 1978. Erosion of Fine-Grained Marine Sediments: Sea-Floor and Laboratory Experiments. Geol. Soc. Am. Bull., v. 89, pp. 663-672.

VITA

Charles Joseph Natale, Jr.

Born in Woburn, Massachusetts, July 28, 1957. Graduated from Woburn Senior High School in that city, June 1975, B.S., Boston College, 1979. Graduate Sea Education Association, Woods Hole, Massachusetts (Joint Program with Boston University and Woods Hole Oceanographic Institute, 1978).

In September, 1979, the author entered the College of William and Mary as a graduate assistant in the Department of Geological Oceanography at the Virginia Institute of Marine Science.